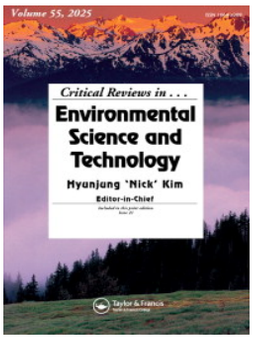

Taylor & Francis
Taylor & Francis Group

Critical Reviews in Environmental Science and Technology

ISSN: 1064-3389 (Print) 1547-6537 (Online) Journal homepage: www.tandfonline.com/journals/best20

Occurrence and remediation of chlorinated paraffins in global environmental matrices: Levels, trends, and future prospects

Yongyi Ma, Qianqian Li, Guijin Su, Huangnan Duan, Tieyu Wang, Jong Seong Khim, Seongjin Hong, Bohua Sun, Jing Meng & Bin Shi

To cite this article: Yongyi Ma, Qianqian Li, Guijin Su, Huangnan Duan, Tieyu Wang, Jong Seong Khim, Seongjin Hong, Bohua Sun, Jing Meng & Bin Shi (06 Oct 2025): Occurrence and remediation of chlorinated paraffins in global environmental matrices: Levels, trends, and future prospects, Critical Reviews in Environmental Science and Technology, DOI: 10.1080/10643389.2025.2566941

To link to this article: https://doi.org/10.1080/10643389.2025.2566941

View supplementary material

Published online: 06 Oct 2025.

Submit your article to this journal

Article views: 1

View related articles

Full Terms & Conditions of access and use can be found at
https://www.tandfonline.com/action/journalInformation?journalCode=best20

CRITICAL REVIEWS IN ENVIRONMENTAL SCIENCE AND TECHNOLOGY
https://doi.org/10.1080/10643389.2025.2566941

Taylor & Francis
Taylor & Francis Group

Check for updates

Occurrence and remediation of chlorinated paraffins in global environmental matrices: Levels, trends, and future prospects

Yongyi Ma[a,b], Qianqian Li[a,b], Guijin Su[a,b,g], Huangnan Duan[c], Tieyu Wang[d], Jong Seong Khim[e], Seongjin Hong[f], Bohua Sun[a,b], Jing Meng[a,b] and Bin Shi[a,b]

[a]Key Laboratory of Environmental Nanotechnology and Health Effects, State Key Laboratory of Environmental Chemistry and Toxicology, Research Center for Eco-Environmental Sciences, Chinese Academy of Sciences, Beijing, China; [b]University of Chinese Academy of Sciences, Beijing, China; [c]Zhangjiakou Municipal Ecological Environment Bureau, Zhangjiakou, China; [d]Guangdong Provincial Key Laboratory of Marine Disaster Prediction and Protection, Shantou University, Shantou, China; [e]School of Earth and Environmental Sciences, Research Institute of Oceanography, Seoul National University, Seoul, Republic of Korea; [f]Department of Marine Environmental Sciences, Chungnam National University, Daejeon, Republic of Korea; [g]Xinjiang Key Laboratory of Environmental Pollution and Ecological Restoration, Xinjiang Institute of Ecology and Geography, Chinese Academy of Sciences, Urumqi, Xinjiang, China

ABSTRACT

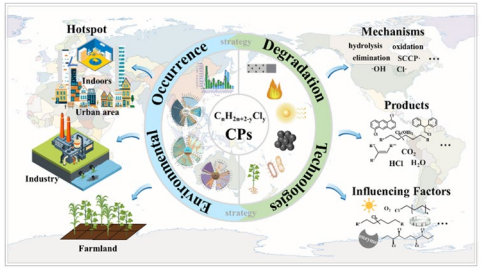

Chlorinated paraffins (CPs), especially short-chain (SCCPs) and medium-chain (MCCPs) homologues, have become a global concern due to their highly toxic and persistent. However, there remains a limited and fragmented understanding of their distribution and hotspots across diverse environmental matrices worldwide, and research on effective control measures is even more deficient. This study investigated the global occurrence of CPs in multiple environmental matrices and reviewed existing degradation technologies. Emissions from industrial activities, product usage and environmental matrices exchanges have led to widespread CPs contamination mainly encompassing SCCPs and MCCPs, with average concentrations of 10^{-3}–10^{3} ng/m^3 in atmosphere, 10–10^{3} ng/L in water and 1–10^{5} ng/g dw in sediment, as well as 1–10^{6} ng/g dw in soil. In contrast, data on long-chain CPs (LCCPs) remain extremely limited. The available long-term atmospheric monitoring demonstrated both the effectiveness of regulatory controls and the delayed environmental response due to long-range atmospheric transport. The environmental migration of CPs is strongly influenced by carbon chain length and degree of chlorination. Current degradation technologies primarily focus on pyrolysis, photolysis, photocatalysis, microbial degradation, and phytoremediation. Mechanisms and efficiency analyses revealed that major challenges include by-products and the limited scalability of technologies beyond laboratory settings. By systematically linking contaminations profiles to suitable treatment options, we proposed a targeted CPs pollution remediation strategy. These insights aim to advance global CPs government and support the implementation of the Stockholm Convention.

KEYWORDS Chlorinated paraffins; environmental occurrence; degradation technologies; remediation strategy

HANDLING EDITORS: Albert Juhasz and Eric van Hullebusch

CONTACT Qianqian Li qqli@rcees.ac.cn; Guijin Su gjsu@rcees.ac.cn Key Laboratory of Environmental Nanotechnology and Health Effects, State Key Laboratory of Environmental Chemistry and Toxicology, Research Center for Eco-Environmental Sciences, Chinese Academy of Sciences, Beijing, China

Supplemental data for this article can be accessed online at https://doi.org/10.1080/10643389.2025.2566941.

© 2025 Taylor & Francis Group, LLC

1. Introduction

Chlorinated paraffins (CPs, $C_nH_{2n+2-y}Cl_y$) are industrial chemicals with complex homologues (Feo et al., 2009). categorized by the carbon chain length (C-length) into short-chain (SCCPs, C_{10-13}), medium-chain (MCCPs, C_{14-17}), and long-chain chlorinated paraffins (LCCPs, $C_{>17}$) (Tomy et al., 1998). Commercial formulations are further distinguished by the degree of chlorination substitution (Cl%), which typically ranges from 30% to 70% by weight, as in CP-42, CP-52 and CP-70 (Tomy et al., 1998; Du et al., 2018). Substantial evidence has demonstrated that the production and usage of CPs far exceed those of many other persistent organic pollutants (POPs) (Chen, Chen, et al., 2022), and CPs are environmentally persistent (Tomy et al., 1999; Iozza et al., 2008), capable of undergoing long-range transport (Ma, Zhang, et al., 2014; Zeng, Zhao, et al., 2012), bioaccumulate in organisms (Houde et al., 2008; Yuan et al., 2019), and ecotoxic (Peng et al., 2020). Regulatory concern over SCCPs emerged in the early 2000s, the Stockholm Convention on Persistent Organic Pollutants (the Stockholm Convention) were officially listed in Annex A in 2017 for global phaseout. In May, 2025, MCCPs were included in Annex A of the Stockholm Convention under the proposed by the United Kingdom of Great Britain and Northern Ireland (UK).

Through life cycle assessment (LCA), a CPs emissions inventory was established by Chen, Chen et al. (2022) identifying major sources from chemical manufacturing and diverse industrial uses, including their application as flame retardants and plasticizers in plastics and rubber, cutting fluids in metalworking, fat liquors in leather processing, and components of sealants and adhesives. With growing public concern and analytical advances, environmental monitoring data on CPs has steadily accumulated (Bayen et al., 2006). CPs have been ubiquitously detected in various environmental matrices (atmosphere (Li et al., 2012), water (Iino et al., 2005), sediment (Ma et al. 2014), and soil (Xu et al., 2019)), biological organisms (marine organism (Zeng et al., 2017), birds (Luo et al., 2015), and humans (Zhou et al., 2020) and everyday items (Wang, Gao, et al., 2018) (plastics, rubber and food packaging). Nevertheless, most reviews have remained narrow in scope, mainly focusing on specific types (Schinkel, Bogdal, et al., 2018), regions (Wei et al., 2016), time periods (van Mourik et al., 2016) or scenario (Beloki Ezker et al., 2024). A systematic global synthesis and cross-matrices comparison of CPs concentrations is still lacking. More critically, the temporal patterns of environmental CPs before and after regulatory actions under the Stockholm Convention remain poorly understood. Such insights are essential for assessing the effectiveness of international regulation and guiding future governance.

Despite increasingly stringent regulations, the chemical stability of CPs leads to persistent environmental contamination, making residual CPs degradation an urgent priority (Tomy et al., 1998; Persistent Organic Pollutants Review Committee, 2015). To date, several degradation technologies have been developed, including pyrolysis (Schinkel et al., 2017), degradation under light (El-Morsi et al., 2002), biodegradation (Heath et al., 2006), zero-valent iron reduction (Zhang et al., 2012), and adsorption (Ding et al., 2018). To broad implementation in practical applications, a systematic review of existing technologies—covering mechanisms, efficiencies, and influencing factors—is essential to identify suitable scenarios and support effective remediation frameworks, which provide a theoretical foundation for constructing targeted scenario-specific remediation strategies.

This review synthesized the global distribution of CPs in major environmental matrices and evaluated current or emerging degradation technologies, thereby facilitating the effective implementation of the Stockholm Convention and advancing to mitigate global CPs pollution. It established correlations between contamination scenarios and degradation technologies, offering scenario-specific recommendations for CPs remediation. This review primarily focused on: (1) the concentrations levels and homologues patterns of CPs across environmental matrices, (2) long-term contamination trends based on multi-decadal monitoring, and (3) mechanistic foundations, influence factors, technological limitations and prospective research directions for existing CPs treatment approaches.

2. Environmental occurrence

2.1. CPs in atmosphere

2.1.1. Concentration distribution

CPs are ubiquitously detected in both gas- and particle-phase of the atmosphere, with reported concentrations spanning from several ng/m³ to several hundred ng/m³, with substantial regional variations (Figure 1, Table S1). Industrial production and application represent the principal emission sources, resulting in elevated concentrations in industrial areas. The peak of SCCPs and MCCPs have been detected at 498.35 ng/m³ and 400.2 ng/m³ near CP production plants in China (Yu et al., 2023; Wang, Zhao, et al., 2018), exceeding those in Tanzania (TZ) electronic waste (e-waste) dismantling area by over 20-fold (Nipen et al., 2022). Regionally, atmospheric CPs concentrations in China surpassed those in other countries, particularly in central and eastern regions where average concentration of SCCPs reached 137 ng/m³ (Li et al., 2012; Diefenbacher et al., 2015) (Table S1, Figure 1), accord with its status as the world's largest producer and consumer. Moreover, concentrations also correlate strongly with population density and anthropogenic activity, Beijing ranks the eighth in urban population density among the global cities, with mean atmospheric SCCPs and MCCPs concentrations of 348 ng/m³ and 148 ng/m³ (Zhou et al., 2024a), respectively, even exceeding those in several industrialized area (Ai et al., 2022; Li, Jiang, et al., 2023). Urban areas generally present higher burdens than rural counterparts, a pattern confirmed in multiple regions worldwide (Niu et al., 2020; Nipen et al., 2022) (Table S1, Figure 1). In Canada (CA), for example, urban SCCPs levels were more than twice those in rural areas (Niu et al., 2021). Indoor environments typically show even greater concentrations due to the intensive use of CP-containing products and limited ventilation, and time people spend indoors exceeds 20h, thereby enhancing exposure potential. (Duan et al., 2014; Gao et al., 2016; Yu et al., 2023) (Table S2, Figure 1). Compared to SCCPs and MCCPs, data on LCCPs remains limited. A study in Shenzhen and Guangzhou, China (CSG), documented average LCCPs concentration of 2.32 ng/m³, comparable to SCCPs and MCCPs levels of 5.06 ng/m³ and 3.53 ng/m³, respectively (Li et al., 2018). This finding highlights significant data gaps in the global occurrence of LCCPs and the need for expanded monitoring.

Continuous monitoring of atmospheric CPs serves as a critical indicator for assessing the effectiveness of pollutant control policies. At present, such monitoring efforts are largely concentrated in polar regions and Xizang, China (CXZ) (Figure 1, Table S3). At Zeppelin in Arctic, over a decade of monitoring revealed a significant decline in SCCPs concentrations, decreasing from 0.361 ng/m³ in 2013 to below 0.052 ng/m³ in 2023. In contrast, MCCPs concentrations rose from 0.023 ng/m³ in 2013 to a peak of 0.750 ng/m³ in 2020, surpassing SCCPs for the first time (Bohlin-Nizzetto et al., 2014, 2021; Halvorsen et al, 2024). Similar temporal patterns were observed in both the King George Island, Antarctica (AQKGI) and CXZ, where SCCPs concentrations exhibited an initial increase followed by a subsequent decline (Jiang, Gao, et al., 2021; Wu et al., 2017, 2019). These rising-then-declining trends in SCCPs atmosphere levels demonstrated the efficacy of international regulatory actions. However, the regulation of SCCPs in some countries beginning in the early twenty first century, peak concentrations in remote areas were still recorded after 2010, underscoring the delayed environmental response due to long-range atmospheric transport of CPs. Therefore, the environmental accumulation of MCCPs also warrants increasing attention.

CPs with longer carbon chains and higher chlorination generally exhibit lower vapor pressure and higher octanol–air partition coefficients (log K_{OA}), favoring particle-phase (Feo et al., 2009). Particle CPs are of concern due to their potential for respiratory deposition and atmospheric transport, leading to accumulation in soil and water. Therefore, increasing attention has been paid to particle-phase CPs. Based on the sampling methodology, research on particulate CPs typically distinguishes between dust (collected by a cleaner) and suspended particulates (collected on quartz fiber filters). Dust samples reveal strong spatial variation, with significantly higher concentrations in industrial and e-waste areas (Figure 2a, Table S4-5). In China, SCCPs and MCCPs reached 30–5600 μg/g and 170–17,800 μg/g in dust from e-waste dismantling areas, respectively (Zeng et al.,

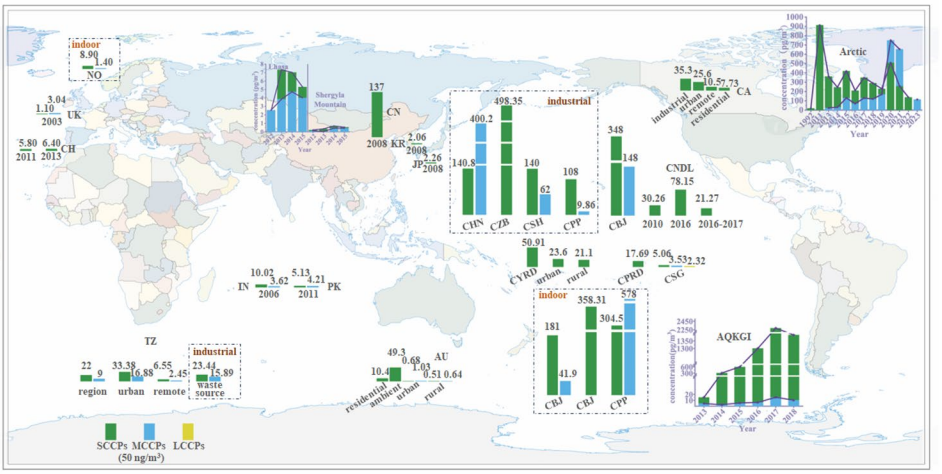

Figure 1. CPs in the global atmosphere. (The map is constructed using the data from Tables S1–S3). Note: UK (United Kingdom), CH (Switzerland), NO (Norway), SE (Sweden), TZ (Tanzania), KR (South Korea), JP (Japan), AU (Australia), CA (Canada), CN (China), CHN (Henan, China), CZB (Zibo, China), CSH (Shanghai, China), CPP (CP production plant, China), CBJ (Beijing, China), CDL (Dalian, China), CPRD (Pearl River Delta, China), CYRD (Yangtze River Delta, China), CSG (Shenzhen and Guangzhou, China), AQKGI (King George Island, Antarctica).

2016; Chen et al., 2018). Nearby residences were also affected, with household dust near Qingyuan, China (CQYerw) containing 580 μg/g of SCCPs and 1760 μg/g of MCCPs (Chen et al., 2018). Plastic-use environments, such as sports courts in Beijing, contained SCCPs and MCCPs exceeding 5429 μg/g and 15157 μg/g, respectively (Cao et al., 2019), which were 2–3 times higher than those detected in residential indoor dust. Notably, in residential environments like offices and households, MCCPs or LCCPs often dominate the CPs profiles in dust, and developing countries exhibit higher than developed (Figure 2a) (Hilger et al., 2013). In Stockholm, Sweden (SWS), office dust contained LCCPs as the predominant homologue, reflecting SCCPs phase-out and increased LCCPs use (Wong et al., 2017). For suspended particulates, concentrations of SCCPs and MCCPs generally remained below 100 ng/m^3. At identical sampling sites, indoor levels were typical 2–3 times higher than outdoor levels, as observed in CBJ and Pearl River Delta, China (CPRD) (Huang et al., 2017; Zhuo et al., 2019). This disparity can be attributed to emissions from indoor sources such as furniture and office supplies, combined with inadequate ventilation. Seasonal temperature and particle size also influenced CPs concentrations in suspended particulates. SCCPs proportions in particulates declined to 2.5% in summer due to volatilization, but rose to 63% in winter (Zhu et al., 2017). SCCPs and MCCPs concentrations in PM_{10}, $PM_{2.5}$, and $PM_{1.0}$ displayed a decreasing trend with smaller particle size in CBJ, (Huang et al., 2017). However, this size-dependent trend was less pronounced in CPRD (Zhuo et al., 2019), warranting further investigation into CPs distribution mechanism in suspended particulates.

2.1.2. Homologues patterns

Investigating the homologues patterns of CPs is essential for tracing their sources, understanding their environmental migration, and so on. For example, variations in CP homologue profiles across regions or industrial processes can aid in tracing the sources of atmospheric CPs contamination (Wang et al., 2016). Specifically, SCCPs homologues exhibited region-specific composition profiles (Table S1). In China, atmospheric SCCPs were predominantly composed of C_{10}, whereas in UK, $C_{11\text{-}12}$ dominated (Li et al., 2012; Niu et al., 2020; J. Peters et al., 2000). In Japan (JP), C_{11} and $Cl_{5\text{-}6}$ were predominant, while in Canada, $C_{12\text{-}13}$ and $Cl_{5\text{-}7}$ were most abundant (Li et al., 2012; Niu et al., 2021). These differences were largely attributed to the variation in homologue compositions of CP commercial mixtures across countries. In contrast, MCCPs displayed more consistent atmospheric distributions worldwide, typical dominated by C_{14} and

$Cl_{6\text{-}8}$ (Niu et al., 2020; Jiang, Gao, et al., 2021; Li, Jiang, et al., 2023). However, studies on the homologues of atmospheric LCCPs remain limited and lack representativeness (Li et al., 2018).

Additionally, the homologous composition of CPs across gas- or particle-phase is closely related to their physicochemical properties resulting from C-length and Cl% primarily. Homologues with short C-length and low Cl% exhibited high vapor pressure, Henry's law constant, and low log K_{OA} (Beloki Ezker et al., 2024), making them more likely to exist in the gas-phase. In contrast, long C-length and high Cl% homologues preferentially associated with particle-phase. In the atmosphere in CBJ, C_{10} and Cl_6 homologues accounted for 72.8% and 52.6% of gas-phase SCCPs, respectively, while their proportions decreased to 48.2% and 39.2% in suspended particulates (Zhou et al., 2024a). In Dalian, China (CDL), $C_{10}H_{16}Cl_6$ (37.12%) and $C_{11}H_{18}Cl_6$ (9.02%) dominated the gas-phase, while $C_{11}H_{16}Cl_8$ (11.34%) and $C_{13}H_{20}Cl_8$ (8.50%) were predominant in suspended particulates (Zhu et al., 2017). In most dust samples, the primary SCCPs homologues were C_{13} and $Cl_{6\text{-}8}$, with a notable enrichment of Cl_7 compared to the gas phase, MCCPs were primarily represented by C_{14} and $Cl_{6\text{-}8}$ (Zeng et al., 2016; Wong et al., 2017; Cao et al., 2019; McGrath et al., 2023; Wu et al., 2023). Accordingly, it can be inferred that SCCPs possessed a greater potential for long-range atmospheric transport compared to MCCPs and LCCPs, as evidenced by the dominance of $C_{10\text{-}11}$ and $Cl_{6\text{-}7}$ homologues in Antarctica atmosphere (Jiang, Gao, et al., 2021).

For atmosphere, industrial point sources and regions with intensive use of CPs constituted critical hotpots areas of pollution, particularly in China, a key producer and consumer of CPs. Indoor atmosphere CPs pollution also warranted urgent attention, especially given that individuals spend the majority of their time indoors (Duan et al., 2014). Long C-length and high Cl% like MCCPs and LCCPs tend to aggregate in the particulate phase than gas phase. Remote areas long-time atmospheric monitoring confirms SCCPs restrictions are effective, yet MCCPs levels continue to rise, reflecting substitution concerns. With MCCPs now listed in Annex A of the Stockholm Convention, urgent efforts are needed for their removal and the development of safer alternatives.

2.2. CPs in water and sediment

2.2.1. Concentration distribution

CPs are ubiquitously detected in global water environments, including surface water bodies such as rivers and lakes, marine environment, and even groundwater (Figure 2b, Table S6). Wastewater discharge is a crucial pathway for CPs into surface water, as 15% of SCCPs can persist in effluents despite tertiary wastewater treatment (Zeng et al., 2013b). For example, SCCPs concentrations in influent samples from wastewater treatment plants in Gaobeidian, China (CGBD) and JP were reported at 4450 ng/L (Zeng, Wang, Wang, et al., 2011) and 280 ng/L (Iino et al., 2005), respectively. In CBGD lake, which receives municipal wastewater, SCCPs concentrations were found to be markedly higher than those observed in other rivers and lakes within the same region (Wang et al., 2018c).

In the early 2000s, elevated concentrations of SCCPs were detected in rivers near industrial regions in developed countries such as UK and Spain (ES), ranging from 200 - 1700 ng/L and 300–1100 ng/L, respectively (Nicholls et al., 2001; Castells et al., 2004), reflecting legacy emissions from extensive CPs production and usage in Europe during twentieth century. The Huangpu River, China (CHPR), flowing through major industrial zones, also contained high MCCPs levels (mean = 1290 ng/L) (Table S6) (Wang et al., 2019). In contrast, rivers in Japan, and Pakistan exhibited much lower concentrations of SCCPs and MCCPs, all below 50 ng/L, consistent with less industries and low population density (Iino et al., 2005; Tahir et al., 2024) (Figure 2b, Table S6). Surface water contamination is a critical pollution source for interconnected systems, notably groundwater and marine environments. Groundwater pollution is particularly concerning due to its persistence, latency, and remediation challenges, threatening soil quality and drinking water safety. Yet, studies remain scarce; one investigation reported highly elevated SCCPs (mean = 9100 ng/L) in groundwater near a CP production plant in China (Wu et al., 2021). Although comprehensive global assessments are currently lacking, rivers play a crucial role in transporting

CPs from terrestrial to marine environment. Existing researches on marine CPs has predominantly focused on Chinese coastal, which reveal a spatial decline from the Bohai Sea (CBS) to the Yellow Sea (CYS) and East China Sea (CECS). The CBS, surrounded by highly industry polluted rivers like the Yellow River, Liao River, and Xiao Qing River, acts as a major pollution sink, and its semi-enclosed geography further limits water exchange and hampers contaminant dispersion. In the intertidal zone of the CBS, SCCPs concentrations have been reported up to 1256 ng/L (Zhao et al., 2019). Concentrations decreased offshore, reflecting marine dilution, while the more open CYS and CECS showed lower levels due to greater hydrodynamic mixing (Zhao et al., 2019; Hu et al., 2022; Cui et al., 2024). It is important to note, however, dilution reduces apparent concentrations only, with total contaminant mass largely unchanged.

Due to their physicochemical properties, CPs tend to accumulate in sludge and sediments *via* adsorption and precipitation, forming spatial distribution patterns in sediments that generally mirror those in overlying water bodies. However, the MCCPs concentrations/SCCPs concentrations ratio (M/S) in precipitates often exceeds 1 (Figure 2b, Table S7–S9). CPs concentrations in sludge were markedly elevated, with SCCPs ranging from 321.43 to 42,000 ng/g and MCCPs from 1560.06 to 180,000 ng/g, and M/S were as high as 2.7 to 12.4 (Nicholls et al., 2001; Stevens et al., 2003; Zeng, Wang, Wang, et al., 2011 Zeng, Wang, 2012; Bogdal et al., 2015; Brandsma et al., 2017). In surface water sediments, higher concentrations of SCCPs had been recorded at an effluent receiving lake in China (CGBDL, mean = 5768.57 ng/g) and landfill ponds in Norway (NO, mean = 4823.33 ng/g). Meanwhile, higher concentrations of MCCPs were found in ponds scattered throughout the e-waste dismantling area in Qingyuan, China (CQY, mean = 21,000 ng/g) (Borgen et al., 2003; Chen et al., 2011). In marine sediments, CPs concentrations are typically lower than those in inland surface water sediments, rarely exceeding 1000 ng/g (Table S8). Nevertheless, concentrations are generally higher in semi-enclosed seas than in open marine systems, due to restricted hydrodynamic conditions limiting dilution and dispersion (Zeng, Zhao, et al., 2012; Cui et al., 2024; Li, Guo, et al., 2023). Meanwhile, most marine sediments from Chinese coasts contained higher levels (mean = 2.55–650.7 ng/g) of SCCPs than those reported in other global marine areas, such as Tokyo Bay, Japan (JP, mean = 10.3 ng/g), and the North and Baltic Sea in Europe (N&BS, mean = 34.59 ng/g), (Li, Guo, et al., 2023; Iino et al., 2005; Hüttig & Oehme, 2006) (Figure 2b, Table S8).

2.2.2. Homologues patterns

The compositional patterns of CPs homologues in surface water and marine environments are relatively simple, with SCCPs dominated by C_{10} and MCCPs by C_{14}, while chlorination is mainly concentrated in $Cl_{5\text{-}7}$ (Table S6). C-length and Cl% largely determine phase partitioning and mobility, as longer C-length and higher Cl% favor sludge and sediment accumulation due to high octanol-water partition coefficient (K_{OW}) and lower solubility (South et al., 2022). At a wastewater treatment plant in CBJ, secondary treatment enriched C_{10} homologues in water from 39.1% to 50.8% and reduced C_{13} from 16.5% to 7.1%, with dominant chlorination shifting from Cl_7 to Cl_6. In contrast, sludge samples were enriched in C_{11} and $Cl_{7\text{-}8}$ (Zeng et al., 2013b). Similar patterns were also observed in the influent and effluent from Japanese wastewater treatment plants (Iino et al., 2005). Shorter-chain and lower-chlorinated homologues exhibit greater mobility and transport potential. In the Xiao Qing River, China, estuarine sediments showed a shift from C_{13} to C_{10} and from $Cl_{8\text{-}9}$ to $Cl_{5\text{-}6}$ relative to upstream water (Pan et al., 2021).

The homologues patterns profile of CPs in sediment cores can provide valuable insights into historical pollutant dynamics and degradation processes. Depth-resolved CPs concentrations are often used to infer temporal variations in environmental contamination, Iozza et al. (2008) collected 135 m sediment core from Lake Thun to examine CPs concentrations in sediments from 1899 to 2004. An investigation of sediment cores from the Pearl River in China revealed that concentrations of $C_{10\text{-}11}$ and $C_{16\text{-}17}$ homologues were notably higher in the upper layers compared to deeper sections, which pattern likely reflected differences in the commercial CPs mixtures used in recent years versus those used a decade ago, or degradation processes occurring

over time in deep layers (Chen et al., 2011). Moreover, a consistent decrease in the Cl% of CPs with the increasing depth was observed, implying a dechlorination during the vertical migration.

For water and sediment, high concentrations of CPs in water and sediments are commonly found in lakes and rivers near wastewater treatment plants and industrial areas. CPs in surface water can vertically migrate into groundwater, enter the sea *via* river discharge, or accumulate in sediments. Additionally, sediments also play a role in adsorbing CPs, with MCCPs being more readily captured than SCCPs. Unfortunately, data LCCPs in water and sediments remain limited.

2.3. CPs in soil

2.3.1. Concentration distribution

Soil acts a significant sink for CPs, with widespread contamination detected globally, particularly in China (Figure 2c, Table S10–S13). Due to their limited migration capacity in soil, CPs' pollution impact is amplified by point source. For example, inner soil of three CP production plants in China (CZBpp, CDLpp, and CGZpp), average concentrations of SCCPs and MCCPs ranged from 1.02×10^3 to 3.06×10^5 ng/g and from 1.61×10^3 to 2.05×10^3 ng/g, respectively (Xu et al., 2016; Wang, Zhao, et al., 2018; Wu et al., 2020b). Notably, the dismantling of CP-containing products contributes more significantly to soil contamination than their production and use. E-waste dismantling, in particular, poses the most severe threat, as demonstrated by roadside soil at e-waste sites in Taizhou, China (CTZ), where average concentrations of SCCPs and MCCPs reached 6.35×10^4 ng/g and 1.26×10^6 ng/g, respectively (Xu et al., 2019). Similarly, soil in Agbogbloshie, Ghana (GH), the world's second-largest e-waste disposal site, showed the average concentrations of 3300 ng/g for SCCPs and 380 ng/g for MCCPs (Moeckel et al., 2020). Both sites in China and GH displayed decreasing CPs concentrations with increasing distance from e-waste dismantling area, highlighting the limited spatial mobility of CPs in soil. Other industrial regions reported average concentrations of SCCPs and MCCPs ranging from 172 to 596.97 and 176.72 to 6987.14 ng/g, respectively, influenced by the local industry types and scales (Huang et al., 2020; Wu et al., 2020a; Weng et al., 2022; Zhou et al., 2023) (Figure 2c, Table S11).

Soil pollution from CPs is also driven by atmosphere/water-soil exchanges, as evidenced by detection in remote areas and farmlands. It can be observed that CPs concentrations in remote soil of developing countries are higher than those in developed countries (Figure 2c). For example, SCCPs averaged 64.51 ng/g on Chongming Island (CCI), a background area distant from urban sources (Wang et al., 2013), while MCCPs reached 325 ng/g In Shergyla Mountain (Zhou et al., 2024b). CPs have also been found in soil of Antarctica and the Arctic (Li et al., 2016, 2017a). A nationwide survey from 31 provinces in China reported mean levels of 374 ng/g SCCPs and 859.59 ng/g MCCPs in farmland soils (Aamir et al., 2019). The spatial distribution of SCCPs was more uniform than MCCPs, likely due to the higher volatility and long-range atmospheric transportation. Farmland irrigated with treated wastewater contained elevated CPs relative to river or groundwater irrigation, highlighting the role of water–soil exchange (Zeng, Wang, Han, et al., 2011). These findings indicate potential threats to food safety and groundwater quality.

CPs in urban-rural soil reflect dual influences from local point sources and environmental partitioning through atmosphere/water -soil exchanges. Soils in the Huangpu River Basin China (CHPB), which contained multiple industrial parks, exhibited notably elevated CPs concentrations (SCCPs mean = 347.12 ng/g; MCCPs mean = 2352.07 ng/g) (Zhou et al., 2023). More CPs levels in most urban-rural areas fell between those observed in industrial and remote regions. For instance, SCCPs concentrations reached 330 ng/g in Dar es Salaam, Tanzanian (TZDS) (Nipen et al., 2022), while soils in the mountainous regions of Yunnan, China (CYN) contained 348 ng/g for SCCPs and 229 ng/g for MCCPs (Wang et al., 2020).

2.3.2. Homologues patterns

Longer C-length and higher Cl% promote the accumulation of CPs in soil. Across surveyed sites, nearly half of the soils showed C_{13} and $Cl_{7\text{-}8}$ as the predominant SCCPs homologues. In Tibetan

agricultural fields, for instance, C_{13} and Cl_8 accounted for 30% and 31% of the total SCCPs, respectively (Zhou et al., 2024b). However, for MCCPs, C_{14} and $Cl_{7\text{-}8}$ remained the dominant homologues, likely due to their absolute dominance in commercial CPs formulations.

Vertical profile analysis further provides insights into CPs persistence and mobility in soil systems. Soil core sampling data revealed an increasing proportion of shorter C-length and lower Cl% homologues with depth, suggesting their greater soil penetration capacity, but this also probably caused by biodegradation from longer-chain counterparts (Aamir et al., 2019). Altitudinal variation in CPs distribution may also shaped by the "mountain cold trapping" effect, a mechanism recognized for its role in retention of organic pollutants. Model predictions suggested that CPs homologues with log K_{OA} values from 8.5 to 11.5 and log K_{WA} values from 3.5 to 6 were more likely to accumulate in high-altitude soil (Aamir et al., 2019a). These findings provide a basis for developing targeted control strategies for MCCPs in mountainous environments.

Point sources and atmosphere/water-soil exchanges are the two primary pathways by which CPs enter soil systems. Therefore, industrial areas with high CPs emissions and farmland with potential for food exposure are priority targets for soil remediation efforts. Compared to atmosphere and water, CPs exhibit poor horizontal migration capacity in soil. Notably, SCCPs in soil display relatively greater vertical penetrating potential and long-range migration than MCCPs, contributing to the spatial expansion of contamination.

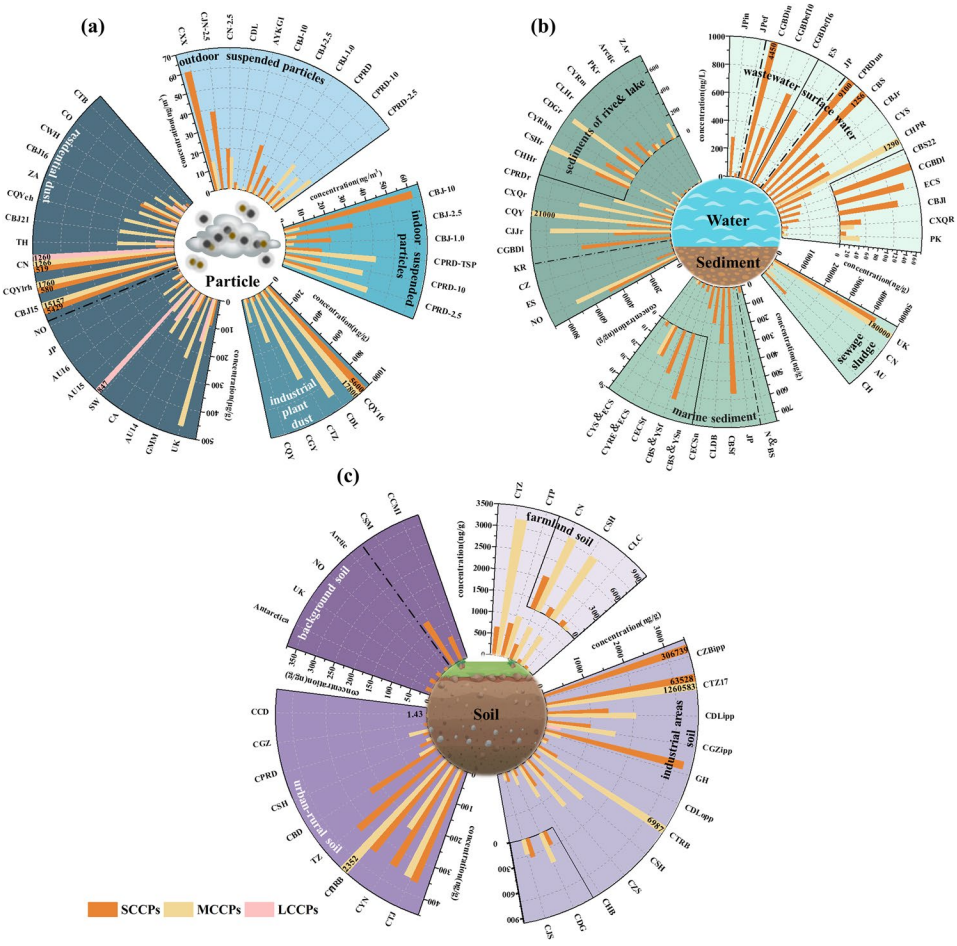

Figure 2. (a) CPs in the global particle-phase; (b) water and sediment; and (c) soil. (The three maps are constructed using the data from Tables S4–S13).

Global assessments indicated that CPs pollution was widespread across multiple environmental matrices, the average concentrations of SCCPs and MCCPs ranged from 10^{-3} to 10^{3} ng/m^3 in the atmosphere, 10–10^{3} ng/L in water, 1–10^{5} ng/g dw in sediments, and 1–10^{6} ng/g dw in soil. Overall, CPs concentrations in dust, wastewater, surface water, surface sediments, and background soils are generally lower in developed countries compared to developing countries, indicating that developing regions currently experience more severe CPs pollution. Society policy exerts a direct and decisive influence on CPs usage and pollution, while socioeconomic factors play a critical role in shaping CP-related regulations and their enforcement, thereby creating pronounced regional concentration disparities between developed and developing countries. High CPs concentrations are typically localized near point sources, irrespective of a country's development status. To better compare and predict CPs concentrations from world while, we attempted employ the available data for meta-analysis and random forest modeling. However, the data in our study is constrained in terms of sample volume, temporal coverage, and geographical representation, thereby limiting the analysis to atmospheric data and reducing the overall accuracy of the results (Text S1 and Figures S1–S4). Nonetheless, the findings still indirectly reflect higher concentrations of CPs in the Chinese atmosphere and highlight population as the dominant driver, which are consistent with Section 2.1. With the accumulation of monitoring data across diverse environmental matrices, the integration of such models with relevant data will enable a more rigorous and comprehensive evaluation of global distribution patterns, temporal dynamics, and key drivers together with their relative contributions.

With SCCPs and MCCPs listed under Annex A, greater attention must be directed toward LCCPs, which are expected to constitute a major fraction of CPs. However, monitoring data for LCCPs in environmental matrices remain markedly scarcer than for SCCPs and MCCPs, primarily due to long-standing analytical challenges. LCCPs' low volatility renders gas chromatography unsuitable, while even advanced two-dimensional GC remains confined to SCCPs and MCCPs (Korytár et al., 2005). Although liquid chromatography has been applied, the commonly used electrospray ionization is poorly suited for nonpolar CPs, limiting reliable detection. With ongoing advances in chromatographic and mass spectrometric techniques, this gap is expected to narrow, enabling more comprehensive assessments in the future. CPs research and management efforts will shift toward residues remediation in environmental matrices. However, distinct distribution patterns characterize CPs in different matrices. Specifically, CPs in the atmosphere exhibit strong long-range transport potential, occurring at low concentrations but across wide spatial scales. In large volume environment water, CPs display certain solubility mobility. In sediment and soil, CPs show strong adsorption and limited mobility. Thus, no single remediation technology is universally applicable for all matrices. The selection of targeted scenario -specific remediation strategies is essential to achieve efficient, economically viable and environmentally friendly outcomes. Systematically evaluation of available technologies is therefore critical, encompassing their underlying mechanisms, scope of applicability, advantages, limitations, cost-effectiveness, and potential for large-scale deployment.

3. Degradation technologies for CPs

Although diverse degradation technologies for CPs—such as pyrolysis, photolysis, photocatalysis, and biodegradation—have been proposed, most remain confined to laboratory evaluations. Several emerging technologies are also expected to be applied to CPs remediation. This chapter comprehensively synthesizes advances, mechanisms, cost-effectiveness and application prospects to inform future environmentally sustainable technologies.

3.1. Pyrolysis

Pyrolysis has long been considered an effective method for the complete removal of organic pollutants. In 1975, Sosa (1975) discovered that synthetic CPs volatilized at 270–330 °C,

undergoing dehydrochlorination to form unsaturated products. Camino and Costa (1980) later observed that CP-70 releases HCl in two temperature range: 275–400 °C and 400–800 °C. This process accompanied with the formation of isolated or short-sequence carbon-carbon double bonds, indicating C–C bond cleavage during pyrolysis. Advancements in analytical techniques have since enabled the detection of more pyrolysis products. For example, gas chromatography-mass spectrometry (GC–MS) revealed that CP-52 and CP-70 generated 25 polychlorinated biphenyls (PCBs) and about 5 polychlorinated naphthalene (PCNs) after 5 min at 504 °C (Bergman et al., 1984). Mono- or di-chlorinated dibenzofurans were also detected after 10 min. At 700 °C, cyclization reactions resulted in the formation of 25 PCBs containing 1–5 chlorine atoms.

Xin, Schinkel et al. elucidated CP pyrolysis mechanisms through experiments, density functional theory (DFT), and deconvolution, dividing the process into three stages (Xin et al., 2017, 2019; Schinkel, Lehner, et al., 2018): the initial stage, the low-temperature stage, and the high-temperature stage (Figure 3). In the initial stage (~200 °C), CPs volatilize and undergo dehydrochlorination and C-C cleavage, producing HCl, chlorinated hydrocarbons, and aliphatic compounds such as alkanes, alkenes, and cycloalkanes. Nowadays, structural analogs of CPs such as chlorinated alkanes are beginning to attract the attention of researchers as emerging contaminants(Chen et al., 2024). At the low-temperature stage (200–400 °C), these intermediates undergo inter- and intramolecular addition, aromatization, cross-linking, and Diels-Alder reactions, yielding monocyclic or bicyclic aromatics rings. In the high-temperature stage (400–800 °C), radical-driven pathways dominate: Cl_2 formed from HCl oxidation dissociates into Cl·, facilitating chlorination of aromatic intermediates to CBz or CBz. Concurrently, thermally generated small molecular radicals condense and cyclize to form phenyl radicals, which intermediates further participated in reactions such as hydrogen abstraction–acetylene addition (HACA), radical addition or other reaction to the form Polycyclic Aromatic Hydrocarbons (PAHs) and Cl-PAHs. At even higher temperatures, more complete decomposition of CPs can be attained. Pilot-scale incineration (~900 °C) achieved destruction efficiencies exceeding 99.9999% for both SCCPs and MCCPs (Figure S5), which can combine with flue gas treatment. Total TEQ concentrations of toxic byproducts (PCB, PCDD/Fs) in bottom and fly ash remained below the Japanese standards (Matsukami & Kajiwara, 2019). Temperature and oxygen are primary governing factors: oxygen enhances dehydrochlorination and radical reactivity (Xin et al., 2017, 2019), but insufficient oxygen may favor toxic chlorinated aromatics, posing secondary pollution risks (Xin et al., 2018).

Pyrolysis degrades CPs into low-chlorinated molecules, which can be mineralized at high temperatures. This technique is particularly suitable for the removal CPs from soil and sediment.

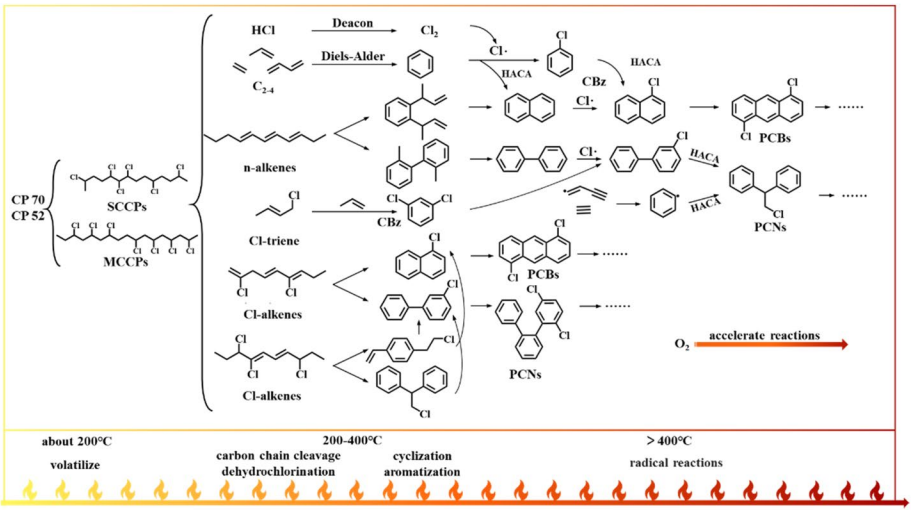

Figure 3. Pyrolysis degradation mechanisms of CPs.

However, pyrolysis need high energy and form toxic byproducts like PAHs at 200-400 °C pose significant ecology and health risks. Therefore, Future developments in pyrolysis should emphasize energy reduction and byproduct control: (1) Integrating CP-containing waste into high-temperature industrial processes (e.g. cement kilns) to completely degrade without extra energy. (2) Applying post-treatment methods, such as thermos-catalysis or photocatalysis, under mild conditions to eliminate hazardous intermediate. These strategies enhance the sustainability and remediation applicability of pyrolysis.

3.2. Degradation under light

The utilization of renewable solar energy for pollutant degradation has consistently attracted the attention of researchers. Based on the presence or absence of catalysts, light-induced treatment technologies can be classified into two types: photolysis and photocatalysis.

3.2.1. Photolysis

Photolysis of CPs has attracted attention since the early twenty first century, though limited UV absorbance in water initially hindered efficiency. Photosensitizers and oxidants significantly improved degradation. Koh & Thiemann (2001) demonstrated that acetone, as a photosensitizer, enabled complete removal of 6 mg/L CPs within 4 h under UV irradiation in a 0.1% acetone-water system (Figure S6a). Similarly, adding H_2O_2 enhanced hydroxyl radical (·OH) generation, accelerating degradation. El-Morsi et al. (2002) confirmed ·OH as the dominant reactive species in the effective photolysis of 1,2,9,10-tetrachlorodecane (T_4C_{10}) under both H_2O_2/UV and photo-Fenton system ($Fe(ClO_4)_2/H_2O_2$/UV). A modified photo-Fenton oxidation system (Fe^{3+}/H_2O_2/UV) further enhanced degradation, reducing the time required for 80% CPs removal from 40 min to 20 min (Figure S6b) (Friesen et al., 2004). The addition of Fe^{3+} promoted ·OH production *via* dual mechanisms: (1) catalytic decomposition of H_2O_2 through the $Fe^{3+} \leftrightharpoons Fe^{2+}$ redox cycle (Equation (1) and (2)), and (2) formation of Fe^{3+}-H_2O_2 complexes that decompose to yield Fe^{2+} and ·OH (Equation 3). Modified photo-Fenton system, when applied to natural lake water in Ontario, Canada, achieved 95% CPs degradation within 3 h (Friesen et al., 2004). Due to the lower bond energy of C–Cl bonds relative to C-C bonds, photolytic pathways predominantly involved dechlorination reactions (Koh & Thiemann, 2001). Photolytic pathways mainly involved dechlorination due to lower C–Cl bond energy, though lower Cl% could favor C–C cleavage. Formation of long-chain n-alkanes ($C_{>25}$) highlighted the complexity of products (Koh & Thiemann, 2001).

$$Fe^{3+} + H_2O_2 \rightarrow Fe^{2+} + \cdot HO_2 + H^+ \quad (1)$$

$$Fe^{2+} + H_2O_2 \rightarrow Fe^{3+} + \cdot OH + OH^- \quad (2)$$

$$Fe(OH)^{2+} \rightarrow h\nu Fe^{2+} + \cdot OH \quad (3)$$

Recent studies continued to reveal ·OH as the primary reactive species in the photolysis process of CPs (Figure 4a). Taking the photolysis of 1-chlorodecane CD in pure water under UV irradiation as an example, ·OH, the triplet excited state $^3CD^*$, superoxide radicals $\cdot O_2^-$, and solvated electrons e_{aq}^- all participated in the photolysis of CD, with ·OH and $^3CD^*$ accounting for 58% and 25.8% of the photolysis process, respectively (Zhang et al., 2019). Upon UV excitation, the $^3CD^*$ was generated from the ground state CD and subsequently dissociated into dechlorination radicals ·CD(–Cl) and reactive chlorine species Cl. The Cl· released into the solution could generate the main reactive species ·OH under UV irradiation. These ·OH radicals then underwent

hydrogen extraction to yield dehydrogenation radicals ·CD(–H), which could also form *via* the decomposition of ionized $CD^{\cdot+}$. Radical-radical reactions between ·CD(–Cl) and ·CD(–H) generated alcohols or long chain products (Figure 4a) (Zhang et al., 2019). Although 5 mg/L CD was completely degraded within 2 h, the mineralization rate was extremely low of 4.96%. This might be attributed to limited ·OH availability or the poor photoreactivity of intermediates, raising concerns about the persistence and bioaccumulation of byproducts in the environment.

The operational simplicity of photolysis has made it a promising technique for CPs removal from the water. However, its efficiency is constrained by factors such as light source intensity, medium absorbance, and ·OH concentration. Moreover, the formation of structurally diverse and potentially toxic intermediates remains a major drawback. Future research should focus on enhancing CPs photo-reactivity and promoting deeper decomposition while minimizing intermediates formation.

3.2.2. Photocatalysis

Light-activated photocatalysts have emerged as promising tools for CPs removal from the environment. El-Morsi et al. (2000) reported that the typical photocatalytic material TiO_2 achieved 62% removal of 1,10-dichlorodecane in water within 15 min, significantly outperforming direct photolysis (Figure S7a). Methanol quenching experiments indicated that photogenerated holes (h^+) and ·OH radicals are the primary reactive species responsible for CPs oxidation (Figure S7b).

Research on photocatalytic degradation materials for CPs remains limited, with existing studies primarily focusing on two composite materials: reduced graphene oxide (RGO)/$CoFe_2O_4$/Ag and Fe_2O_3@polydopamine (PDA)-Ag (Figure 4b) (Chen et al., 2016; Xiong et al., 2018). These materials enhance photogenerated electron-hole (e^-/h^+) separation *via* interfacial interactions, where e^- reduce O_2 to $\cdot O_2^-$ and h^+ oxidize H_2O to ·OH, which subsequently mineralize SCCPs into CO_2, H_2O, and HCl. (Figure 4b). These reactive oxygen species oxidized SCCPs into CO_2, H_2O, and HCl. Accordingly, RGO/$CoFe_2O_4$/Ag achieved a SCCPs degradation rate of 91.9% within 12 h, over fourfold higher than TiO_2 P25 (Figure S8) (Chen et al., 2016), due to the Ag surface plasmon resonance effect and the high conductivity of graphene, both of which significantly promoted the separation of e^- and h^+. For Fe_2O_3@PDA-Ag hybrids, degradation efficiency increased by 1.3-, 1.8-, and 2.9-fold compared compare to Fe_2O_3@PDA, P25, and Fe_2O_3, respectively (Figure S8) (Xiong et al., 2018). Ag nanoparticles not only had the SPR effect but also accumulated the photogenerated electrons produced by Fe_2O_3, while the PDA shell facilitated interfacial electron transfer and broadened the light absorption spectrum. Additionally, DFT calculations further elucidated the specific degradation pathway of SCCPs. The ·OH first conducted nonselective H-abstraction to form ·SCCP, followed by sequential dichlorination and deep oxidation by ·OH, ultimately achieving mineralization (Equations (4) and (5)).

$$\mathrm{SCCP} + \cdot\mathrm{OH} \rightarrow \mathrm{SCCP} + \mathrm{H_2O} \tag{4}$$

$$\cdot\mathrm{SCCP} + \cdot\mathrm{OH} \rightarrow \mathrm{HCl} + \mathrm{H_2O} + \mathrm{CO_2} \tag{5}$$

Compared with direct photolysis, photocatalytic degradation driven by ·OH provides a more efficient and sustainable strategy for mineralizing CPs into CO_2, H_2O, and HCl. Nonetheless, limited progress has been made in photocatalyst synthesis, application, and recovery, while economic feasibility and environmental risks remain unclear. Future studies should focus on the development of advanced photocatalysts: (1) Enhancing separation of photogenerated electron-hole pairs through effective modification strategies; (2) Reducing production and operational costs to improve economic feasibility. (3) Extending the catalyst lifespan and establishing practical recycling and regeneration methods; and (4) Using LCA assessing potential environmental risks to guide the development of green and sustainable photocatalysts.

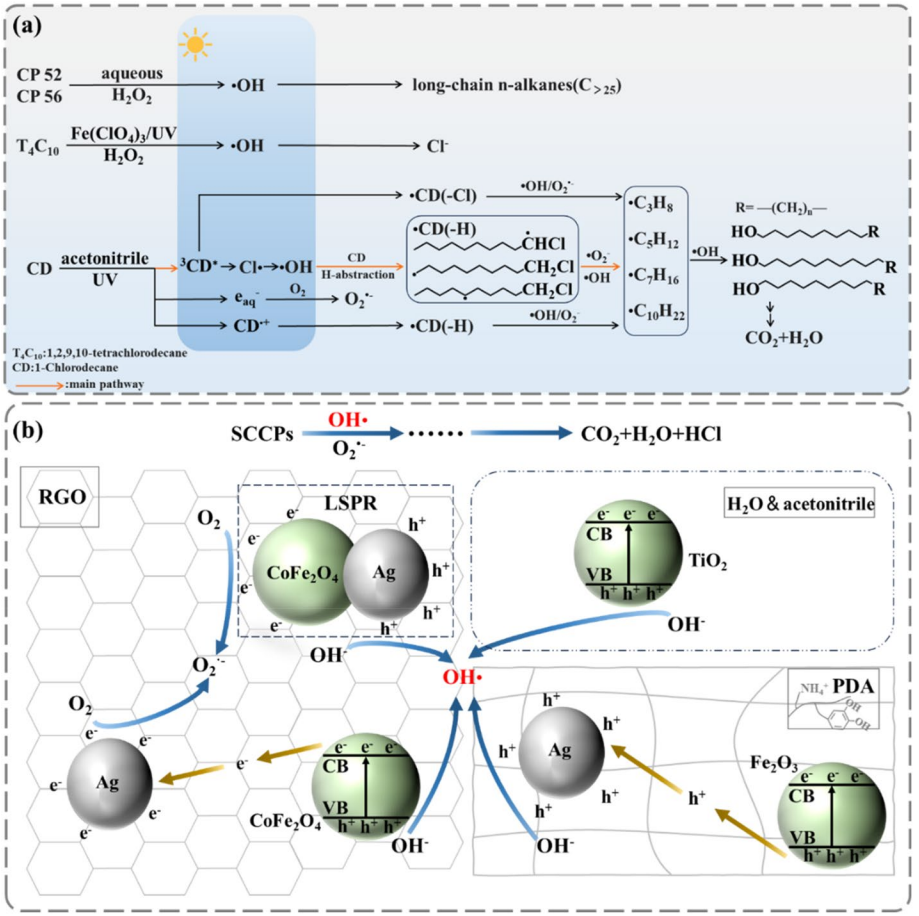

Figure 4. (a) photolysis degradation mechanisms of CPs; (b) photocatalysis degradation mechanisms of CPs.

3.3. Microbial degradation

Since the 1970s, studies on the dehalogenation of halogenated hydrocarbons have confirmed that these compounds can serve as carbon and energy sources for specific microorganisms (Omori & Alexander, 1978; Sallis et al., 1990). Identifying CPs-degrading microbes is therefore essential for developing effective bioremediation strategies. Early research highlighted the superior degradation performance of microbial consortia through synergistic metabolism (Omori et al., 1987). Subsequent studies identified *Rhodococcus* species as typical microbial strains for CPs degradation. Notably, *Rhodococcus rhodochrous* NCIMB 13064, isolated from contaminated industrial site, achieved 100% degradation of 1-chlorohexadecane within 70 h and an 80% mineralization rate of organic chloride within 20 d (Olaniran et al., 2004). Building on this, Allpress and Gowland (1999) first reported that *Rhodococcus* strain S45-1 could utilize 1-chlorinated $C_{12\text{-}18}$ alkanes as its sole carbon and energy source, demonstrating substrate-specific CPs degradation. This advancement reflects the evolution of CPs biodegradation technologies from community-level co-metabolism to the isolation of individual functional strains, and more recently, to the extraction and purification of dehalogenase enzymes.

To enhance the efficiency and feasibility of microbial degradation for CPs, extensive studies have examined mechanisms and influencing factors. The primary pathways involve elimination, hydrolysis, and oxidation, yielding products such as alkenes, alcohols, short-chain alkanes and acids (Figure 5a). Transformation is strongly affected by chain length, chlorination degree, stereoisomers, microbial strains, and environmental conditions. The dehydrohalogenase enzyme LinA2 expressed

in *Sphingobium Indicum* B90A catalyzed HCl elimination reaction of CPs, forming chlorinated alkenes. Transformation RATES of CPs mediated by LinA2 reached 20%–40% within 24h and 50-70% within 168 h, with higher Cl% homologs being preferentially converted (Heeb et al., 2019). LinA2 also exhibited stereoselectivity of CPs, favoring 2-Diaxial in (*RR*/*SS*) configurations. LinB from the same strain, hydrolyzed chlorinated alkenes and SCCPs to mono- or di-hydroxy derivatives, achieving complete degradation within 144 h, with higher efficiency for less-chlorinated compounds (Knobloch et al., 2022). Both enzymes cleaved C–Cl bonds, Cl% exerted a greater influence than C-length. Additionally, *Escherichia coli* strain 2 could degrade SCCPs *via* oxidative dechlorination, cleaving both C–Cl and C–C bonds and producing Cl^- and short-chain alkanes such as 2,4-dimethylheptane (C_9H_{20}) and 3,3-dimethylhexane (C_8H_{18}) (Qian et al., 2022). Appropriately elevated oxygen pressure (0.15 MPa) to promote bacterial growth enhanced growth and dehydrogenase activity, achieving 85.61% removal within 7 d (Figure S9). In addition, oxygenase secreted by *Rhodococcus* NCIMB 13064 targeted non-chlorinated positions on 1-chlorohexadecane, initiating β-oxidation to yield 4-chlorobutyric acid. These intermediates spontaneously cyclized to form γ-butyrolactone, which was further metabolized in trace amounts to 4-hydroxybutyric acid and subsequently entering the metabolic pathways through succinic acid and tricarboxylic acid cycle.

Building upon the understanding of microbial degradation mechanisms, research on CPs has gradually extended from controlled laboratory studies to more application-oriented investigations in contaminated environments. However, current reports on field-scale microbial degradation of CPs are limited. Wu et al. (2020b) analyzed microbial communities in soils from CP production industry and identified *Acinetobacter* and *Stenotrophomonas* as the most abundant genera across all samples, suggesting their potential role in the bioremediation of CP-contaminated soil. Lu (2013) isolated *Pseudomonas* sp. N35 from soil and applied it to dewatered sludge from a wastewater treatment plant in Beijing, China. Within 30 d, N35 achieved a 73.4% degradation rate for SCCPs initially present at 66.1 mg/kg. Notably, the release of chloride was significantly lower than the degradation efficiencies of SCCPs, indicating the accumulation of intermediate products like chlorinated alkanes($C_{<10}$), which warrant further attention.

Microbial degradation has environmentally friendly and in suit application potential, making it a promising strategy for the removal of CPs from soil and sediment. Its effectiveness depends on CPs' physicochemical traits, matrix conditions (e.g. pH, moisture, and redox), and microbial activity. Its effectiveness depends on CPs' physicochemical property, matrix conditions (e.g. pH, moisture, and redox potential), and enzymatic activity (Figure 5a). Microbial degradation face challenges including isolating efficient strains, slow metabolism, and incomplete degradation. Future work should prioritize screening strains with high efficiency, adaptability, and cost-effectiveness to enhance practical applicability.

3.4. Phytodegradation

Phytoremediation has been considered an environmentally friendly and promising technology for *in situ* soil remediation since the 1990s, particularly for shallow soils. However, its application to CPs has only recently garnered attention and interest. This process can be divided into two main mechanisms: (a) plant absorption and (b) plant metabolism.

CPs can be absorbed from water, soil and atmosphere by various plants *via* root uptake and leaf diffusion, (Klánová et al., 2009; Li et al., 2019; Chen et al. 2022b). In mature rice plants, roots CPs concentrations exceed surrounding soil levels by 2.1 times and was 1.7 to 7.0 times higher than in aerial tissues (Du et al., 2022). Uptake efficiency correlated negatively with soil organic carbon, which limited availability, but positively with nitrogen, which promoted root growth (Yu et al., 2024). Hydroponic pumpkin studies showed >95% SCCPs removal within 10 d, confirming root uptake dominance (Li et al., 2019). Meanwhile, in mature corn plants, SCCPs and MCCPs were more abundant in outer tissues (such as stalk and leaves) than in internal parts like corn cobs and kernels (Chen et al., 2021), indicating a greater role of leaf diffusion. CPs can translocate among different organs, with the transport capacity decreasing as C-length

and Cl% increase (Yu et al., 2024). Conifer needle, whose CPs concentrations have been shown to correlate with passive sampler data over long-term monitoring, may serve as environmentally friendly cleaner for of CPs Current phytoremediation focus on crops, raising potential food safety concerns (Klánová et al., 2009).

Once absorbed by plants, CPs undergo metabolic degradation. Research on CPs plant metabolism mainly focused on soybean, pumpkin, and rice (Figure 5b). Soybean and pumpkin detoxify SCCPs through dechlorination, chlorine rearrangement, and carbon chain cleavage (Li et al., 2019). Pumpkin seedlings degraded 1,2,5,5,6,9,10-heptachlorodecane, with recovery of dechlorinated products lower than total conversion, indicating subsequent hydroxylation, methoxylation, and related reactions (Li, Fu, et al., 2017; Li, Hou, et al., 2017). Chen et al. (2020) discovered that rice cells exhibited strong metabolic activity toward both 1,2,5,6,9,10-hexachlorodecane (CP-4) and a commercial 52%-MCCPs. After 5 d of exposure, only 0.27% of CP-4 and 7.62% of 52%-MCCP remained, with >40 metabolites identified, including HCl elimination, hydroxylation, sulfation, glycosylation, and conjugatio products. Authors proposed a metabolic mechanism of CPs involving intracellular enzyme and extracellular enzyme secretion catalysis. Cells also exhibited absorption/adsorption to CPs, with 99.67% for CP-4 and 102.58% for 52%-MCCP recovery rates in nonviable cell (Figure S10) (Chen et al., 2020). Building upon the cellular experiments, the team further examined the CP-4 metabolism in rice seedlings. The seedlings removed 78.6% of CP-4 from the solution with 61 transformation products detected (Chen, Hou, et al., 2022).

Phytoremediation offers an eco-friendly in-situ approach to remediate CPs-contaminated soils, providing ecological and economic benefits without disturbing the site. However, it is time-intensive

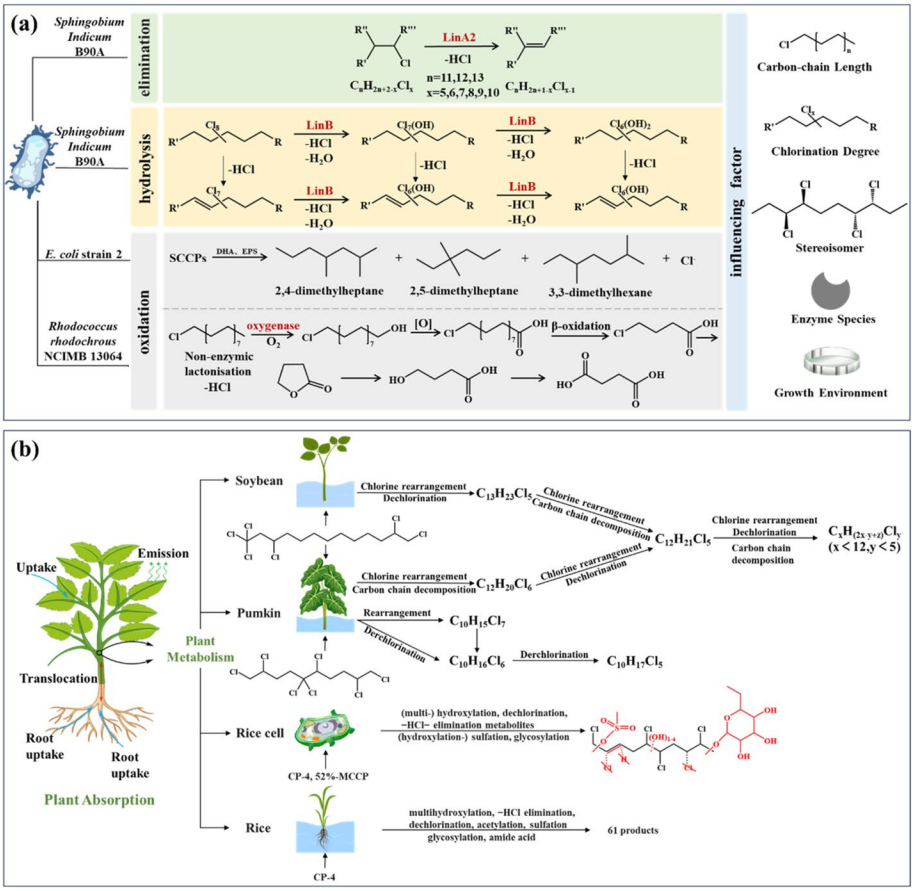

Figure 5. (a) Microbial degradation mechanisms of CPs; (b) Phytodegradation mechanisms of CPs.

and complicated due to plant metabolic byproducts. Soil conditions can directly influence plants' ability to adsorb and metabolize CPs. Consequently, phytoremediation practical application requires careful plant selection, Plant species considered suitable for practical CPs remediation are expected to possess the following attributes: (1) strong CPs uptake and metabolic capacities to minimize the formation of intermediate by-products; (2) adaptability to local soil environments; and (3) ease of harvesting and disposal, ensuring sustainability while minimizing secondary pollution.

3.5. Other degradation technology

In addition to the primary remediation techniques mentioned above, several approaches have been investigated for CPs removal. Zhang et al. (2012) demonstrated the rapid removal of SCCPs using nanoscale zero-valent iron (NZVI) under ambient temperature and pressure conditions, with dechlorination identified as the primary degradation mechanism. However, the efficiency of NZVI is constrained by factors such as loading, temperature, pH, humic acid content and initial pollutant concentration (Zhang et al., 2012), and issues like material passivation and agglomeration further limit its practical application (Stefaniuk et al., 2016). Ding et al. (2018) have established the theoretical feasibility of using carbon nanotubes as adsorbents for CPs *via* physical adsorption, though the captures pollutants still require environmentally sound disposal.

3.6. Emerging technologies

Emerging remediation technologies offer promising avenues for addressing the persistence of CPs in the environment. Here, we delve into the subject using persulfate oxidation (PS) and electrochemical technology as examples.

PS has attracted increasing attention owing to its cost-effectiveness, operational simplicity, and high degradation efficiency, which has *via* radical and non-radical pathways (Lee et al., 2020; Jing et al., 2023). In the radical pathway, strong oxidants such as peroxymonosulfate and peroxydisulfate are activated by light (Shen et al., 2020), microwave (Gujar et al., 2023; Qu et al., 2023), reducing metals (e.g. Fe and Co) (Zhang et al., 2022; Liu et al., 2023), and metal oxides (e.g., Fe_3O_4 and $CoFe_2O_4$) (Tan et al., 2014; Zhang et al., 2020), generating sulfate radicals ($SO_4^{\cdot-}$). With a robust oxidation potential (2.60 V), rapid reaction rates (10^6–10^9 M/s), relatively long lifetime ($t_{1/2}$=30–40 μs), and broad pH applicability, $SO_4^{\cdot-}$ is more effective, stable, and cost-efficient than ·OH (Ushani et al., 2020). Non-radical pathways involve the formation of singlet oxygen ($^1O_2$) through the self-decay of peroxy acids (Evans & Upton, 1985). PS is influenced by pH, temperature, activators, and coexisting ions (Ushani et al., 2020). PS have been widely applied to degrade other chlorinated organics in water and soil. Qu et al. (2023) demonstrated that microwave-activated PS system achieving 89.2% degradation of chlordane in soil. Huang et al. (2022) designed Fe-biochar composites for PS activation, achieving 95.9% removal of hexachlorophene in water with 60 min. However, $SO_4^{\cdot-}$ reacts with Cl^- to form Cl· radicals, reducing efficiency and producing toxic byproducts (Lee et al., 2020). Thus, the development of cost-effective, environmentally and efficient activation methods and the inhibition of chlorine radicals remains a key challenge for advancing PS-based CPs remediation.

Electrochemical technology is a promising strategy for degrading chlorinated pollutants *via* cathodic dechlorination and anodic dechlorination and oxidation, with effectiveness determined by chlorination degree, molecular structure, and electrode materials (Chen et al., 2019, Jiang, Zhao, et al., 2021; Pei et al., 2024). Deng et al. (2021) achieved >95% dechlorination of trichloroethylene in actual wastewater using Fe–N–doped carbon cathodes within 8 h. Cai et al. (2020) employed boron-doped diamond anodes with carbon-black-modified cathodes, enabling complete degradation of 2,4-dichlorophenoxyacetic acid within 2 h, dominated by ·OH oxidation. This process was influenced by factors such as electrode material, current density, solution pH, and

electrolyte concentration. Offering high stability, rapid kinetics, and scalability, electrochemical technology is attractive for CPs remediation, though cost-effective, durable, and recyclable electrodes remain essential for practical applications.

Based on the above analysis, we summarize CPs remediation technologies regarding environmental applicability, influencing factors, byproducts, advantages, disadvantages, economic feasibility (Table S14) and feasibility of large-scale application. Pyrolysis requires high energy and large-scale facilities but has had pilot scale: a rotary kiln incineration in Japan achieved >99.9999% removal of SCCPs and MCCPs above 900 °C, with emissions below Japanese regulatory standards (Matsukami & Kajiwara, 2019). Photocatalysis faces cost and sustainability issues related to catalyst synthesis, regeneration, and recycling. In contrast, bioremediation, including microbial and phytoremediation, is highly environmentally friendly. Nonetheless, it presents challenges such as long remediation periods, species selection difficulty, and complex metabolic by-products, with main cost of biological species selection, cultivation, and processing. Lu (2013) reported 73.4% SCCPs degradation in Beijing sewage sludge by *Pseudomonas sp.* N35 within 30 d, underscoring the metabolic potential of microorganisms toward CPs even in complex environments. Adsorption technique can effectively remove but requires follow-up disposal, while redox-based technologies hold promises for rapid and complete treatment but face constraints in materials and reactor design. Like photocatalysis, their economic feasibility largely governed by materials and required reactors. Technology Effectiveness depends on C-length, Cl%, environmental conditions, and catalysts or organisms' type. Most technologies remain confined to the laboratory stage due to issues such as low efficiency, secondary pollution, and high operational costs. Future advances may rely on integrated strategies, such as combining low-temperature pyrolysis with photocatalysis or catalytic processes, to enhance remediation efficiency and sustainability. This review is intended to inform and promote the development of more effective, sustainable, and economically feasible technologies for CP remediation.

4. Targeted scenario-specific remediation strategies for CPs removal

To achieve more effective control of CPs pollution, we have developed an implementation framework outlining priority pollution sources and optimal technology combinations, proposed targeted scenario-specific remediation strategies, as shown in Figure 6.

By comprehensively analyzing matrices characteristics and the applicability of various technologies, we identified CPs production plants and historically contaminated sites as major sources of environmental pollution, where observed elevated CPs levels. Concentrations were particularly high in soil and sediment, ranging from 1 to 10^6 ng/g dw and 1 to 10^5 ng/g dw, respectively, while notable levels also occurred in air and water, with maxima reaching 10^3 ng/m^3 and 10^3 ng/L. Based on the characteristics of each matrix, we have established optimal matches between environmental scenarios and remediation technologies, proposing targeted scenario-specific remediation strategies for CPs removal. For soil and sediment, in-situ strategies such as bioremediation offer distinct ecological and economic advantages. Given the diffusivity and long-range atmospheric transport potential of CPs, adsorption is prioritized for air, followed by centralized treatment of adsorbents and particulates *via* pyrolysis or thermal catalysis. In water, chemical or biological agents provide larger contact surfaces, rending chemical catalytic degradation technologies such as photocatalysis and NZVI reduction particularly effective. In addition, emerging techniques like PS and electrochemical technology also hold promise for high-efficiency CPs remediation in soil or water.

Notably, due to significant socioeconomic disparities, developed and developing countries exhibit a marked temporal misalignment in multiple dimensions like CPs production and policy formulation, with developed countries consistently at the forefront. Consequently, the challenges and strategies in CPs control diverge substantially between the two groups. Developed countries have generally undergone a trajectory of "pollution first, remediation later", with mid-twentieth century CPs production causing environmental pollution. Regulatory frameworks, such as the

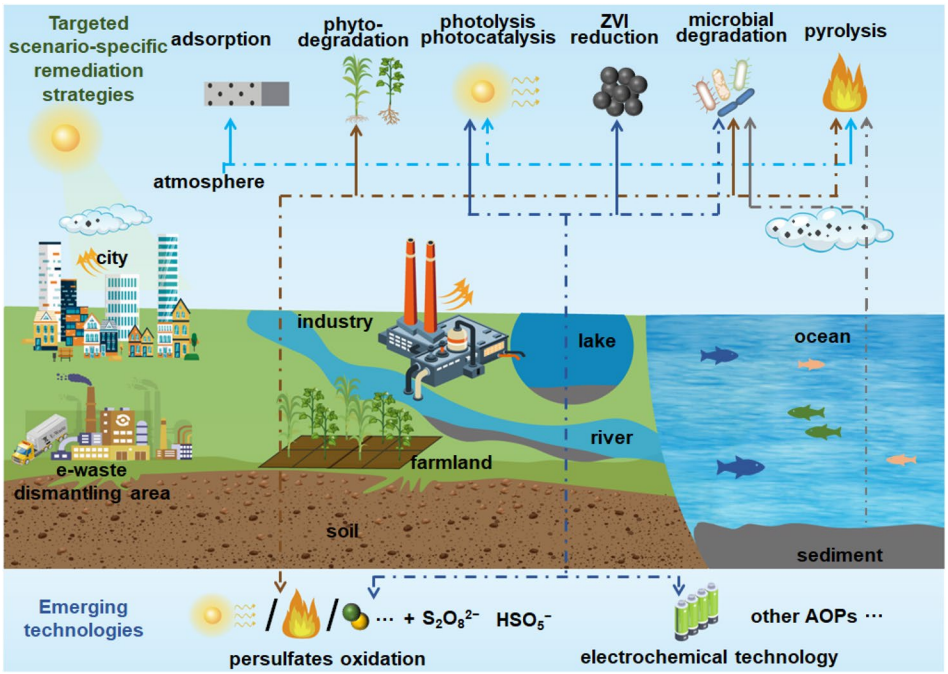

Figure 6. Environmental metrices CPs and corresponding remediation technologies. (Solid line lines represent optimal technology combinations for corresponding matrices.).

U.S. Environmental Protection Agency and Canadian Environmental Protection Act designated of SCCPs as pollutants of concern (Tomy et al., 1998). With growing attention to MCCPs, countries such as the European Union and the United States have progressively tightened restrictions (USEPA, 2009; ECHA, 2021). Today, developed countries face the challenge of remediating legacy CPs contamination, requiring long-term investment and scalable technologies. In contrast, developing countries, such as China, entered large-scale CPs production and use later, with regulatory measures delayed. Although China comprehensively eliminates SCCPs in 2023, other developed countries like India and South Africa have yet to implement comparable restrictions (Ministry of Ecology and Environment, PRC, 2023). Current challenges for developing countries are twofold: first, sound policies and regulatory systems remain inadequate; second, control technologies development and application are still at an early stage. Moving forward, developing countries can draw on these lessons from developing countries, future progress depends on accelerating regulation, advancing control technologies, and fostering innovation in CPs alternatives.

5. Conclusion and outlook

We summarized the occurrence of CPs across environmental matrices worldwide and examined the current development of remediation technologies, aiming to provide targeted scenario-specific strategies for CPs abatement. The main conclusions and outlook are as follows.

1. Strengthen regular monitoring of CPs, especially LCCPs
   Available data demonstrate the global prevalence of CPs, with particularly high levels in China. The main sources include industrial sources and human activities. The detection data of CPs are mostly clustered in SCCPs and MCCPs, and their average concentrations in atmosphere, water, sediment and soil were 10^{-3}–10^{3} ng/m^3, 10^{2}–10^{4} ng/L, 10^{1}–10^{5} ng/g dw and 10^{2}–106 ng/g dw, respectively. Soil and sediment serve as major sinks, while short C-chain, low-Cl% CPs show greater mobility and long-range transport. Long-term monitoring revealed

an initial increase followed by a decline in SCCPs, reflecting regulatory effectiveness and delayed response. Although MCCPs were recently listed in Annex A of the Stockholm Convention, Ongoing monitoring is crucial for real-time pollution assessment and early warning. Analytical challenges, especially for LCCPs, have constrained monitoring.

2. Promote the integration of multiple catalytic remediation approaches
Current CPs remediation technologies mainly focused on pyrolysis, photolytic/photocatalysis, and biological degradation. While pyrolysis and photolytic processes demonstrate the potential for complete degradation capacity and efficiency, they often require high energy consumption or operation complexity. Moreover, the use of photocatalysts may introduce secondary environmental risks. Biotechnologies are environmentally friendly but face challenges such as extended treatment durations, difficulty in selecting effective species, and the production of complex metabolic by-products. Each technique is influenced by various factors, including C-length and Cl%, environmental parameters, and the nature of the catalyst or biological organism. A single remediation technology may not adequately address practical requirements, underscoring the value of combined approaches. For instance, photothermal catalysis has demonstrated promising potential by enhancing material activity and improving degradation efficiency. Additionally, advanced oxidation technologies such as electrochemical technology and Fenton's reagent exhibit robust degradation capabilities for other organic pollutants, potentially offering new perspectives for future CPs remediation.
3. Develop a targeted scenario-specific remediation strategy
To bridge the gap between laboratory research and practical application, we developed a targeted remediation strategy by systematically linking contaminated environmental matrices with appropriate treatment technologies. Photocatalytic adsorption is particularly promising for atmospheric CPs removal at industrial sources, in urban environment, and indoors. CPs in water can be effectively treated through photocatalysis, microbial degradation, or NZVI reduction. Sediment remediation approaches include both *in situ* methods, such as adsorption, microbial degradation, and phytoremediation, and ex situ techniques like dredging followed by thermal catalysis. For soil, particularly agricultural land, *in situ* remediation techniques including microbial degradation, phytoremediation, and redox catalysis are better suited to ensure sustained land usability. Meanwhile, LCA can play a significant role in predictive insights and guidance on the economic costs and environmental impacts of emerging technologies (Johanning et al., 2023; Erakca et al., 2024). Moving forward, greater emphasis should be placed on pollution-specific scenarios when developing and applying remediation technologies to ensure relevance and effectiveness in real-world conditions.

Disclosure statement

The authors declare that they have no known competing financial interests or personal relationships that could have appeared to influence the work reported in this paper.

Funding

This work was supported by the National Key R&D Program of China (2024YFC3908803), the Strategic Priority Research Program of the Chinese Academy of Sciences, Grant NO. XDB0750400, Supported by Beijing Natural Science Foundation (Grant NO. 8252035), National Natural Science Foundation of China (22376210, 22406195) and National Funding Program for Postdoctoral Researchers (GZC20232886) and the Tianchi Talents Recruitment Program.

ORCID

Jong Seong Khim http://orcid.org/0000-0001-7977-0929
Seongjin Hong http://orcid.org/0000-0002-6305-8731

References

Aamir, M., Yin, S., Zhou, Y., Xu, C., Liu, K., & Liu, W. (2019). Congener-specific C_{10}—C_{13} and C_{14}—C_{17} chlorinated paraffins in Chinese agricultural soils: Spatio-vertical distribution, homologue pattern and environmental behavior. *Environmental Pollution (Barking, Essex: 1987)*, *245*, 789–798. https://doi.org/10.1016/j.envpol.2018.10.132

Ai, Q., Zhang, P., Gao, L., Zhou, X., Liu, Y., Huang, D., Qiao, L., Weng, J., & Zheng, M. (2022). Air–soil exchange of and risks posed by short- and medium-chain chlorinated paraffins: Case study in a contaminated area in China. *Chemosphere*, *297*, 134230. https://doi.org/10.1016/j.chemosphere.2022.134230

Allpress, J. D., & Gowland, P. C. (1999). Biodegradation of chlorinated paraffins and long-chain chloroalkanes by *Rhodococcus* sp. S45-1. *International Biodeterioration & Biodegradation*, *43*(4), 173–179. https://doi.org/10.1016/S0964-8305(99)00050-5

Bayen, S., Obbard, J. P., & Thomas, G. O. (2006). Chlorinated paraffins: A review of analysis and environmental occurrence. *Environment International*, *32*(7), 915–929. https://doi.org/10.1016/j.envint.2006.05.009

Beloki Ezker, I., Yuan, B., Bohlin-Nizzetto, P., Borgen, A. R., & Wang, T. (2024). Polychlorinated alkanes in indoor environment: A review of levels, sources, exposure, and health implications for chlorinated paraffin mixtures. *Chemosphere*, *365*, 143326. https://doi.org/10.1016/j.chemosphere.2024.143326

Bergman, A., Hagman, A., Jacobsson, S., Jansson, B., & Ahlman, M. (1984). Thermal degradation of polychlorinated alkanes. *Chemosphere*, *13*(2), 237–250. https://doi.org/10.1016/0045-6535(84)90130-9

Bogdal, C., Alsberg, T., Diefenbacher, P. S., MacLeod, M., & Berger, U. (2015). Fast quantification of chlorinated paraffins in environmental samples by direct injection high-resolution mass spectrometry with pattern deconvolution. *Analytical Chemistry*, *87*(5), 2852–2860. https://doi.org/10.1021/ac504444d

Bohlin-Nizzetto, P., Aas, W., & Krogseth, I. (2014). Monitoring of environmental contaminants in air and precipitation, annual report 2013. M-202-1014. Norwegian Institute for Air Research. (NILU report, 29/2014).

Bohlin-Nizzetto, P., Aas, W., Halvorsen, H. L., Nikiforov, V., & Pfaffhuber, K. A. (2021). Monitoring of environmental contaminants in air and precipitation, annual report 2020. M-2060-2021. Norwegian Institute for Air Research. (NILU report, 12/2021).

Borgen, A. R., Schlabach, M., & Mariussen, E. (2003). Screening of chlorinated paraffins in Norway. *Organohalogen Compounds*, *60*, 331–334.

Brandsma, S. H., van Mourik, L., O'Brien, J. W., Eaglesham, G., Leonards, P. E. G., de Boer, J., Gallen, C., Mueller, J., Gaus, C., & Bogdal, C. (2017). Medium-chain chlorinated paraffins (CPs) dominate in Australian sewage sludge. *Environmental Science & Technology*, *51*(6), 3364–3372. https://doi.org/10.1021/acs.est.6b05318

Cai, J., Zhou, M., Pan, Y., & Lu, X. (2020). Degradation of 2,4-dichlorophenoxyacetic acid by anodic oxidation and electro-Fenton using BDD anode: Influencing factors and mechanism. *Separation and Purification Technology*, *230*, 115867. https://doi.org/10.1016/j.seppur.2019.115867

Camino, G., & Costa, L. (1980). Thermal degradation of a highly chlorinated paraffin used as a fire retardant additive for polymers. *Polymer Degradation and Stability*, *2*(1), 23–33. https://doi.org/10.1016/0141-3910(80)90013-0

Cao, D., Gao, W., Wu, J., Lv, K., Xin, S., Wang, Y., & Jiang, G. (2019). Occurrence and human exposure assessment of short- and medium-chain chlorinated paraffins in dusts from plastic sports courts and synthetic turf in Beijing, China. *Environmental Science & Technology*, *53*(1), 443–451. https://doi.org/10.1021/acs.est.8b04323

Castells, P., Santos, F. J., & Galceran, M. T. (2004). Solid-phase extraction versus solid-phase microextraction for the determination of chlorinated paraffins in water using gas chromatography–negative chemical ionisation mass spectrometry. *Journal of Chromatography A*, *1025*(2), 157–162. https://doi.org/10.1016/j.chroma.2003.10.069

Chen, Z., Liu, Y., Wei, W., & Ni, B.-J. (2019). Recent advances in electrocatalysts for halogenated organic pollutant degradation. *Environmental Science Nano*, *6*(8), 2332–2366. https://doi.org/10.1039/C9EN00411D

Chen, C., Chen, A., Zhan, F., Wania, F., Zhang, S., Li, L., & Liu, J. (2022). Global historical production, use, in-use stocks, and emissions of short-, medium-, and long-chain chlorinated paraffins. *Environmental Science & Technology*, *56*(12), 7895–7904. https://doi.org/10.1021/acs.est.2c00264

Chen, H., Lam, J. C. W., Zhu, M., Wang, F., Zhou, W., Du, B., Zeng, L., & Zeng, E. Y. (2018). Combined effects of dust and dietary exposure of occupational workers and local residents to short- and medium-chain chlorinated paraffins in a mega e-waste recycling industrial park in South China. *Environmental Science & Technology*, *52*(20), 11510–11519. https://doi.org/10.1021/acs.est.8b02625

Chen, M., Luo, X., Zhang, X., He, M., Chen, S., & Mai, B. (2011). Chlorinated paraffins in sediments from the Pearl River Delta, South China: Spatial and temporal distributions and implication for processes. *Environmental Science & Technology*, *45*(23), 9936–9943. https://doi.org/10.1021/es202891a

Chen, W., Hou, X., Liu, Y., Hu, X., Liu, J., Schnoor, J. L., & Jiang, G. (2021). Medium- and short-chain chlorinated paraffins in mature maize plants and corresponding agricultural soils. *Environmental Science & Technology*, *55*(8), 4669–4678. https://doi.org/10.1021/acs.est.0c05111

Chen, W., Hou, X., Mao, X., Jiao, S., Wei, L., Wang, Y., Liu, J., & Jiang, G. (2022b). Biotic and abiotic transformation pathways of a short-chain chlorinated paraffin congener, 1,2,5,6,9,10-$C_{10}H_{16}Cl_6$, in a rice seedling hydroponic exposure system. *Environmental Science & Technology*, *56*(13), 9486–9496. https://doi.org/10.1021/acs.est.2c01119

Chen, W., Yu, M., Zhang, Q., Hou, X., Kong, W., Wei, L., Mao, X., Liu, J., Schnoor, J. L., & Jiang, G. (2020). Metabolism of SCCPs and MCCPs in suspension rice cells based on paired mass distance (PMD) analysis. *Environmental Science & Technology*, *54*(16), 9990–9999. https://doi.org/10.1021/acs.est.0c01830

Chen, W., Ren, D., Liu, Q., Zhou, Q., Liu, J., & Jiang, G. (2024). Enhanced research needed on the structural analogues of chlorinated paraffins as emerging contaminants of concern. *Environment & Health (Washington, D.C.)*, *2*(10), 681–683. https://doi.org/10.1021/envhealth.4c00099

Chen, X., Zhao, Q., Li, X., & Wang, D. (2016). Enhanced photocatalytic activity of degrading short chain chlorinated paraffins over reduced graphene oxide/$CoFe_2O_4$/Ag nanocomposite. *Journal of Colloid and Interface Science*, *479*, 89–97. https://doi.org/10.1016/j.jcis.2016.06.053

Cui, Q., Han, D., Qin, H., Li, H., Liu, Y., Guo, W., Song, M., Li, J., Sun, Y., Luo, J., Xue, J., & Xu, Y. (2024). Investigating the levels, spatial distribution, and trophic transfer patterns of short-chain chlorinated paraffins in the Southern Bohai Sea, China. *Water Research*, *253*, 121337. https://doi.org/10.1016/j.watres.2024.121337

Deng, J., Hu, X.-M., Gao, E., Wu, F., Yin, W., Huang, L.-Z., & Dionysiou, D. D. (2021). Electrochemical reductive remediation of trichloroethylene contaminated groundwater using biomimetic iron-nitrogen-doped carbon. *Journal of Hazardous Materials*, *419*, 126458. https://doi.org/10.1016/j.jhazmat.2021.126458

Diefenbacher, P. S., Bogdal, C., Gerecke, A. C., Glüge, J., Schmid, P., Scheringer, M., & Hungerbühler, K. (2015). Short-chain chlorinated paraffins in Zurich, Switzerland—Atmospheric concentrations and emissions. *Environmental Science & Technology*, *49*(16), 9778–9786. https://doi.org/10.1021/acs.est.5b02153

Ding, Q., Ding, N., Chen, X., & Wu, C.-M. L. (2018). Chlorinated paraffins wrapping of carbon nanotubes: A theoretical investigation. *Applied Surface Science*, *436*, 277–282. https://doi.org/10.1016/j.apsusc.2017.12.009

Du, X., Yuan, B., Li, J., Yin, G., Qiu, Y., Zhao, J., Duan, X., Wu, Y., Lin, T., & Zhou, Y. (2022). Distribution, behavior, and risk assessment of chlorinated paraffins in paddy plants throughout whole growth cycle. *Environment International*, *167*, 107404. https://doi.org/10.1016/j.envint.2022.107404

Du, X., Yuan, B., Zhou, Y., Benskin, J. P., Qiu, Y., Yin, G., & Zhao, J. (2018). Short-, medium-, and long-chain chlorinated paraffins in wildlife from paddy fields in the Yangtze River Delta. *Environmental Science & Technology*, *52*(3), 1072–1080. https://doi.org/10.1021/acs.est.7b05595

Duan, X., Zhao, X., Wang, B., Chen, Y., & Cao, S. (2014). *Highlights of the Chinese exposure factors (Adults)*. Science Press.

ECHA. (2021). Inclusion of substances of very high concern in the Candidate List for eventual inclusion in Annex XIV.

El-Morsi, T. M., Budakowski, W. R., Abd-El-Aziz, A. S., & Friesen, K. J. (2000). Photocatalytic degradation of 1,10-dichlorodecane in aqueous suspensions of TiO_2: A reaction of adsorbed chlorinated alkane with surface hydroxyl radicals. *Environmental Science & Technology*, *34*(6), 1018–1022. https://doi.org/10.1021/es9907360

El-Morsi, T. M., Emara, M. M., Abd El Bary, H. M. H., Abd-El-Aziz, A. S., & Friesen, K. J. (2002). Homogeneous degradation of 1,2,9,10-tetrachlorodecane in aqueous solutions using hydrogen peroxide, iron and UV light. *Chemosphere*, *47*(3), 343–348. https://doi.org/10.1016/S0045-6535(01)00305-8

Erakca, M., Baumann, M., Helbig, C., & Weil, M. (2024). Systematic review of scale-up methods for prospective life cycle assessment of emerging technologies. *Journal of Cleaner Production*, *451*, 142161. https://doi.org/10.1016/j.jclepro.2024.142161

Evans, D. F., & Upton, M. W. (1985). Studies on singlet oxygen in aqueous solution. Part 3. The decomposition of peroxy-acids. *Journal of the Chemical Society, Dalton Transactions*, (6), 1151–1153. https://doi.org/10.1039/dt9850001151

Feo, M. L., Eljarrat, E., Barceló, D., & Barceló, D. (2009). Occurrence, fate and analysis of polychlorinated n-alkanes in the environment. *TRAC Trends in Analytical Chemistry*, *28*(6), 778–791. https://doi.org/10.1016/j.trac.2009.04.009

Friesen, K. J., El-Morsi, T. M., & Abd-El-Aziz, A. S. (2004). Photochemical oxidation of short-chain polychlorinated n-alkane mixtures using H_2O_2/UV and the photo-Fenton reaction. *International Journal of Photoenergy*, *6*, 631879. https://doi.org/10.1155/S1110662X04000121

Gao, W., Wu, J., Wang, Y., & Jiang, G. (2016). Distribution and congener profiles of short-chain chlorinated paraffins in indoor/outdoor glass window surface films and their film-air partitioning in Beijing, China. *Chemosphere*, *144*, 1327–1333. https://doi.org/10.1016/j.chemosphere.2015.09.075

Gujar, S. K., Divyapriya, G., Gogate, P. R., & Nidheesh, P. V. (2023). Environmental applications of ultrasound activated persulfate/peroxymonosulfate oxidation process in combination with other activating agents. *Critical Reviews in Environmental Science and Technology*, *53*(6), 780–802. https://doi.org/10.1080/10643389.2022.2085965

Halvorsen, H. L., Pfaffhuber, K. A., Nipen, M., Bohlin-Nizzetto, P., Berglen, T. F., Nikiforov, V., & Hartz, W. (2024). Monitoring of environmental contaminants in air and precipitation. Annual report 2023. (NILU report 18/2024).

Heath, E., Brown, W. A., Jensen, S. R., & Bratty, M. P. (2006). Biodegradation of chlorinated alkanes and their commercial mixtures by *Pseudomonas* sp. strain 273. *Journal of Industrial Microbiology & Biotechnology*, *33*(3), 197–207. https://doi.org/10.1007/s10295-004-0186-x

Heeb, N. V., Schalles, S., Lehner, S., Schinkel, L., Schilling, I., Lienemann, P., Bogdal, C., & Kohler, H.-P. E. (2019). Biotransformation of short-chain chlorinated paraffins (SCCPs) with LinA2: A HCH and HBCD converting bacterial dehydrohalogenaseLinA2. *Chemosphere*, *226*, 744–754. https://doi.org/10.1016/j.chemosphere.2019.03.169

Hilger, B., Fromme, H., Völkel, W., & Coelhan, M. (2013). Occurrence of chlorinated paraffins in house dust samples from Bavaria, Germany. *Environmental Pollution (Barking, Essex: 1987)*, *175*, 16–21. https://doi.org/10.1016/j.envpol.2012.12.011

Houde, M., Muir, D. C. G., Tomy, G. T., Whittle, D. M., Teixeira, C., & Moore, S. (2008). Bioaccumulation and trophic magnification of short- and medium-chain chlorinated paraffins in food webs from Lake Ontario and Lake Michigan. *Environmental Science & Technology*, *42*(10), 3893–3899. https://doi.org/10.1021/es703184s

Hu, H., Jin, H., Li, T., Guo, Y., Wu, P., Xu, K., Zhu, W., Zhou, Y., & Zhao, M. (2022). Spatial distribution, partitioning, and ecological risk of short chain chlorinated paraffins in seawater and sediment from East China Sea. *The Science of the Total Environment*, *811*, 151932. https://doi.org/10.1016/j.scitotenv.2021.151932

Huang, D., Gao, L., Qiao, L., Cui, L., Xu, C., Wang, K., & Zheng, M. (2020). Concentrations of and risks posed by short-chain and medium-chain chlorinated paraffins in soil at a chemical industrial park on the southeast coast of China. *Environmental Pollution (Barking, Essex: 1987)*, *258*, 113704. https://doi.org/10.1016/j.envpol.2019.113704

Huang, H., Gao, L., Xia, D., Qiao, L., Wang, R., Su, G., Liu, W., Liu, G., & Zheng, M. (2017). Characterization of short- and medium-chain chlorinated paraffins in outdoor/indoor $PM_{10}/PM_{2.5}/PM_{1.0}$ in Beijing, China. *Environmental Pollution (Barking, Essex: 1987)*, *225*, 674–680. https://doi.org/10.1016/j.envpol.2017.03.054

Huang, P., Zhang, P., Wang, C., Tang, J., & Sun, H. (2022). Enhancement of persulfate activation by Fe-biochar composites: Synergism of Fe and N-doped biochar. *Applied Catalysis B: Environmental*, *303*, 120926. https://doi.org/10.1016/j.apcatb.2021.120926

Hüttig, J., & Oehme, M. (2006). Congener group patterns of chloroparaffins in marine sediments obtained by chloride attachment chemical ionization and electron capture negative ionization. *Chemosphere*, *64*(9), 1573–1581. https://doi.org/10.1016/j.chemosphere.2005.11.042

Iino, F., Takasuga, T., Senthilkumar, K., Nakamura, N., & Nakanishi, J. (2005). Risk assessment of short-chain chlorinated paraffins in Japan based on the first market basket study and species sensitivity distributions. *Environmental Science & Technology*, *39*(3), 859–866. https://doi.org/10.1021/es049221l

Iozza, S., Müller, C. E., Schmid, P., Bogdal, C., & Oehme, M. (2008). Historical profiles of chlorinated paraffins and polychlorinated biphenyls in a dated sediment core from Lake Thun (Switzerland). *Environmental Science & Technology*, *42*(4), 1045–1050. https://doi.org/10.1021/es702383t

J. Peters, A., T. Tomy, G., Jones, K. C., Coleman, P., & Stern, G. A. (2000). Occurrence of C_{10}–C_{13} polychlorinated *n*-alkanes in the atmosphere of the United Kingdom. *Atmospheric Environment*, *34*(19), 3085–3090. https://doi.org/10.1016/S1352-2310(99)00479-3

Jing, B., Li, J., Nie, C., Zhou, J., Li, D., & Ao, Z. (2023). Flow line of density functional theory in heterogeneous persulfate-based advanced oxidation processes for pollutant degradation: A review. *Critical Reviews in Environmental Science and Technology*, *53*(4), 483–503. https://doi.org/10.1080/10643389.2022.2070404

Jiang, L., Gao, W., Ma, X., Wang, Y., Wang, C., Li, Y., Yang, R., Fu, J., Shi, J., Zhang, Q., Wang, Y., & Jiang, G. (2021). Long-term investigation of the temporal trends and gas/particle partitioning of short- and medium-chain chlorinated paraffins in ambient air of King George Island, Antarctica. *Environmental Science & Technology*, *55*(1), 230–239. https://doi.org/10.1021/acs.est.0c05964

Johanning, M., Widenmeyer, M., Cano, G. E., Zeller, V., Klemenz, S., Chen, G., Feldhoff, A., & Weidenkaff, A. (2023). Recycling process development with integrated life cycle assessment – a case study on oxygen transport membrane material. *Green Chemistry*, *25*(12), 4735–4749. https://doi.org/10.1039/D3GC00391D

Jiang, Y., Zhao, H., Liang, J., Yue, L., Li, T., Luo, Y., Liu, Q., Lu, S., Asiri, A. M., Gong, Z., & Sun, X. (2021). Anodic oxidation for the degradation of organic pollutants: Anode materials, operating conditions and mechanisms. A mini review. *Electrochemistry Communications*, *123*, 106912. https://doi.org/10.1016/j.elecom.2020.106912

Klánová, J., Cupr, P., Baráková, D., Seda, Z., Andel, P., & Holoubek, I. (2009). Can pine needles indicate trends in the air pollution levels at remote sites? *Environmental Pollution (Barking, Essex: 1987)*, *157*(12), 3248–3254. https://doi.org/10.1016/j.envpol.2009.05.030

Knobloch, M. C., Mathis, F., Fleischmann, T., Kohler, H.-P. E., Kern, S., Bleiner, D., & Heeb, N. V. (2022). Enzymatic synthesis and formation kinetics of mono- and di-hydroxylated chlorinated paraffins with the bacterial dehalogenase LinB from *Sphingobium indicum*. *Chemosphere*, *291*(Pt 2), 132939. https://doi.org/10.1016/j.chemosphere.2021.132939

Koh, I.-O., & Thiemann, W. (2001). Study of photochemical oxidation of standard chlorinated paraffins and identification of degradation products. *Journal of Photochemistry and Photobiology A: Chemistry*, *139*(2–3), 205–215. https://doi.org/10.1016/S1010-6030(00)00427-5

Korytár, P., Leonards, P. E. G., de Boer, J., & Brinkman, U. (2005). Group separation of organohalogenated compounds by means of comprehensive two-dimensional gas chromatography. *Journal of Chromatography A*, *1086*(1–2), 29–44. https://doi.org/10.1016/j.chroma.2005.05.087

Lee, J., Von Gunten, URS., & Kim, J.-H. (2020). Persulfate-Based Advanced Oxidation: Critical Assessment of Opportunities and Roadblocks. *Environmental Science & Technology*, *54*(6), 3064–3081. https://doi.org/10.1021/acs.est.9b07082

Li, H., Fu, J., Pan, W., Wang, P., Li, Y., Zhang, Q., Wang, Y., Zhang, A., Liang, Y., & Jiang, G. (2017a). Environmental behaviour of short-chain chlorinated paraffins in aquatic and terrestrial ecosystems of Ny-Ålesund and London Island, Svalbard, in the Arctic. *The Science of the Total Environment*, *590-591*, 163–170. https://doi.org/10.1016/j.scitotenv.2017.02.192

Li, H., Fu, J., Zhang, A., Zhang, Q., & Wang, Y. (2016). Occurrence, bioaccumulation and long-range transport of short-chain chlorinated paraffins on the Fildes Peninsula at King George Island, Antarctica. *Environment International*, *94*, 408–414. https://doi.org/10.1016/j.envint.2016.05.005

Li, Q., Jiang, S., Li, Y., Su, J., Shangguan, J., Zhan, M., Wang, Y., Su, X., Li, J., & Zhang, G. (2023). The impact of three related emission industries on regional atmospheric chlorinated paraffins pollution. *Environmental Pollution (Barking, Essex: 1987)*, *316*(Pt 2), 120564. https://doi.org/10.1016/j.envpol.2022.120564

Li, Q., Li, J., Wang, Y., Xu, Y., Pan, X., Zhang, G., Luo, C., Kobara, Y., Nam, J.-J., & Jones, K. C. (2012). Atmospheric short-chain chlorinated paraffins in China, Japan, and South Korea. *Environmental Science & Technology*, *46*(21), 11948–11954. https://doi.org/10.1021/es302321n

Li, T., Gao, S., Ben, Y., Zhang, H., Kang, Q., & Wan, Y. (2018). Screening of chlorinated paraffins and unsaturated analogues in commercial mixtures: Confirmation of their occurrences in the atmosphere. *Environmental Science & Technology*, *52*(4), 1862–1870. https://doi.org/10.1021/acs.est.7b04761

Liu, B., Huang, B., Wang, Z., Tang, L., Ji, C., Zhao, C., Feng, L., & Feng, Y. (2023). Homogeneous/heterogeneous metal-catalyzed persulfate oxidation technology for organic pollutants elimination: A review. *Journal of Environmental Chemical Engineering*, *11*(3), 109586. https://doi.org/10.1016/j.jece.2023.109586

Li, X., Guo, H., Hong, J., Gao, Y., Ma, X., & Chen, J. (2023). Short- and medium-chain chlorinated paraffins in the sediment of the East China Sea and Yellow Sea: Distribution, composition, and ecological risks. *Toxics*, *11*(7), 558. https://doi.org/10.3390/toxics11070558

Li, Y., Hou, X., Chen, W., Liu, J., Zhou, Q., Schnoor, J. L., & Jiang, G. (2019). Carbon chain decomposition of short chain chlorinated paraffins mediated by pumpkin and soybean seedlings. *Environmental Science & Technology*, *53*(12), 6765–6772. https://doi.org/10.1021/acs.est.9b01215

Li, Y., Hou, X., Yu, M., Zhou, Q., Liu, J., Schnoor, J. L., & Jiang, G. (2017). Dechlorination and chlorine rearrangement of 1,2,5,5,6,9,10-heptachlorodecane mediated by the whole pumpkin seedlings. *Environmental Pollution (Barking, Essex: 1987)*, *224*, 524–531. https://doi.org/10.1016/j.envpol.2017.02.035

Lu, M. (2013). Degradation of short chain polychlorinated paraffins by a new isolate: Tests in pure culture and sewage sludge. *Journal of Chemical Technology & Biotechnology*, *88*(7), 1273–1279. https://doi.org/10.1002/jctb.3971

Luo, X., Sun, Y., Wu, J., Chen, S., & Mai, B. (2015). Short-chain chlorinated paraffins in terrestrial bird species inhabiting an e-waste recycling site in South China. *Environmental Pollution (Barking, Essex: 1987)*, *198*, 41–46. https://doi.org/10.1016/j.envpol.2014.12.023

Ma, X., Chen, C., Zhang, H., Gao, Y., Wang, Z., Yao, Z., Chen, J., & Chen, J. (2014). Congener-specific distribution and bioaccumulation of short-chain chlorinated paraffins in sediments and bivalves of the Bohai Sea, China. *Marine Pollution Bulletin*, *79*(1–2), 299–304. https://doi.org/10.1016/j.marpolbul.2013.11.020

Ma, X., Zhang, H., Zhou, H., Na, G., Wang, Z., Chen, C., Chen, J., & Chen, J. (2014). Occurrence and gas/particle partitioning of short- and medium-chain chlorinated paraffins in the atmosphere of Fildes Peninsula of Antarctica. *Atmospheric Environment*, *90*, 10–15. https://doi.org/10.1016/j.atmosenv.2014.03.021

Matsukami, H., & Kajiwara, N. (2019). Destruction behavior of short- and medium-chain chlorinated paraffins in solid waste at a pilot-scale incinerator. *Chemosphere*, *230*, 164–172. https://doi.org/10.1016/j.chemosphere.2019.05.048

McGrath, T. J., Poma, G., Hutinet, S., Fujii, Y., Dodson, R. E., Johnson-Restrepo, B., Muenhor, D., Dervilly, G., Cariou, R., & Covaci, A. (2023). An international investigation of chlorinated paraffin concentrations and homologue distributions in indoor dust. *Environmental Pollution (Barking, Essex: 1987)*, *333*, 121994. https://doi.org/10.1016/j.envpol.2023.121994

Ministry of Ecology and Environment, PRC. (2023). Lists of new pollutants under control.

Moeckel, C., Breivik, K., Nøst, T. H., Sankoh, A., Jones, K. C., & Sweetman, A. (2020). Soil pollution at a major West African E-waste recycling site: Contamination pathways and implications for potential mitigation strategies. *Environment International*, *137*, 105563. https://doi.org/10.1016/j.envint.2020.105563

Nicholls, C. R., Allchin, C. R., & Law, R. J. (2001). Levels of short and medium chain length polychlorinated *n*-alkanes in environmental samples from selected industrial areas in England and Wales. *Environmental Pollution (Barking, Essex: 1987)*, *114*(3), 415–430. https://doi.org/10.1016/S0269-7491(00)00230-X

Nipen, M., Vogt, R. D., Bohlin-Nizzetto, P., Borgå, K., Mwakalapa, E. B., Borgen, A. R., Jørgensen, S. J., Ntapanta, S. M., Mmochi, A. J., Schlabach, M., & Breivik, K. (2022). Spatial trends of chlorinated paraffins and dechloranes in air and soil in a tropical urban, suburban, and rural environment. *Environmental Pollution (Barking, Essex: 1987)*, *292*(Pt A), 118298. https://doi.org/10.1016/j.envpol.2021.118298

Niu, S., Chen, R., Zou, Y., Dong, L., Hai, R., & Huang, Y. (2020). Spatial distribution and profile of atmospheric short-chain chlorinated paraffins in the Yangtze River Delta. *Environmental Pollution (Barking, Essex: 1987)*, *259*, 113958. https://doi.org/10.1016/j.envpol.2020.113958

Niu, S., Harner, T., Chen, R., Parnis, J. M., Saini, A., & Hageman, K. (2021). Guidance on the application of polyurethane foam disk passive air samplers for measuring nonane and short-chain chlorinated paraffins in air: Results from a screening study in urban air. *Environmental Science & Technology*, *55*(17), 11693–11702. https://doi.org/10.1021/acs.est.1c02428

Olaniran, A. O., Pillay, D., & Pillay, B. (2004). Haloalkane and haloacid dehalogenases from aerobic bacterial isolates indigenous to contaminated sites in Africa demonstrate diverse substrate specificities. *Chemosphere*, *55*(1), 27–33. https://doi.org/10.1016/j.chemosphere.2003.10.067

Omori, T., & Alexander, M. (1978). Bacterial and spontaneous dehalogenation of organic compounds. *Applied and Environmental Microbiology*, *35*(3), 512–516. https://journals.asm.org/doi/10.1128/aem.35.3.512-516.1978 https://doi.org/10.1128/aem.35.3.512-516.1978

Omori, T., Kimura, T., & Kodama, T. (1987). Bacterial cometabolic degradation of chlorinated paraffins. *Applied Microbiology and Biotechnology*, *25*(6), 553–557. https://doi.org/10.1007/BF00252016

Pei, X., Shang, R., Chen, B., Wang, Z., Yao, X., & Zhu, H. (2024). Advances in the electrochemical degradation of environmental persistent organochlorine pollutants: Materials, mechanisms, and applications. *Frontiers of Environmental Science & Engineering*, *18*(11), 144. https://doi.org/10.1007/s11783-024-1904-4

Pan, X., Zhen, X., Tian, C., & Tang, J. (2021). Distributions, transports and fates of short- and medium-chain chlorinated paraffins in a typical river-estuary system. *The Science of the Total Environment*, *751*, 141769. https://doi.org/10.1016/j.scitotenv.2020.141769

Peng, Y., Fang, W., Yan, L., Wang, Z., Wang, P., Yu, J., & Zhang, X. (2020). Early life stage bioactivity assessment of short-chain chlorinated paraffins at environmentally relevant concentrations by concentration-dependent transcriptomic analysis of zebrafish embryos. *Environmental Science & Technology*, *54*(2), 996–1004. https://doi.org/10.1021/acs.est.9b04879

Persistent Organic Pollutants Review Committee. (2015). UNEP/POPS/POPRC/11/10/Add.2: Report of the Persistent Organic Pollutants Review Committee on the work of its eleventh meeting.

Qu, J., Liu, R., Bi, X., Li, Z., Li, K., Hu, Q., Zhang, X., Zhang, G., Ma, S., & Zhang, Y. (2023). Remediation of atrazine contaminated soil by microwave activated persulfate system: Performance, mechanism and DFT calculation. *Journal of Cleaner Production*, *399*, 136546. https://doi.org/10.1016/j.jclepro.2023.136546

Qian, Y., Han, W., Zhou, F., Ji, B., Zhang, H., & Zhang, K. (2022). Effects of pressurized aeration on the biodegradation of short-chain chlorinated paraffins by *Escherichia coli* strain 2. *Membranes*, *12*(6), 634. https://doi.org/10.3390/membranes12060634

Shen, C.-H., Wen, X.-J., Fei, Z.-H., Liu, Z.-T., & Mu, Q.-M. (2020). Visible-light-driven activation of peroxymonosulfate for accelerating ciprofloxacin degradation using CeO_2/Co_3O_4 p-n heterojunction photocatalysts. *Chemical Engineering Journal*, *391*, 123612. https://doi.org/10.1016/j.cej.2019.123612

Schinkel, L., Bogdal, C., Canonica, E., Cariou, R., Bleiner, D., McNeill, K., & Heeb, N. V. (2018). Analysis of medium-chain and long-chain chlorinated paraffins: The urgent need for more specific analytical standards. *Environmental Science & Technology Letters*, *5*(12), 708–717. https://doi.org/10.1021/acs.estlett.8b00537

Schinkel, L., Lehner, S., Heeb, N. V., Lienemann, P., McNeill, K., & Bogdal, C. (2017). Deconvolution of mass spectral interferences of chlorinated alkanes and their thermal degradation products: Chlorinated alkenes. *Analytical Chemistry*, *89*(11), 5923–5931. https://doi.org/10.1021/acs.analchem.7b00331

Schinkel, L., Lehner, S., Knobloch, M., Lienemann, P., Bogdal, C., McNeill, K., & Heeb, N. V. (2018). Transformation of chlorinated paraffins to olefins during metal work and thermal exposure–Deconvolution of mass spectra and kinetics. *Chemosphere*, *194*, 803–811. https://doi.org/10.1016/j.chemosphere.2017.11.168

Sosa, J. M. (1975). Thermal stability of chlorinated paraffins. *Journal of Polymer Science: Polymer Chemistry Edition*, *13*(10), 2397–2405. https://doi.org/10.1002/pol.1975.170131021

South, L., Saini, A., Harner, T., Niu, S., Parnis, J. M., & Mastin, J. (2022). Medium- and long-chain chlorinated paraffins in air: A review of levels, physicochemical properties, and analytical considerations. *The Science of the Total Environment*, *843*, 157094. https://doi.org/10.1016/j.scitotenv.2022.157094

Stefaniuk, M., Oleszczuk, P., & Ok, Y. S. (2016). Review on nano zerovalent iron (nZVI): From synthesis to environmental applications. *Chemical Engineering Journal*, *287*, 618–632. https://doi.org/10.1016/j.cej.2015.11.046

Stevens, J. L., Northcott, G. L., Stern, G. A., Tomy, G. T., & Jones, K. C. (2003). PAHs, PCBs, PCNs, organochlorine pesticides, synthetic musks, and polychlorinated n-alkanes in U.K. sewage sludge: Survey results and implications. *Environmental Science & Technology*, *37*(3), 462–467. https://doi.org/10.1021/es020161y

Sallis, P. J., Armfield, S. J., Bull, A. T., & Hardman, D. J. (1990). Isolation and characterization of a haloalkane halidohydrolase from *Rhodococcus erythropolis* Y2. *Journal of General Microbiology*, *136*(1), 115–120. https://doi.org/10.1099/00221287-136-1-115

Tahir, A., Abbasi, N. A., He, C., Ahmad, S. R., Baqar, M., & Qadir, A. (2024). Spatial distribution and ecological risk assessment of short and medium chain chlorinated paraffins in water and sediments of river Ravi, Pakistan. *The Science of the Total Environment*, *926*, 171964. https://doi.org/10.1016/j.scitotenv.2024.171964

Tan, C., Gao, N., Deng, Y., Deng, J., Zhou, S., Li, JUN., & Xin, X. (2014). Radical induced degradation of acetaminophen with Fe_3O_4 magnetic nanoparticles as heterogeneous activator of peroxymonosulfate. *Journal of Hazardous Materials*, *276*, 452–460. https://doi.org/10.1016/j.jhazmat.2014.05.068

Tomy, G. T., Fisk, A. T., Westmore, J. B., & Muir, D. C. G. (1998). Environmental chemistry and toxicology of polychlorinated n-alkanes. In G.W. Ware (Ed.), *Reviews of environmental contamination and toxicology: Continuation of residue reviews* (pp. 53–128). Springer-Verlag.

Tomy, G. T., Stern, G. A., Lockhart, W. L., & Muir, D. C. G. (1999). Occurrence of C_{10}–C_{13} polychlorinated n-alkanes in Canadian midlatitude and Arctic lake sediments. *Environmental Science & Technology*, *33*(17), 2858–2863. https://doi.org/10.1021/es990107q

USEPA. (2009). Short-Chain Chlorinated Paraffins (SCCPs) and Other Chlorinated Paraffins Action Plan.

Ushani, U., Lu, X., Wang, J., Zhang, Z., Dai, J., Tan, Y., Wang, S., Li, W., Niu, C., Cai, T., Wang, N., & Zhen, G. (2020). Sulfate radicals-based advanced oxidation technology in various environmental remediation: A state-of-the–art review. *Chemical Engineering Journal*, *402*, 126232. https://doi.org/10.1016/j.cej.2020.126232

van Mourik, L. M., Gaus, C., Leonards, P. E. G., & de Boer, J. (2016). Chlorinated paraffins in the environment: A review on their production, fate, levels and trends between 2010 and 2015. *Chemosphere*, *155*, 415–428. https://doi.org/10.1016/j.chemosphere.2016.04.037

Wang, C., Gao, W., Liang, Y., Wang, Y., & Jiang, G. (2018a). Concentrations and congener profiles of chlorinated paraffins in domestic polymeric products in China. *Environmental Pollution (Barking, Essex: 1987)*, *238*, 326–335. https://doi.org/10.1016/j.envpol.2018.02.078

Wang, K., Gao, L., Zhu, S., Cui, L., Qiao, L., Xu, C., Huang, D., & Zheng, M. (2020). Spatial distributions and homolog profiles of chlorinated nonane paraffins, and short and medium chain chlorinated paraffins in soils from Yunnan, China. *Chemosphere*, *247*, 125855. https://doi.org/10.1016/j.chemosphere.2020.125855

Wang, P., Zhao, N., Cui, Y., Jiang, W., Wang, L., Wang, Z., Chen, X., Jiang, L., & Ding, L. (2018). Short-chain chlorinated paraffin (SCCP) pollution from a CP production plant in China: Dispersion, congener patterns and health risk assessment. *Chemosphere*, *211*, 456–464. https://doi.org/10.1016/j.chemosphere.2018.07.136

Wang, X., Jia, H., Hu, B., Cheng, H., Zhou, Y., & Fu, R. (2019). Occurrence, sources, partitioning and ecological risk of short- and medium-chain chlorinated paraffins in river water and sediments in Shanghai. *The Science of the Total Environment*, *653*, 475–484. https://doi.org/10.1016/j.scitotenv.2018.10.391

Wang, X., Zhang, Y., Miao, Y., Ma, L., Li, Y., Chang, Y., & Wu, M. (2013). Short-chain chlorinated paraffins (SCCPs) in surface soil from a background area in China: Occurrence, distribution, and congener profiles. *Environmental Science and Pollution Research International*, *20*(7), 4742–4749. https://doi.org/10.1007/s11356-012-1446-3

Wang, X., Zhou, J., Lei, B., Zhou, J., Xu, S., Hu, B., Wang, D., Zhang, D., & Wu, M. (2016). Atmospheric occurrence, homologue patterns and source apportionment of short- and medium-chain chlorinated paraffins in Shanghai, China: Biomonitoring with Masson pine (*Pinus massoniana* L.) needles. *The Science of the Total Environment*, *560-561*, 92–100. https://doi.org/10.1016/j.scitotenv.2016.03.240

Wang, Y., Wang, Y., & Jiang, G. (2018c). Solid-phase extraction for analysis of short-chain chlorinated paraffins in water sample. *Chinese Journal of Analytical Chemistry*, *46*(7), 1102–1108. https://doi.org/10.11895/j.issn.0253-3820.181008

Wei, G., Liang, X., Li, D., Zhuo, M., Zhang, S., Huang, Q., Liao, Y., Xie, Z., Guo, T., & Yuan, Z. (2016). Occurrence, fate and ecological risk of chlorinated paraffins in Asia: A review. *Environment International*, *92-93*, 373–387. https://doi.org/10.1016/j.envint.2016.04.002

Weng, J., Zhang, P., Gao, L., Zhu, S., Liu, Y., Qiao, L., Zhao, B., Liu, Y., Xu, M., & Zheng, M. (2022). Concentrations, homolog profiles, and risk assessment of short- and medium-chain chlorinated paraffins in soil around factories in a non-ferrous metal recycling park. *Environmental Pollution (Barking, Essex: 1987)*, *293*, 118456. https://doi.org/10.1016/j.envpol.2021.118456

Wong, F., Suzuki, G., Michinaka, C., Yuan, B., Takigami, H., & de Wit, C. A. (2017). Dioxin-like activities, halogenated flame retardants, organophosphate esters and chlorinated paraffins in dust from Australia, the United Kingdom, Canada, Sweden and China. *Chemosphere*, *168*, 1248–1256. https://doi.org/10.1016/j.chemosphere.2016.10.074

Wu, J., Cao, D., Gao, W., Lv, K., Liang, Y., Fu, J., Gao, Y., Wang, Y., & Jiang, G. (2019). The atmospheric transport and pattern of medium chain chlorinated paraffins at Shergyla Mountain on the Tibetan Plateau of China. *Environmental Pollution (Barking, Essex: 1987)*, *245*, 46–52. https://doi.org/10.1016/j.envpol.2018.10.112

Wu, J., Gao, W., Liang, Y., Fu, J., Gao, Y., Wang, Y., & Jiang, G. (2017). Spatiotemporal distribution and alpine behavior of short chain chlorinated paraffins in air at Shergyla mountain and Lhasa on the Tibetan Plateau of China. *Environmental Science & Technology*, *51*(19), 11136–11144. https://doi.org/10.1021/acs.est.7b03457

Wu, Y., Gao, S., Ji, B., Liu, Z., Zeng, X., & Yu, Z. (2020a). Occurrence of short- and medium-chain chlorinated paraffins in soils and sediments from Dongguan City, South China. *Environmental Pollution (Barking, Essex: 1987)*, *265*(Pt A), 114181. https://doi.org/10.1016/j.envpol.2020.114181

Wu, Y., Gao, S., Zeng, X., Liang, Y., Liu, Z., He, L., Yuan, J., & Yu, Z. (2023). Levels and diverse composition profiles of chlorinated paraffins in indoor dust: Possible sources and potential human health related concerns. *Environmental Geochemistry and Health*, *45*(7), 4631–4642. https://doi.org/10.1007/s10653-023-01524-9

Wu, Y., Wu, J., Tan, H., Song, Q., Zhang, J., Zhong, X., Zhou, J., Wu, W., Cai, X., Zhang, W., & Liu, X. (2020b). Distributions of chlorinated paraffins and the effects on soil microbial community structure in a production plant brownfield site. *Environmental Pollution (Barking, Essex: 1987)*, *262*, 114328. https://doi.org/10.1016/j.envpol.2020.114328

Wu, Y., Wu, J., Wu, Z., Zhou, J., Zhou, L., Lu, Y., Liu, X., & Wu, W. (2021). Groundwater contaminated with short-chain chlorinated paraffins and microbial responses. *Water Research*, *204*, 117605. https://doi.org/10.1016/j.watres.2021.117605

Xin, S., Gao, W., Cao, D., Lv, K., Liu, Y., Zhao, C., Wang, Y., & Jiang, G. (2019). The thermal transformation mechanism of chlorinated paraffins: An experimental and density functional theory study. *Journal of Environmental Sciences (China)*, *75*, 378–387. https://doi.org/10.1016/j.jes.2018.05.022

Xin, S., Gao, W., Wang, Y., & Jiang, G. (2017). Thermochemical emission and transformation of chlorinated paraffins in inert and oxidizing atmospheres. *Chemosphere*, *185*, 899–906. https://doi.org/10.1016/j.chemosphere.2017.07.019

Xin, S., Gao, W., Wang, Y., & Jiang, G. (2018). Identification of the released and transformed products during the thermal decomposition of a highly chlorinated paraffin. *Environmental Science & Technology*, *52*(17), 10153–10162. https://doi.org/10.1021/acs.est.8b01729

Xiong, W., Li, X., Zhao, Q., Shi, Y., & Hao, C. (2018). Insight into the photocatalytic mineralization of short chain chlorinated paraffins boosted by polydopamine and Ag nanoparticles. *Journal of Hazardous Materials*, *359*, 186–193. https://doi.org/10.1016/j.jhazmat.2018.07.066

Xu, C., Zhang, Q., Gao, L., Zheng, M., Qiao, L., Cui, L., Wang, R., & Cheng, J. (2019). Spatial distributions and transport implications of short- and medium-chain chlorinated paraffins in soils and sediments from an e-waste dismantling area in China. *The Science of the Total Environment*, *649*, 821–828. https://doi.org/10.1016/j.scitotenv.2018.08.355

Xu, J., Gao, Y., Zhang, H., Zhan, F., & Chen, J. (2016). Dispersion of short- and medium-chain chlorinated paraffins (CPs) from a CP production plant to the surrounding surface soils and coniferous leaves. *Environmental Science & Technology*, *50*(23), 12759–12766. https://doi.org/10.1021/acs.est.6b03595

Yu, J., Tang, Q., Yin, G., Chen, W., Lv, J., Li, L., Zhang, C., Ye, Y., Song, X., Zhao, X., Tang, T., Zhang, C., Zeng, L., & Xu, Z. (2024). Uptake, accumulation and toxicity of short chain chlorinated paraffins to wheat (*Triticum aestivum* L.). *Journal of Hazardous Materials*, *464*, 132954. https://doi.org/10.1016/j.jhazmat.2023.132954

Yu, S., Gao, Y., Zhu, X., Yu, H., Zhang, Y., & Chen, J. (2023). Gas/particle partitioning of short and medium chain chlorinated paraffins from a CP production plant using passive air sampler and occupational exposure assessment. *The Science of the Total Environment*, *858*(Pt 1), 159875. https://doi.org/10.1016/j.scitotenv.2022.159875

Yuan, B., Vorkamp, K., Roos, A. M., Faxneld, S., Sonne, C., Garbus, S. E., Lind, Y., Eulaers, I., Hellström, P., Dietz, R., Persson, S., Bossi, R., & de Wit, C. A. (2019). Accumulation of short-, medium-, and long-chain chlorinated paraffins in marine and terrestrial animals from Scandinavia. *Environmental Science & Technology*, *53*(7), 3526–3537. https://doi.org/10.1021/acs.est.8b06518

Zeng, L., Lam, J. C. W., Chen, H., Du, B., Leung, K. M. Y., & Lam, P. K. S. (2017). Tracking dietary sources of short- and medium-chain chlorinated paraffins in marine mammals through a subtropical marine food web. *Environmental Science & Technology*, *51*(17), 9543–9552. https://doi.org/10.1021/acs.est.7b02210

Zeng, L., Li, H., Wang, T., Gao, Y., Xiao, K., Du, Y., Wang, Y., & Jiang, G. (2013b). Behavior, fate, and mass loading of short chain chlorinated paraffins in an advanced municipal sewage treatment plant. *Environmental Science & Technology*, *47*(2), 732–740. https://doi.org/10.1021/es304237m

Zeng, L., Wang, T., Han, W., Yuan, B., Liu, Q., Wang, Y., & Jiang, G. (2011a). Spatial and vertical distribution of short chain chlorinated paraffins in soils from wastewater irrigated farmlands. *Environmental Science & Technology*, *45*(6), 2100–2106. https://doi.org/10.1021/es103740v

Zeng, L., Wang, T., Ruan, T., Liu, Q., Wang, Y., & Jiang, G. (2012). Levels and distribution patterns of short chain chlorinated paraffins in sewage sludge of wastewater treatment plants in China. *Environmental Pollution (Barking, Essex: 1987)*, *160*(1), 88–94. https://doi.org/10.1016/j.envpol.2011.09.004

Zeng, L., Wang, T., Wang, P., Liu, Q., Han, S., Yuan, B., Zhu, N., Wang, Y., & Jiang, G. (2011). Distribution and trophic transfer of short-chain chlorinated paraffins in an aquatic ecosystem receiving effluents from a sewage treatment plant. *Environmental Science & Technology*, *45*(13), 5529–5535. https://doi.org/10.1021/es200895b

Zeng, L., Zhao, Z., Li, H., Wang, T., Liu, Q., Xiao, K., Du, Y., Wang, Y., & Jiang, G. (2012). Distribution of short chain chlorinated paraffins in marine sediments of the East China sea: Influencing factors, transport and implications. *Environmental Science & Technology*, *46*(18), 9898–9906. https://doi.org/10.1021/es302463h

Zhang, Q., He, D., Li, X., Feng, W., Lyu, C., & Zhang, Y. (2020). Mechanism and performance of singlet oxygen dominated peroxymonosulfate activation on CoOOH nanoparticles for 2,4-dichlorophenol degradation in water. *Journal of Hazardous Materials*, *384*, 121350. https://doi.org/10.1016/j.jhazmat.2019.121350

Zhang, X., Xu, B., Wang, S., Li, X., Wang, C., Liu, B., Han, F., Xu, Y., Yu, P., & Sun, Y. (2022). Tetracycline degradation by peroxymonosulfate activated with CoNx active sites: Performance and activation mechanism. *Chemical Engineering Journal*, *431*, 133477. https://doi.org/10.1016/j.cej.2021.133477

Zeng, Y., Tang, B., Luo, X., Zheng, X., Peng, P., & Mai, B. (2016). Organohalogen pollutants in surface particulates from workshop floors of four major e-waste recycling sites in China and implications for emission lists. *The Science of the Total Environment*, *569-570*, 982–989. https://doi.org/10.1016/j.scitotenv.2016.06.053

Zhang, W., Gao, Y., Qin, Y., Wang, M., Wu, J., Li, G., & An, T. (2019). Photochemical degradation kinetics and mechanism of short-chain chlorinated paraffins in aqueous solution: A case of 1-chlorodecane. *Environmental Pollution (Barking, Essex: 1987)*, *247*, 362–370. https://doi.org/10.1016/j.envpol.2019.01.065

Zhang, Z., Lu, M., Zhang, Z., Xiao, M., & Zhang, M. (2012). Dechlorination of short chain chlorinated paraffins by nanoscale zero-valent iron. *Journal of Hazardous Materials*, *243*, 105–111. https://doi.org/10.1016/j.jhazmat.2012.10.004

Zhao, N., Cui, Y., Wang, P., Li, S., Jiang, W., Luo, N., Wang, Z., Chen, X., & Ding, L. (2019). Short-chain chlorinated paraffins in soil, sediment, and seawater in the intertidal zone of Shandong Peninsula, China: Distribution and composition. *Chemosphere*, *220*, 452–458. https://doi.org/10.1016/j.chemosphere.2018.12.063

Zhou, Q., Xu, C., Shen, C., Li, F., Liu, S., & Aamir, M. (2023). Congener profiles, air-soil exchange, and potential risks of short- and medium-chain chlorinated paraffins in demonstration zone of Yangtze River Delta. *Atmospheric Pollution Research*, *14*(1), 101639. https://doi.org/10.1016/j.apr.2022.101639

Zhou, T., Yang, Q., Weng, J., Gao, L., Liu, Y., Xu, M., Zhao, B., & Zheng, M. (2024a). Characterization and health risks of short- and medium-chain chlorinated paraffins in the gas and size-fractionated particulate phases in ambient air. *Chemosphere*, *358*, 142225. https://doi.org/10.1016/j.chemosphere.2024.142225

Zhou, W., Huang, K., Bu, D., Zhang, Q., Fu, J., Hu, B., Zhou, Y., Chen, W., Fu, Y., Zhang, A., Fu, J., & Jiang, G. (2024b). Remarkable contamination of short- and medium-chain chlorinated paraffins in free-range chicken eggs from rural Tibetan Plateau. *Environmental Science & Technology*, *58*(11), 5093–5102. https://doi.org/10.1021/acs.est.3c08815

Zhou, Y., Yuan, B., Nyberg, E., Yin, G., Bignert, A., Glynn, A., Odland, J. Ø., Qiu, Y., Sun, Y., Wu, Y., Xiao, Q., Yin, D., Zhu, Z., Zhao, J., & Bergman, Å. (2020). Chlorinated paraffins in human milk from urban sites in China, Sweden, and Norway. *Environmental Science & Technology*, *54*(7), 4356–4366. https://doi.org/10.1021/acs.est.9b06089

Zhu, X., Bai, H., Gao, Y., Chen, J., Yuan, H., Wang, L., Wang, W., Dong, X., & Li, X. (2017). Concentrations and inhalation risk assessment of short-chain polychlorinated paraffins in the urban air of Dalian, China. *Environmental Science and Pollution Research International*, *24*(26), 21203–21212. https://doi.org/10.1007/s11356-017-9775-x

Zhuo, M., Ma, S., Li, G., Yu, Y., & An, T. (2019). Chlorinated paraffins in the indoor and outdoor atmospheric particles from the Pearl River Delta: Characteristics, sources, and human exposure risks. *The Science of the Total Environment*, *650*(Pt 1), 1041–1049. https://doi.org/10.1016/j.scitotenv.2018.09.107

Supporting information

Occurrence and remediation of chlorinated paraffins in global environmental matrices: Levels, trends, and future prospects

Yongyi Ma[a,b], Qianqian Li[a,b,*], Guijin Su[a,b,*], Huangnan Duan[c], Tieyu Wang[d], Jong Seong Khim[e], Seongjin Hong[f], Bohua Sun[a,b],Jing Meng[a,b], Bin Shi[a,b]

[a]Key Laboratory of Environmental Nanotechnology and Health Effects, State Key Laboratory of Environmental Chemistry and Ecotoxicology, Research Center for Eco-Environmental Sciences, Chinese Academy of Sciences, Beijing 100085, China;

[b]University of Chinese Academy of Sciences, Beijing 100049, China;

[c]Zhangjiakou Municipal Ecological Environment Bureau, Hebei Province, Zhangjiakou 075000, China

[d]Institute of Marine Sciences, Shantou University, Shantou 515063, China

[e]School of Earth and Environmental Sciences, Research Institute of Oceanography, Seoul National University, Seoul 08826, Republic of Korea

[f]Department of Marine Environmental Sciences, Chungnam National University, Daejeon 34134, Republic of Korea

*Corresponding author: Dr. Qianqian Li; Tel: +86 10 62844310; Fax: + 86 10 62923563; E-mail address: qqli@rcees.ac.cn

Dr. Guijin Su; Tel: +86 10 62847550; Fax: + 86 10 62923563; E-mail address: gjsu@rcees.ac.cn

Text S1 Meta-analysis and random forest

We sincerely thank you for this suggestion. We performed a meta-analysis and random forest model to uncover underlying patterns in the existing data.

For the meta-analysis, rigorous data screening was needed. The exiting concentration data of CPs in this study were retrieved from the Web of Science database for the period 2000 to June 2024 using the search query *TS = chlorinated paraffins or* polychlorinated alkanes. Literature screening focused on studies reporting the occurrence of CPs in the atmosphere, water, sediment, and soil. Studies were included if they met the following criteria: (1) Complete environmental sampling information (e.g., sampling sites and methods); (2) Scientifically reliable sample pretreatment and detection methodologies; (3) Quantitative CPs concentration data in environmental matrices, reported in tables, figures, or text, including mean values and standard deviations. For studies presenting data only in graphical form, data were extracted using WebPlotDigitizer. Based on these criteria, the screened dataset formed the basis of Table S1-S13 and Figure S1-2. For meta-analysis, an additional inclusion principle was applied: each country or region had to be represented by at least two independent studies meeting the above conditions. Ultimately, 24 publications or reports were identified, comprising 41 valid data entries across Australia (2), Alert, Arctic (2), Zeppelin, Arctic (8), Antarctica (6), and China (6). Notably, after comprehensive review, only atmospheric data fulfilled the requirements for meta-analysis, as most other environmental matrices were represented by single-location studies, precluding robust comparative analysis.

Based on these extracted data, we calculated the weighted means and weighted standard errors as effect sizes for each region and pollutant. The regional information was classified into different zones such as the Arctic, Antarctic, and China. We then performed a multilevel Meta-analysis with "region/year" as a random effect to estimate the average effect of pollutant concentrations across different regions and years. Unlike fixed-effect models, random effect models account for differences between independent studies. The results were presented as forest plots (Figure S1-2) to illustrate pollutant concentration data and their confidence intervals across regions and years.

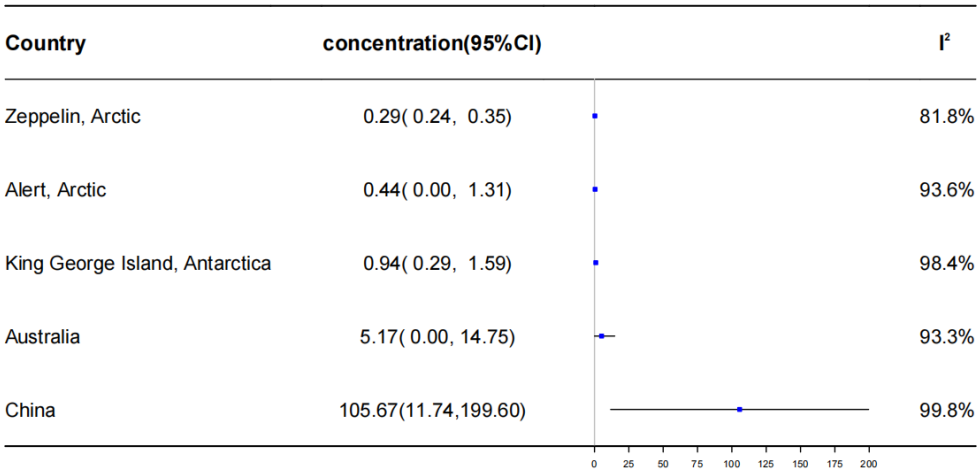

Figure S1. Forest plot of SCCPs concentrations in the atmosphere (ng/m^3)

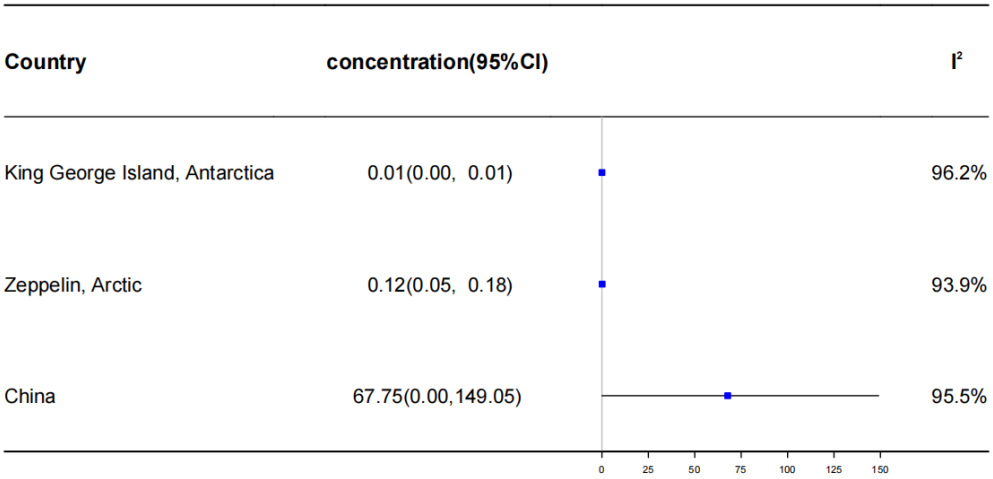

Figure S2 Forest plot of MCCPs concentrations in the atmosphere (ng/m^3)

As shown in Figure S1-2, the overall I^2 values for both SCCPs and MCCPs are relatively high, indicating substantial heterogeneity. This might be attributed to two key factors: (1) the limited number of available datasets, and (2) considerable variability in both the reported concentrations and their standard deviations. Although the present results do not allow for mapping CPs and offer a concentration scale from world while, they nonetheless provide valuable information on regional differences. In particular, CPs concentrations in China are generally higher than those in other regions, consistent with China's current status as the world's largest producer and consumer of CPs. By contrast, atmosphere CPs levels in the Arctic and Antarctic remain relatively low, reflecting the scarcity of pollution sources and sparse human activity in these regions. These observations align well with the conclusions drawn in the main text.

Random forest is a machine learning model based on decision trees. Theoretically, it can predict CPs

concentrations in environmental matrices by integrating multiple driving factors and corresponding contributions. As indicated by the meta-analysis, atmospheric data are the most abundant. Therefore, we used atmospheric CPs as the primary case study for random forest modeling. We first attempted to systematically compile natural factors that may affect CPs concentrations in the atmosphere. However, only a few studies reported parameters such as wind speed, temperature, humidity, or total suspended particulate (TSP) concentrations, which constrained their use in modeling. Based on our analysis, industrial point sources and densely populated urban areas are the dominant contributors to atmospheric CPs emissions, while social policies and socioeconomic conditions also shape CPs use and pollution levels. Accordingly, we incorporated socioeconomic indicators from the World Bank, including GDP per capita ($), urbanization rate, industrial added value (as a percentage of GDP), population (people), and population density (person/km^2), as input variables for the random forest model to construct a quantitative relationship between pollutant concentrations and these factors. Given the limited dataset, we partitioned the data at a 1:1 ratio, with 50% used for model training and optimization and the remaining 50% for validation. The results revealed an R^2 of -0.1475, which falls outside the expected range (0-1), mean absolute error (MAE) of 37.7462, and RSME=57.83 (Figure S3). While the negative R^2 indicates that no reliable relationship could be established between atmospheric CPs concentrations and the selected socioeconomic predictors, lower MAE might suggest higher the model prediction accuracy, and lower RMSE suggest smaller the deviation between the predicted results and the actual values. RMSE > MAE indicates that some data exhibit large errors. This limitation stems primarily from the small dataset used for model construction and validation, which is insufficient to produce robust conclusions.

Despite these constraints, we further employed SHAP (Shapley Additive Explanations) analysis to explore the relative importance of predictors (Figure S4). Each point represents a sample's SHAP value; the x-axis reflects the direction and magnitude of each feature's influence on model output, while the y-axis ranks feature by importance. The color gradient from blue to red denotes low to high feature values. The results highlighted population as the dominant factor, followed sequentially by urbanization rate, industrial output, population density, and GDP per capita. These findings were consistent with our main-text conclusion that CPs concentrations are generally higher in urban than in rural environments.

Although the current data is insufficient to support robust modeling of the global distribution, prediction, and driving factors of CPs, future improvements are anticipated. With rising public awareness and the accumulation of monitoring data across diverse environmental matrices, the integration of such models with relevant data will enable a more rigorous and comprehensive evaluation of global distribution patterns, temporal dynamics, and key drivers together with their relative contributions.

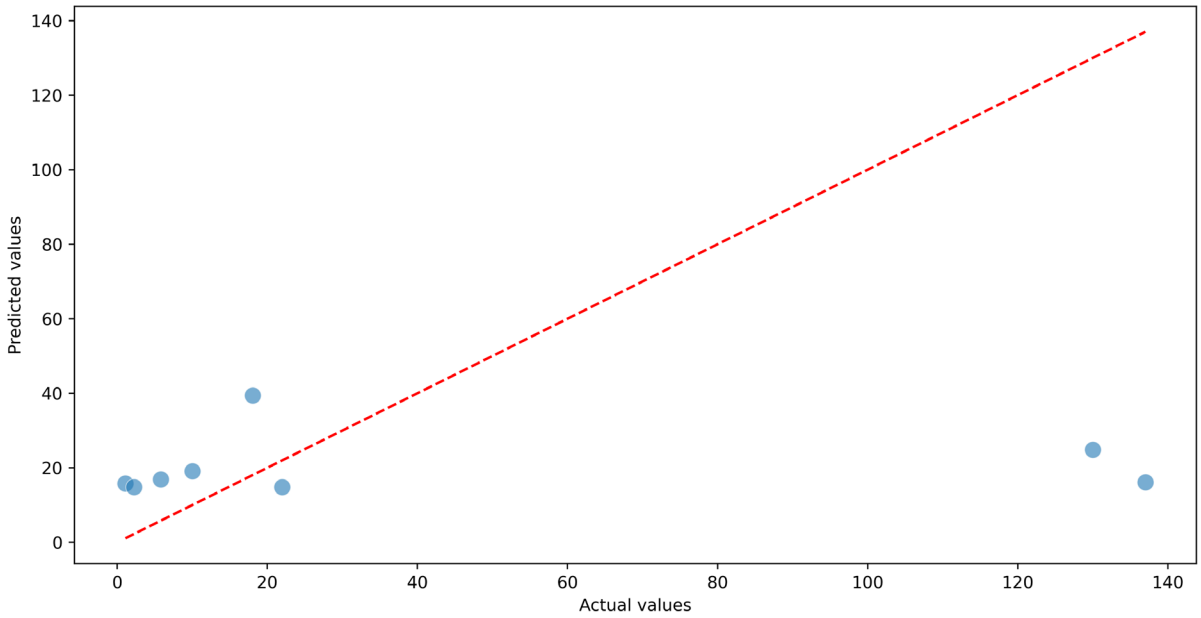

Figure S3. Random Forest Precipitation. Note：R^2=-0.1475, MAE=37.7462, RMSE=57.83

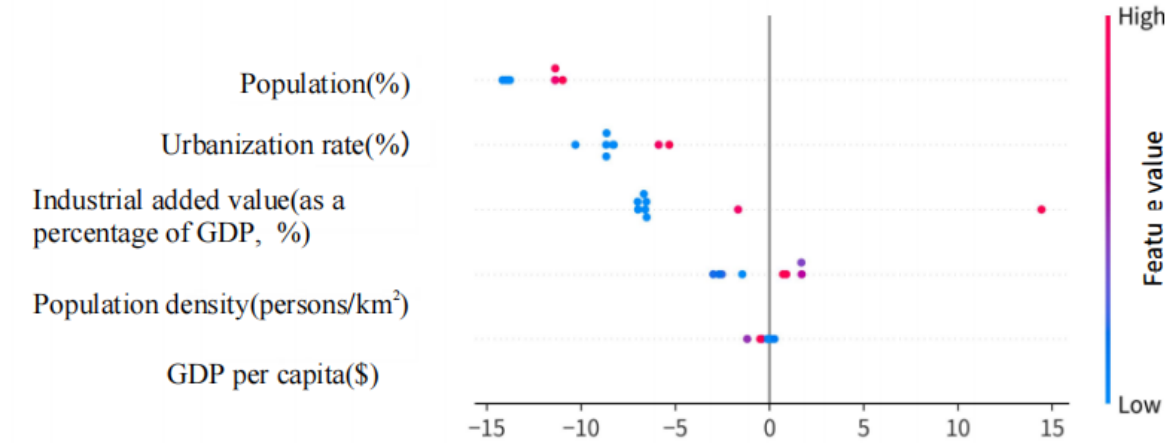

Figure S4. Contribution of different driving factors to CPs concentration

Text 2Data filtering methods

Indeed, the development of environmental regulations, industrial practices, and monitoring methodologies over the past decade can result in temporal discrepancies in comparisons. Therefore, for more valid comparisons, we must restrict the analysis within a narrower timeframe. However, a careful examination of the datasets collected in our study revealed a pronounced temporal misalignment between developed and developing countries in terms of CPs monitoring. This discrepancy is closely linked to socioeconomic factors. Historically, the United States, Western Europe, and other developed nations dominated CPs production and consumption, which explains why most of the earlier environmental monitoring data originated from these regions (Zitko, 1980). These countries were also the first to recognize the risks associated with SCCPs and subsequently introduced regulatory measures, resulting in a scarcity of recent monitoring data. By contrast, since the early 21century, CPs production has expanded rapidly in developing countries, with China emerging as the largest global producer and consumer. This has led to a surge in CPs monitoring data from these regions. Consequently, monitoring data from developing countries are predominantly concentrated in recent years. This poses a paradox: defining overly narrow time windows may inadvertently exclude most datasets from developed countries, thereby undermining the global comparability of certain environmental matrices.

To address this, we customized time frames for different environmental matrices by considering national distribution, monitoring years, and data volume, aiming to achieve a more scientific, rational, and effective analysis. For the atmosphere, where abundant monitoring data are available, we retained a broader temporal span to capture historical trends of CPs pollution and indirectly reflect the effectiveness of Stockholm Convention implementation. For other matrices, we adopted a selective retention strategy that incorporates both historical data from developed countries and recent data from developing countries. Specifically, for suspended particulate matter, data prior to 2000 were excluded, and the residual records were restricted to within ±2 years; for dust, CPs data were limited to within ±5 years; and for water, sediment, and soil, to within ±6 years.

Table S1 S/M/LCCPs in ambient atmosphere

Year	Location	Abbreviations	S/M/LCCPs	Average (ng/m^3)	Range (ng/m^3)	Dominant chain length	Dominant chlorinated homologues	Reference
2003	United Kingdom	UK	SCCPs	1.10	< 0.185-3.43	——	——	(Barber et al., 2005)
2003	United Kingdom	UK	MCCPs	3.04	< 0.81-14	——	——	
2006	India	IN	SCCPs	10.02	n.d.-47.4	C10	Cl7, Cl8	(Chaemfa et al., 2014)
2006	India	IN	MCCPs	3.62	n.d.-38.2	——	——	
2008	Japan	JP	SCCPs	2.26	0.28-14.2	C11	Cl5, Cl6	(Li et al., 2012)
2008	South Korea	KR	SCCPs	2.06	0.6-8.96	C11	Cl6, Cl7	
2011	Punjab, Pakistan	PK	SCCPs	5.13	0.37-14.2	C10	Cl7, Cl8	(Chaemfa et al., 2014)
2011	Punjab, Pakistan	PK	MCCPs	4.21	0.29-9.45	——	——	
2011	Zurich, Switzerland	CH	SCCPs	5.80	1.8-17	C10, C11	Cl6, Cl7	(Diefenbacher et al., 2015)
2013	Zurich, Switzerland	CH	SCCPs	6.40	1.1-42	C10, C11	Cl7, Cl8	
2013-2014	Australia (ambient)	AU (ambient)	SCCPs	10.40	1.8-28.4	——	——	(Gillett et al., 2017)
2013-2014	Australia (residential)	AU (residential)	SCCPs	49.30	28.2-82.0	——	——	
2016	Australia (urban)	AU (urban)	SCCPs	0.68	0.38-1.1	C10, C11	Cl5, Cl6	(van Mourik et al., 2020)
2016	Australia (urban)	AU (urban)	MCCPs	1.03	0.47-1.8	C14	Cl5, Cl7	
2016	Australia (rural)	AU (rural)	SCCPs	0.51	0.24-1.3	C10, C11	Cl5, Cl6	
2016	Australia (rural)	AU (rural)	MCCPs	0.64	< MDL-1.7	C14	Cl5, Cl7	
2017-2018	Greater Toronto Area, Canada (industrial)	CA (industrial)	SCCPs	35.30	13.5-78.5	C12, C13	Cl5-7	(Niu et al., 2021)
2017-2018	Greater Toronto Area, Canada (urban)	CA (urban)	SCCPs	25.60	2.96-66.2	C12, C13	Cl7	
2017-2018	Greater Toronto Area, Canada (remote)	CA (remote)	SCCPs	10.50	3.82-15.9	C10, C11 (Spr. Sum) C12, C13 (Fal. Win)	Cl6, Cl7	

2017-2018	Greater Toronto Are, Canada (residential)	CA (residential)	SCCPs	7.73	< MDL-17.6	C10, C11 (Spr. Sum) C12, C13 (Fal. Win)	Cl7, Cl8	
2019	Dar es Salaam, Tanzania (whole)	TZ (whole)	SCCPs	22.00	0.3–63	——	——	
2019	Dar es Salaam, Tanzania (whole)	TZ (whole)	MCCPs	9.00	< 0.4–35	——	——	
2019	Dar es Salaam, Tanzania（urban）	TZ (urban)	SCCPs	33.38	11-59	——	——	
2019	Dar es Salaam, Tanzania (urban)	TZ (urban)	MCCPs	16.88	3-35	——	——	
2019	Dar es Salaam, Tanzania (urban)	TZ (rural)	SCCPs	6.55	0.3-18	——	——	(Nipen et al., 2022)
2019	Dar es Salaam, Tanzania(rural)	TZ (rural)	MCCPs	2.45	< 0.4-5	——	——	
2019	Dar es Salaam, Tanzania (waste-source transect)	TZ (waste-source transect)	SCCPs	23.44	4-59	——	——	
2019	Dar es Salaam, Tanzania (waste-source transect)	TZ (waste-source transect)	MCCPs	15.89	1-33	——	——	
2008	China	CN	SCCPs	137.00	13.5-517	C10, C11	Cl5, Cl6	(Li et al., 2012)
2010	Pearl River Delta, China	CPRD	SCCPs	17.69	0.95-106	C10	Cl6, Cl7	(Wang et al., 2013b)
2011-2012	Yangtze River Delta, China	CYRD	SCCPs	59.10	6.08-63.2	C10	Cl6-8	
2011-2012	Yangtze River Delta, China (urban)	CYRD (urban)	SCCPs	23.60	——	C10	Cl6-8	(Niu et al., 2020)
2011-2012	Yangtze River Delta, China (rural)	CYRD (rural)	SCCPs	21.10	——	C10	Cl6-8	

2014	Shenzhen and Guangzhou, China	CSG	SCCPs	5.06	1.11-39.8	C13	Cl6-9	
2014	Shenzhen and Guangzhou, China	CSG	MCCPs	3.53	0.7-12.2	C14	Cl6-9	(Li et al., 2018b)
2014	Shenzhen and Guangzhou, China	CSG	LCCPs	2.32	0.25–8.38	C23-25	Cl7-10	
2010	Dalian, China	CDL	SCCPs	30.26	15.12-66.44	C10, C11	Cl7	(Zhu et al., 2017)
2016	Dalian, China	CDL	SCCPs	78.15	65.3-91	——	——	
2016-2017	Dalian, China	CDL	SCCPs	21.27	4.98-78	——	——	(Wang et al., 2019b)
2016	Henan, China	CHN	SCCPs	140.00	260-770	C10	Cl6, Cl7	(Li et al., 2023a)
2016	Henan, China	CHN	MCCPs	62.00	210-430	C14	Cl7, Cl8	
2016	Zibo, China (CP production plant)	CZB	SCCPs	498.35	102-1441.8	C10	Cl6, Cl7	(Wang et al., 2018a)
2021	Shanghai, China (shipyards and waste incinerators)	CSH	SCCPs	108.00	57–208	C10	Cl6	(Ai et al., 2022)
2021	Shanghai, China (shipyards and waste incinerators)	CSH	MCCPs	9.86	1.8–25	C14	Cl7, Cl8	
2021	China (CP production plant)	CPP	SCCPs	140.80	63.5-299.1	——	——	(Yu et al., 2023)
2021	China (CP production plant)	CPP	MCCPs	400.20	151.6-1136.4	C14	Cl7, Cl8	
2022-2023	Beijing, China	CBJ	SCCPs	348.00	57-881	C10	Cl6, Cl7	(Zhou et al., 2024a)
2022-2024	Beijing, China	CBJ	MCCPs	148.00	30-385	C14	Cl7, Cl8	

Table S2 S/MCCPs in indoor atmosphere

Year	Location	Abbreviations	S/M/CCPs	Average (ng/m^3)	Range (ng/m^3)	Dominant chain length	Dominant chlorinated homologues	Reference
2006-2007	Stockholm, Sweden	SE	CPsa	69.00	5-210	——	——	(Fridén et al., 2011)
2012	Oslo and Akershus, Norway	NO	SCCPs	8.90	1.7-54	——	——	(Sakhi et al., 2019)
2012	Oslo and Akershus, Norway	NO	MCCPs	1.40	< 0.35-13	——	——	
2014	Beijing, China	CBJ	SCCPs	181.00	9.77-966	C10	Cl6, Cl7	(Gao et al., 2018)
2014	Beijing, China	CBJ	MCCPs	41.90	< LOD-613	C14	Cl5, Cl6	
2013-2014	Beijing, China	CBJ	SCCPs	358.31	60-1350	C10	Cl6, Cl7	(Gao et al., 2016)
2021	China (CP production plant)	CPP	SCCPs	304.50	119.1-732.3	——	——	(Yu et al., 2023)
2021	China (CP production plant)	CPP	MCCPs	578.00	249.4-998.8	——	——	

Table S3 S/MCCPs in remote regions ambient atmosphere

Year	Location	Abbreviations	S/MCCPs	Average (ng/mv)	Range (ng/m^3)	Reference
1992	Alert, Arctic	Arctic	SCCPs	0.020	< 0.002-0.067	(J. Peters et al., 2000)
2011	Alert, Arctic	Arctic	SCCPs	0.913	0.206-2.876	(AINA, 2015)
2013	Zeppelin, Arctic	Arctic	SCCPs	0.361	——	(Bohlin-Nizzetto et al., 2014)
2013	Zeppelin, Arctic	Arctic	MCCPs	0.023	——	
2014	Zeppelin, Arctic	Arctic	SCCPs	0.245	——	(Bohlin-Nizzetto et al., 2015)
2014	Zeppelin, Arctic	Arctic	MCCPs	0.031	——	
2015	Zeppelin, Arctic	Arctic	SCCPs	0.420	——	(Bohlin-Nizzetto and Aas, 2016)
2015	Zeppelin, Arctic	Arctic	MCCPs	0.130	——	
2016	Zeppelin, Arctic	Arctic	SCCPs	0.210	——	(Bohlin-Nizzetto et al., 2017)
2016	Zeppelin, Arctic	Arctic	MCCPs	0.070	——	
2017	Zeppelin, Arctic	Arctic	SCCPs	0.350	——	(Bohlin-Nizzetto et al., 2018)
2017	Zeppelin, Arctic	Arctic	MCCPs	0.130	——	
2018	Zeppelin, Arctic	Arctic	SCCPs	0.290	——	(Bohlin-Nizzetto et al., 2019)
2018	Zeppelin, Arctic	Arctic	MCCPs	0.120	——	
2019	Zeppelin, Arctic	Arctic	SCCPs	0.230	——	(Bohlin-Nizzetto et al., 2020)
2019	Zeppelin, Arctic	Arctic	MCCPs	0.170	——	
2020	Zeppelin, Arctic	Arctic	SCCPs	0.510	<0.120-6.600	(Bohlin-Nizzetto et al., 2021)
2020	Zeppelin, Arctic	Arctic	MCCPs	0.750	<0.320-5.200	
2021	Zeppelin, Arctic	Arctic	SCCPs	0.260	< 0.370-0.640	(Bohlin-Nizzetto et al., 2022)
2021	Zeppelin, Arctic	Arctic	MCCPs	0.655	< 1.252-1.336	
2022	Zeppelin, Arctic	Arctic	SCCPs	0.138	0.039-0.363	(Halvorsen et al., 2023)

2022	Zeppelin, Arctic	Arctic	MCCPs	<0.172	<0.172-0.686	(Halvorsen et al., 2024)
2023	Zeppelin, Arctic	Arctic	SCCPs	< 0.052	< 0.052-0.198	
2023	Zeppelin, Arctic	Arctic	MCCPs	0.114	< 0.062-1.780	
2013	King George Island, Antarctica	AQKGI	SCCPs	0.0149	0.010-0.021	(Ma et al., 2014a)
2013	King George Island, Antarctica	AQKGI	MCCPs	0.0045	0.0037-0.0052	
2014	King George Island, Antarctica	AQKGI	SCCPs	0.3080	——	(Jiang et al., 2021)
2014	King George Island, Antarctica	AQKGI	MCCPs	0.0025	——	
2015	King George Island, Antarctica	AQKGI	SCCPs	0.6000	——	
2015	King George Island, Antarctica	AQKGI	MCCPs	0.0055	——	
2016	King George Island, Antarctica	AQKGI	SCCPs	1.3000	——	
2016	King George Island, Antarctica	AQKGI	MCCPs	0.0065	——	
2017	King George Island, Antarctica	AQKGI	SCCPs	2.2900	——	
2017	King George Island, Antarctica	AQKGI	MCCPs	0.0154	——	
2018	King George Island, Antarctica	AQKGI	SCCPs	1.3900	——	
2018	King George Island, Antarctica	AQKGI	MCCPs	0.0102	——	
2012	Lhasa, China	Lhasa	SCCPs	2.48	1.104-5.998	(Wu et al., 2017)
2013	Lhasa, China	Lhasa	SCCPs	7.33	1.805-10.260	
2014	Lhasa, China	Lhasa	SCCPs	7.02	3.270-14.444	
2015	Lhasa, China	Lhasa	SCCPs	5.31	1.371-12.096	
2012	Shergyla Mountain, China	Shergyla Mountain	SCCPs	0.23	0.132-0.365	
2013	Shergyla Mountain, China	Shergyla Mountain	SCCPs	0.35	0.168-0.769	

2014	Shergyla Mountain, China	Shergyla Mountain	SCCPs	0.70	0.314-1．267	
2015	Shergyla Mountain, China	Shergyla Mountain	SCCPs	0.55	0.345-0.667	
2012	Lhasa, China	Lhasa	MCCPs	2.57	1.563-4.2066	
2013	Lhasa, China	Lhasa	MCCPs	3.86	0.8452-5.3945	
2014	Lhasa, China	Lhasa	MCCPs	4.73	2.6285-6.6603	
2015	Lhasa, China	Lhasa	MCCPs	4.03	2.3434-5.7504	(Wu et al., 2019)
2012	Shergyla Mountain, China	Shergyla Mountain	MCCPs	0.13	0.0526-0.2891	
2013	Shergyla Mountain, China	Shergyla Mountain	MCCPs	0.34	0.1274-0.5955	
2014	Shergyla Mountain, China	Shergyla Mountain	MCCPs	0.43	0.182-0.6652	
2015	Shergyla Mountain, China	Shergyla Mountain	MCCPs	0.42	0.208-0.6875	

Table S4 S/MCCPs in suspended particles

Year	Location	Abbreviations	S/MCCPs	Average (ng/m^3)	Range (ng/m^3)	Dominant chain length	Dominant chlorinated homologues	Reference
2014	King George Island, Antarctica	AYKGI	SCCPs	0.11	0.00348-533	C10, C11	Cl6, Cl7	(Jiang et al., 2021)
2014	King George Island, Antarctica	AYKGI	MCCPs	1.60	< 0.26-6.28	C14	Cl7, Cl8	
2013-2014	China (PM2.5)	CN-2.5	SCCPs	19.90	1.98–274	C11	Cl7, Cl8	(Liu et al., 2020)
2013-2014	China (PM2.5)	CN-2.5	MCCPs	15.60	1.27–312	C14	Cl6, Cl7	
2010	Dalian, China (outdoor)	CDL	SCCPs	3.38	0.52-10.47	C11, C13	Cl7, Cl8	(Zhu et al., 2017)
2016	Dalian, China (outdoor)	CDL	SCCPs	1.84	1.72-01.95	——	——	
2016	Beijing, China (indoor PM10)	CBJ-10	SCCPs	61.10	38.3-87.7	C10, C11	Cl7, Cl8	
2016	Beijing, China (indoor PM10)	CBJ-10	MCCPs	6.90	3.2-9.6	C14	Cl7, Cl8	
2016	Beijing, China (indoor PM2.5)	CBJ-2.5	SCCPs	31.40	16.8-49.4	C10, C11	Cl7, Cl8	
2016	Beijing, China (indoor PM2.5)	CBJ-2.5	MCCPs	4.80	1.6-7.5	C14	Cl7, Cl8	
2016	Beijing, China (indoor PM1.0)	CBJ-1.0	SCCPs	20.70	6.4-32.5	C10, C11	Cl7, Cl8	(Huang et al., 2017)
2016	Beijing, China (indoor PM1.0)	CBJ-1.0	MCCPs	3.40	1.0-6.4	C14	Cl7, Cl8	
2016	Beijing, China (outdoor PM10)	CBJ-10	SCCPs	23.90	16.9-28.8	C10, C11	Cl7, Cl8	
2016	Beijing, China (outdoor PM10)	CBJ-10	MCCPs	3.60	3.2-9.6	C14	Cl7, Cl8	
2016	Beijing, China (outdoor PM2.5)	CBJ-2.5	SCCPs	14.90	9.2-19.6	C10, C11	Cl7, Cl8	

2016	Beijing, China (outdoor PM2.5)	CBJ-2.5	MCCPs	1.70	0.6–2.7	C14	Cl7, Cl8	
2016	Beijing, China (outdoor PM1.0)	CBJ-1.0	SCCPs	10.40	4.1-15.4	C10, C11	Cl7, Cl8	
2016	Beijing, China (outdoor PM1.0)	CBJ-1.0	MCCPs	1.00	0.3–1.3	C14	Cl7, Cl8	
2016	Jinan, China	CJN-2.5	SCCPs	38.75	9.8-105	C11	Cl7	(Li et al., 2019)
2017	Pearl River Delta, China (indoor)	CPRD	SCCPs	16.45	3.3-43.2	C11	Cl6, Cl7	
2017	Pearl River Delta, China (indoor)	CPRD	MCCPs	41.63	7.3-110	C14	Cl7, Cl8	
2017	Pearl River Delta, China (indoor PM10)	CPRD-10	SCCPs	16.48	5.2-51.8	C11	Cl6, Cl7	
2017	Pearl River Delta, China (indoor PM10)	CPRD-10	MCCPs	36.50	14.2-116	C14	Cl7, Cl8	
2017	Pearl River Delta, China (indoor PM2.5)	CPRD-2.5	SCCPs	15.58	2.9-45.5	C11	Cl6, Cl7	(Zhuo et al., 2019)
2017	Pearl River Delta, China (indoor PM2.5)	CPRD-2.5	MCCPs	40.53	5.4-182	C14	Cl7, Cl8	
2017	Pearl River Delta, China (outdoor)	CPRD	SCCPs	8.45	1.8-32.5	C11	Cl6, Cl7	
2017	Pearl River Delta, China (outdoor)	CPRD	MCCPs	22.97	4.8-132	C14	Cl7, Cl8	
2017	Pearl River Delta, China (outdoor PM10)	CPRD-10	SCCPs	8.45	1.8-32.8	C11	Cl6, Cl7	

2017	Pearl River Delta, China (outdoor PM10)	CPRD-10	MCCPs	19.27	4.9-62.9	C14	Cl7, Cl8	
2017	Pearl River Delta, China (outdoor PM2.5)	CPRD-2.5	SCCPs	7.80	1.6-27.1	C11	Cl6, Cl7	
2017	Pearl River Delta, China (outdoor PM2.5)	CPRD-2.5	MCCPs	23.15	4.5-180	C14	Cl7, Cl8	
2017-2018	Xinxiang, China	CXX	SCCPs	60.40	3.55-359	——	——	(Li et al., 2021b)
2017-2018	Xinxiang, China	CXX	MCCPs	14.20	1.95-59.8	——	——	

Table S5 S/M/LCCPs in dusts

Year	Location	Abbrevia-tions	S/M/LCCPs	Average (μg/g dw)	Range (μg/g dw)	Dominant chain length	Dominant chlorinated homologues	Reference
——	Munich, Germany	GMM	SCCPs	10.30	4.0-27.0	C12	Cl7	(Hilger et al., 2013)
——	Munich, Germany	GMM	MCCPs	229.30	8-892	C14	Cl6	
2008-2009	United Kingdom	UK	SCCPs	92.69	——	C13	Cl5-7	
2008-2009	United Kingdom	UK	MCCPs	463.45	——	C14	Cl5-7	(Wong et al., 2017)
2008-2009	United Kingdom	UK	LCCPs	156.86	——	C18	Cl7, Cl8	
2013-2014	Oslo, Norway	NO	SCCPs	5.8 (median)	0.76-460	——	——	
2013-2014	Oslo, Norway	NO	MCCPs	21 (median)	2.3-840	——	——	(Yuan et al., 2021)
2013-2014	Oslo, Norway	NO	LCCPs	8.1 (median)	0.66–340	——	——	
2014	Australia	AU14	SCCPs	61.20	——	C13	Cl5-7	
2014	Australia	AU14	MCCPs	180.00	——	C14	Cl5-8	(Wong et al., 2017)
2014	Australia	AU14	LCCPs	98.60	——	C18	Cl8	
2012	China	CN	SCCPs	518.66	106.2-807.5	C13	Cl5-7	
2012	China	CN	MCCPs	1265.74	330.4-1974.5	C14	Cl5-7	
2012	China	CN	LCCPs	1259.60	153.4-1995	C18	Cl7-9	
2014	Canada	CA	SCCPs	49.33	21.9-65.11	C13	Cl5-7	
2014	Canada	CA	MCCPs	175.54	140-191.5	C14	Cl5-7	(Wong et al., 2017)
2014	Canada	CA	LCCPs	130.13	92.4-160.6	C18	Cl6-8	
2014	Sweden	SW	SCCPs	6.72	4.73-8.77	C13	Cl5, Cl6	
2014	Sweden	SW	MCCPs	108.54	66.5-157.86	C17	Cl5, Cl6	
2014	Sweden	SW	LCCPs	846.96	567-1263.5	C18	Cl7, Cl8	
2015	Brisbane, Sydney and Canberra, Australia	AU15	SCCPs	9.4 (median)	0.29-58	——	——	(He et al., 2019)
2015	Brisbane, Sydney and Canberra, Australia	AU15	MCCPs	95 (median)	5.1-530	——	——	

2015	Brisbane, Sydney and Canberra, Australia	AU15	LCCPs	——	< 0.0014-27	——	——	
2016	Australia	AU16	SCCPs	46.92	9.2-210	C13	Cl6-8	
2016	Australia	AU16	MCCPs	93.00	7-250	C14	Cl6-9	
2016	Australia	AU16	LCCPs	15.41	< 1-65	C18-20	Cl7	
2016	Colombia	CO	SCCPs	45.30	17-110	C13	Cl6-8	
2016	Colombia	CO	MCCPs	75.00	16-200	C14	Cl6-8	
2016	Colombia	CO	LCCPs	17.37	2.6-60	C18-20	Cl9	(McGrath et al., 2023)
2017	Japan	JP	SCCPs	28.87	7.3-100	C13	Cl6-8	
2017	Japan	JP	MCCPs	36.09	6.9-95	C14	Cl6-8	
2017	Japan	JP	LCCPs	4.33	< 9.5	C18-20	Cl8	
2019	Thailand	TH	SCCPs	62.44	4-290	C13	Cl6-8	
2019	Thailand	TH	MCCPs	199.00	17-540	C14	Cl6-8	
2019	Thailand	TH	LCCPs	65.36	1.3-230	C18-20	Cl8	
2013	Taizhou, China	CTZ	SCCPs	38.00	7.8-240	C13	Cl7-9	
2013	Taizhou, China	CTZ	MCCPs	670.00	190-3500	C14	Cl7, Cl8	
2013	Guiyu, China	CGY	SCCPs	33.00	4.9-110	C13	Cl7-9	
2013	Guiyu, China	CGY	MCCPs	340.00	13-1900	C14	Cl7, Cl8	
2013	Dali, China	CDL	SCCPs	61.00	41-98	C13	Cl7-9	(Zeng et al., 2016)
2013	Dali, China	CDL	MCCPs	890.00	420-1700	C14	Cl7, Cl8	
2013	Qingyuan, China	CQY	SCCPs	30.00	1.8-75	C12	Cl8-10	
2013	Qingyuan, China	CQY	MCCPs	170.00	12-360	C14	Cl7, Cl8	
2013	Wuhan, China	CWH	SCCPs	64.30	4.23–304	C13	Cl6-8	
2013	Wuhan, China	CWH	MCCPs	115.00	6.70–495	C14	Cl6-8	(Wu et al., 2023)
2013	Wuhan, China	CWH	LCCPs	45.00	3.68–331	C18	Cl8-9	
2015	Beijing, China	CBJ15	SCCPs	5429.00	819-49118	C13	Cl7, Cl8	(Cao et al., 2019)
2015	Beijing, China	CBJ15	MCCPs	15157.00	2323-85739	C14	Cl7, Cl8	
——	Taibei, China	CTB	SCCPs	12.42	1.2-31.2	C12	——	(Chen et al., 2016)
2016	Beijing, China	CBJ16	SCCPs	148.00	5.35-1022	C11, C13	Cl7, Cl8	(Gao et al., 2018)

2016	Beijing, China	CBJ16	MCCPs	139.00	2.10-725	C14	Cl8	
2016-2017	Qingyuan, China (e-waste dismantling area)	CQYerw	SCCPs	5600.00	246-19900	——	——	
2016-2017	Qingyuan, China (e-waste dismantling area)	CQYerw	MCCPs	17800.00	874-48000	——	——	
2016-2017	Qingyuan, China (local residential homes)	CQYlrh	SCCPs	580.00	34.5–2030	——	——	(Chen et al., 2018)
2016-2017	Qingyuan, China (local residential homes)	CQYlrh	MCCPs	1760.00	79.2–6510	——	——	
2016-2017	Qingyuan, China (control homes)	CQYch	SCCPs	59.00	27.8–173	——	——	
2016-2017	Qingyuan, China (control homes)	CQYch	MCCPs	185.00	74.0–539	——	——	
2018	Pretoria, South Africa	ZA	SCCPs	62.00	5.4-353	C13	Cl6, Cl7	
2018	Pretoria, South Africa	ZA	MCCPs	142.00	21-498	C14	Cl6, Cl7	(Brits et al., 2020)
2018	Pretoria, South Africa	ZA	LCCPs	24.00	1.9-108	C18	Cl7, Cl8	
2021	Beijing, China	CBJ21	SCCPs	2.84	0.112-207	C13	Cl7, Cl8	(Lu et al., 2023)
2021	Beijing, China	CBJ21	MCCPs	194.00	0.135–2903	C14	Cl7, Cl8	

Table S6 S/MCCPs in water

Year	Location	Abbreviations	S/MCCPs	Average (ng/L)	Range (ng/L)	Dominant chain length	Dominant chlorinated homologues	Reference
2002	Tokyo, Japan	JP	SCCPs	17.03	7.6-31	C11	Cl6, Cl7	(Iino et al., 2005)
2002	Tokyo, Japan (influent)	JPin	SCCPs	280.00	220-360	C11-13	Cl7	
2002	Tokyo, Japan (effluent)	JPef	SCCPs	25.67	16-35	C11	Cl6, Cl7	
2003	Llobregat river and Riera del Tenes river, Spain	ES	SCCPs	603.00	300-1100	——	——	(Castells et al., 2004)
2010	Gaobeidian sewage treatment plant, China (influent)	CGBDin	SCCPs	4450.00	4200-4700	C11, C12	Cl7, Cl8	(Zeng et al., 2011b)
2010	Gaobeidian sewage treatment plant, China (effluent)	CGBDef10	SCCPs	390.00	364-416	C11, C12	Cl6-8	
2010	Gaobeidian Lake, China	CGBDl	SCCPs	169.00	162-176	C11, C12	Cl7, Cl8	
2014	Xiaoqing River, China	CXQR	SCCPs	43.00	nd-470	C10, C11	Cl6, Cl7	(Pan et al., 2021)
2014	Xiaoqing River, China	CXQR	MCCPs	28.00	nd-120	C14	Cl7, Cl8	
2016	Rivers in Beijing, China	CBJr	SCCPs	457.00	77-652	C11	Cl6, Cl7	(Wang et al., 2018a)
2016	Lake in Beijing, China	CBJl	SCCPs	124.00	< LOD-377	C11, C12	Cl6, Cl7	
2016	Huangpu River, China	CHPR	SCCPs	448.00	15-1640	C13	Cl7, Cl8	(Wang et al., 2019)
2016	Huangpu River, China	CHPR	MCCPs	1290.00	40.3–3870	C14	Cl5-7	

2016	Gaobeidian sewage treatment plant, China (effluent)	CGBDef16	SCCPs	682.00	——	C11, C12	Cl6, Cl7	(Wang et al., 2018b)
2017	Bohai Sea, China	CBS17	SCCPs	1256.00	572.6–1978	C10, C11	Cl6-8	(Zhao et al., 2019)
2017	Yellow Sea, China	CYS	SCCPs	449.30	370.0-548.3	C10, C11	Cl6-8	(Zhao et al., 2019)
2018	Pearl River Delta, China	CPRDun	SCCPs	9100.00	n.d.-70300	C13	Cl6, Cl7	(Wu et al., 2021)
2019	East China Sea, China	CECS	SCCPs	144.00	12.2-430	C10, C11	Cl5-7	(Hu et al., 2022)
2020	River Ravi, Pakistan	PK	SCCPs	11.00	n.d.-17	C10, C13	Cl7, Cl8	(Tahir et al., 2024)
2020	River Ravi, Pakistan	PK	MCCPs	40.00	25-50	C16, C17	Cl7-9	
2022	Bohai Sea, China	CBS22	SCCPs	268.50	57.5-1150.4	C10, C11	Cl6, Cl7	(Cui et al., 2024)

Table S7 S/M/LCCPs in sewage sludge

Year	Location	Abbrevia -tions	S/M/LCCPs	Average (ng/g dw)	Range (ng/g dw)	Dominant chain length	Dominant chlorinated homologues	Reference
2002	United Kingdom	UK	SCCPs	42000.00	6900-200000	——	——	(Stevens et al., 2003)
2002	United Kingdom	UK	MCCPs	180000.00	30000-9700000	——	——	
2007	Zurich, Switzerland	CH	SCCPs	321.43	135-584	C13	Cl6-8	(Bogdal et al., 2015)
2007	Zurich, Switzerland	CH	MCCPs	3971.43	1070-8960	C14	Cl6-8	
2010-2011	China	CN	SCCPs	10700.00	800–52700	C11	Cl7, Cl8	(Zeng et al., 2012a)
2014	Australian	AU	SCCPs	587.88	< 57-1421	C13	Cl6, Cl7	(Brandsma et al., 2017)
2014	Australian	AU	MCCPs	1560.06	542-3645	C14	Cl6-8	
2014	Australian	AU	LCCPs	374.56	116–960	C18	Cl5-8	

Table S8 S/MCCPs in marine sediment

Year	Location	Abbreviations	S/MCCPs	Average (ng/g dw)	Range (ng/g dw)	Dominant chain length	Dominant chlorinated homologues	Reference
2003	Tokyo, Japan	JP	SCCPs	10.30	1.3-27.4	——	——	(Iino et al., 2005)
2003	Tokyo, Japan	JP	MCCPs	19.20	3.2-56.8	——	——	
2003-2004	North and Baltic Sea	N&BS	SCCPs	34.59	8-82	——	——	(Hüttig & Oehme, 2006)
2011	East China Sea, China	CECSf	SCCPs	25.90	5.8-64.8	C10, C11	Cl5-7	(Zeng et al., 2012b)
2012	Bohai Sea and Yellow Sea, China	CBS&YSf	SCCPs	38.40	14.5-85.2	C10, C11	Cl5-7	(Zeng et al., 2013)
——	Liaodong Bay, China	CLDB	SCCPs	299.00	65-541	C10, C11	Cl5-7	(Ma et al., 2014b)
2017	Bohai Sea and Yellow Sea, China	CBS&YSn	SCCPs	120.92	25.96-452.9	C10	Cl5-7	(Zhao et al., 2019)
2017	Yangtze River Estuary and East China Sea, China	CYRE&ECS	SCCPs	18.60	2.85-94.7	C13	Cl5-7	(Ji et al., 2022)
2017	Yangtze River Estuary and East China Sea, China	CYRE&ECS	MCCPs	18.50	3.33-77.8	C14	Cl6-8	
2019	East China Sea and Yellow Sea, China	CYS&ECS	SCCPs	2.55	0.703-13.4	C10, C11	Cl5-7	(Li et al., 2023b)
2019	East China Sea and Yellow Sea, China	CYS&ECS	MCCPs	0.50	0.0936-4.19	C14, C15	Cl5-7	
2019	East China Sea, China	CECSn	SCCPs	194.00	89.6-351	C10, C11	Cl5-7	(Hu et al., 2022)
2022	Bohai Sea, China	CBSf	SCCPs	568.00	167.7–1105.9	C10, C11	Cl6, Cl7	(Cui et al., 2024)

Table S9 S/M/LCCPs in sediment of rivers and lakes

Year	Location	Abbrevia-tions	S/M/LCCPs	Average (ng/g dw)	Range (ng/g dw)	Dominant chain length	Dominant chlorinated homologues	Reference
——	Norway (landfills)	NO	SCCPs	4823.33	330-19400	——	——	(Borgen et al., 2003)
——	Norway (landfills)	NO	MCCPs	7050.00	2700-11400	——	——	
——	Besòs River, Spain	ES	SCCPs	1210.00	270-3260	——	——	(Parera et al., 2004)
2001-2002	Zlín, Czech Republic	CZ	SCCPs	106.21	16.30–180.75	——	——	(Štejnarová et al., 2005)
2006	Vaal River, South Africa	ZAr	SCCPs	15.09	4.1-47	——	——	(Quinn et al., 2009)
2006	Vaal River, South Africa	ZAr	MCCPs	134.81	1.8-1200	——	——	
2009-2010	Rivers in Pearl River Delta, China	CPRDr	SCCPs	1200.00	——	C10, C11	Cl7, Cl8	(Chen et al., 2011)
2009-2010	Rivers in Pearl River Delta, China	CPRDr	MCCPs	3900.00	——	C14	Cl7, Cl8	
2010	Gaobeidian Lake, China	CGBDl	SCCPs	5768.57	1100-8700	C11	Cl7, Cl8	(Zeng et al., 2011b)
2010	Qingyuan, China (e-waste dismantling areas)	CQY	SCCPs	2800.00	——	C10	Cl8-10	(Chen et al., 2011)
2010	Qingyuan, China (e-waste dismantling areas)	CQY	MCCPs	21000.00	——	C14	Cl6, Cl7	
2010	Liaohe River Basin, China	CLHr	SCCPs	212.20	39.8-480.3	C10, C11	Cl5, Cl6	(Gao et al., 2012)
2011-2012	Arctic	Arctic	SCCPs	49.90	23.28-94.65	C10	Cl6, Cl7	(Li et al., 2017)

2011	Reservoirs and Rivers in Dongguan, China	CDGr	SCCPs	219.00	6.01-613	C13	Cl6, Cl7	(Wu et al., 2020a)
2011	Reservoirs and Rivers in Dongguan, China	CDGr	MCCPs	694.00	14-1581	C14	Cl7, Cl8	
2014	Xiaoqing River, China	CXQr	SCCPs	1300.00	48-16000	C10, C11	Cl6-8	(Pan et al., 2021)
2014	Xiaoqing River, China	CXQr	MCCPs	6020.00	130-27000	C14	Cl7, Cl8	
2014	Henan section of the Yellow River, China	CYRhn	SCCPs	262.00	11.8-2792	C10, C11	Cl6, Cl7	(Li et al., 2018a)
2014	Henan section of the Yellow River, China	CYRhn	MCCPs	97.10	1.56-1558	C14	Cl6, Cl7	
2016	Rivers in Shanghai, China	CSHr	SCCPs	308.00	nd-2020	C13	Cl6-8	(Wang et al., 2019)
2016	Rivers in Shanghai, China	CSHr	MCCPs	2520.00	10.1-10800	C14	Cl6-8	
2017	Jiaojiang River, China	CJJr	SCCPs	3643.36	32.5-1.29 × 104	C13	Cl7, Cl8	(Xu et al., 2019)
2017	Jiaojiang River, China	CJJr	MCCPs	7743.29	271-2.72 × 104	C14	Cl6, Cl7	
——	Middle Reaches of the Yellow River, China	CYRm	SCCPs	165.35	11.6-9.76×103	C10, C11	Cl6, Cl7	(Qiao et al., 2016)
——	Middle Reaches of the Yellow River, China	CYRm	MCCPs	44.82	8.33-168	C14	Cl7, Cl8	

2018	Nakdong, Namhan and Yeongsan, South Korea	KR	SCCPs	90.70	27.4-146	——	——	(Choo et al., 2020)
2020	River Ravi, Pakistan	PKr	SCCPs	62.00	<LOD-170	C10, C13	Cl7, Cl8	(Tahir et al., 2024)
2020	River Ravi, Pakistan	PKr	MCCPs	44.00	<LOD-100	C14	Cl7, Cl8	
2021	Haihe River, China	CHHr	SCCPs	688.00	132–1768	C10, C11	Cl6, Cl7	(Cao et al., 2024)
2021	Haihe River, China	CHHr	MCCPs	558.00	90–1443	C14	Cl7, Cl8	

Table S10 S/MCCPs in farmland soil

Year	Location	Abbreviations	S/MCCPs	Average (ng/g dw)	Range (ng/g dw)	Dominant chain length	Dominant chlorinated homologues	Reference
2016	China	CN	SCCPs	374.00	38.7-1609	C10	Cl5-7	(Aamir et al., 2019)
2016	China	CN	MCCPs	859.59	127.3-1969	C14	Cl5-8	
2017	Liaocheng, China	CLC	SCCPs	64.81	5.41-381	C10	Cl6, Cl7	(Chen et al., 2021)
2017	Liaocheng, China	CLC	MCCPs	37.53	< 1.51-188	C14	Cl7, Cl8	
2017	Taizhou, China	CTZ	SCCPs	658.00	156-1160	C12, C13	Cl7, Cl8	(Xu et al., 2019)
2017	Taizhou, China	CTZ	MCCPs	3190.00	1050-5330	C14	Cl7, Cl8	
——	Tibetan Plateau, China	CTP	SCCPs	794.00	89.1-1961	C13	Cl7, Cl8	(Zhou et al., 2024b)
——	Tibetan Plateau, China	CTP	MCCPs	1003.00	66.8-3395	C14	Cl7-9	
2019	Shanghai, China	CSH	SCCPs	99.80	52.6-237.6	C10	Cl7	(Xu et al., 2023)
2019	Shanghai, China	CSH	MCCPs	801.00	417.2-1691	C14	Cl7	

Table S11 S/M/LCCPs in industrial soil

Year	Location	Abbrevia-tions	S/M/LCCPs	Average (ng/g dw)	Range (ng/g dw)	Dominant chain length	Dominant chlorinated homologues	Reference
2013-2014	Dalian, China (in-CP production plant)	CDLipp	SCCPs	1421.40	1018.4-1824.4	C10	Cl6-8	(Xu et al., 2016)
2013-2014	Dalian, China (in-CP production plant)	CDLipp	MCCPs	2051.40	2028.0-2074.8	C14	Cl7, Cl8	
2013-2014	Dalian, China (out-CP production plant)	CDLopp	SCCPs	141.90	24.8-481.6	C10, C11	Cl6, Cl7	
2013-2014	Dalian, China (out-CP production plant)	CDLopp	MCCPs	119.40	19.3-1460.6	C14	Cl7, Cl8	
2015	Agbogbloshie, Ghana (e-waste dismantling area)	GH	SCCPs	3300.00	145-28000	——	——	(Moeckel et al., 2020)
2015	Agbogbloshie, Ghana (e-waste dismantling area)	GH	MCCPs	380.00	n.d.-1400	——	——	
2016	Zibo, China (in-CP production plant)	CZBipp	SCCPs	306739.00	27508.4-554160.8	C12, C13	Cl8-10	(Wang et al., 2018a)
2017	Taizhou, China (e-waste dismantling area)	CTZ	SCCPs	63528.33	1.90×103-2.20×105	C13	Cl7, Cl8	(Xu et al., 2019)
2017	Taizhou, China (e-waste dismantling area)	CTZ	MCCPs	1260583.33	2.08×104-4.40 ×106	C14	Cl7, Cl8	
2018	Guangzhou, China (in-CP production plant)	CGZipp	SCCPs	1017.39	n.d.-5090	C13	Cl7, Cl8	(Wu et al., 2020b)
2018	Guangzhou, China (in-CP production plant)	CGZipp	MCCPs	1607.93	n.d.-6670	——	——	
2018	Guangzhou, China (in-CP production plant)	CGZipp	LCCPs	338.75	n.d.-1450	——	——	
2018	Jiangsu, China	CJS	SCCPs	225.42	37.5-995.7	C10, C13	Cl6-8	(Huang et al., 2020)
2018	Jiangsu, China	CJS	MCCPs	176.72	15.1-739.6	C14	Cl7-9	
2019	Hebei, China	CHB	SCCPs	596.97	121-5159	C10	Cl6, Cl7	(Weng et al., 2022)
2019	Hebei, China	CHB	MCCPs	846.88	47-6079	C14, C15	Cl5	

——	Zhoushan, China	CZS	SCCPs	515.40	72-3842	C11, C13	Cl7, Cl8	(Ai et al., 2022)
——	Zhoushan, China	CZS	MCCPs	1365.40	117-8819	C14	Cl8, Cl9	
2019-2021	Shanghai, China	CSH	SCCPs	178.00	98.3-977.1	C10	Cl7	(Xu et al., 2023)
2019-2021	Shanghai, China	CSH	MCCPs	1533.00	370.9-10713	C14	Cl7	
2021	Taipu River Basin, China	CTRB	SCCPs	493.57	191-996	——	——	(Zhou et al., 2023)
2021	Taipu River Basin, China	CTRB	MCCPs	6987.14	2230-13800	——	——	

Table S12 S/MCCPs in background soil

Year	Location	Abbrevia-tions	S/MCCPs	Average (ng/g dw)	Range (ng/g dw)	Dominant chain length	Dominant chlorinated homologues	Reference
2008	United Kingdom	UK	SCCPs	16.00	0.8-179	——	——	(Halse et al., 2015)
2008	Norway	NO	SCCPs	12.00	0.8-281	——	——	
——	Shergyla Mountain, China	CSM	SCCPs	125.00	81.4-164	C10	Cl6, Cl7	(Zhou et al., 2024b)
——	Shergyla Mountain, China	CSM	MCCPs	325.00	n.d.-632	C14	Cl6-8	
2011	Chongming Island, China	CCMI	SCCPs	64.51	0.42-420	C13	Cl7, Cl8	(Wang et al., 2013a)
2011-2012	Ny-Ålesund and London Island, Arctic	Arctic	SCCPs	7.10	6.03-8.17	C10	Cl6	(Li et al., 2017)
2012-2013	King George Island, Antarctica	Antarctica	SCCPs	14.80	3.5–32.8	C10	Cl6, Cl7	(Li et al., 2016)

Table S13 S/MCCPs in urban-rural soil

Year	Location	Abbrevia-tions	S/MCCPs	Average (ng/g dw)	Range (ng/g dw)	Dominant chain length	Dominant chlorinated homologues	Reference
2016	Yunnan, China	CYN	SCCPs	348.00	79-948	C10	Cl6, Cl7	(Wang et al., 2020)
2016	Yunnan, China	CYN	MCCPs	229.00	20-1206	C14	Cl6, Cl7	
2017-2018	Tianjin, China	CTJ	SCCPs	361.00	n.d.-14285	C13	Cl7, Cl8	(Li et al., 2021a)
2017-2018	Tianjin, China	CTJ	MCCPs	356.00	n.d.-6760	C14	Cl7, Cl8	
2019	Dar es Salaam, Tanzania	TZ	SCCPs	330.00	< 11-5300	——	——	(Nipen et al., 2022)
2020-2021	Huangpu River Basin, China	CHRB	SCCPs	347.12	140-1130	——	——	(Zhou et al., 2023)
2020-2021	Huangpu River Basin, China	CHRB	MCCPs	2352.07	277-10200	——	——	
——	Baoding, China	CBD	SCCPs	234.00	19-1456	C10	Cl6, Cl7	(Wang et al., 2022)
——	Baoding, China	CBD	MCCPs	54.00	<10-385	C14	Cl7, Cl8	

Table S14. Summary of the characteristics of existing CPs remediation technologies.

Remediation Technology	Applied Environmental Compartment	Influencing Factors	Advantages	Disadvantages	Products	Main Cost Sources
Pyrolysis	Soil Sediment	temperature, oxygen, etc.	1)High conversion rates 2)Synergistically remove other pollutants	1)High energy consumption 2)Complex equipment and operational conditions, high costs 3)Generation of toxic by-products, significant secondary pollution	CBz PAHs PCBs etc.	1)Energy 2)Incineration equipment
Photolysis degradation	Water	light intensity, solution absorbance, concentration of reactive species, etc.	1)Simple equipment and operations 2)Low cost 3)Environmentally friendly	1)Low degradation efficiency 2)By-products with ecological toxicity 3)Limited light sources	Alkanes long-chain alcohols etc.	1)Chemical reagents 2)Light source energy
Photocatalysis degradation	Water Atmosphere	light intensity, types and concentration of catalyst, initial concentration of pollutants, etc.	1)Broad spectrum absorption 2)Strong oxidation capability 3)Both adsorption and degradation	1)Difficult to develop ideal photocatalysts 2)Low mineralization rate 3)Difficult to catalyst recovery	CO_2 H_2O HCl byproducts etc.	1)Material development, synthesis, regeneration, and recycling 2) required reactors
Microbial degradation	Soil Sediment	soil condition, strain species and abundance, C-length, Cl%, etc.	1)Environmentally friendly 2)Low costs 3)In-situ remediation 4)No recovery and treatment	1)Difficulties in microbial strain selection 2)Low efficiency 3)Diverse by-products	Alcohols Acids Alkenes etc.	Biological species selection, cultivation, and processing

Phytodegradation	Soil	environmental condition plant species C-length, Cl%, etc.	1)In situ remediation 2)Economic and ecological benefits 3)Low energy consumption	1)Long remediation cycles 2)Difficulty in selecting appropriate plant species 3)Complex and diverse by-products	-	Biological species selection, cultivation, and processing
NZVI reduction	Water	pH temperature C-length, Cl%, etc.	1)High reactivity 2)Strong reducing capacity 3)Simple preparation 4)Low cost	1)NZVI reunion and deactivation 2)Short lifespan 3)Ecological risks of NZVI	Alkanes	1)Material development, synthesis, regeneration, and recycling 2) required reactors
Adsorption	Atmosphere Water	material size specific surface area C-length, etc.	No byproducts	1)Require appropriate follow-up disposal 2)Complexity of recovery and treatment	-	1)Material development, synthesis, regeneration, and recycling 2) required reactors

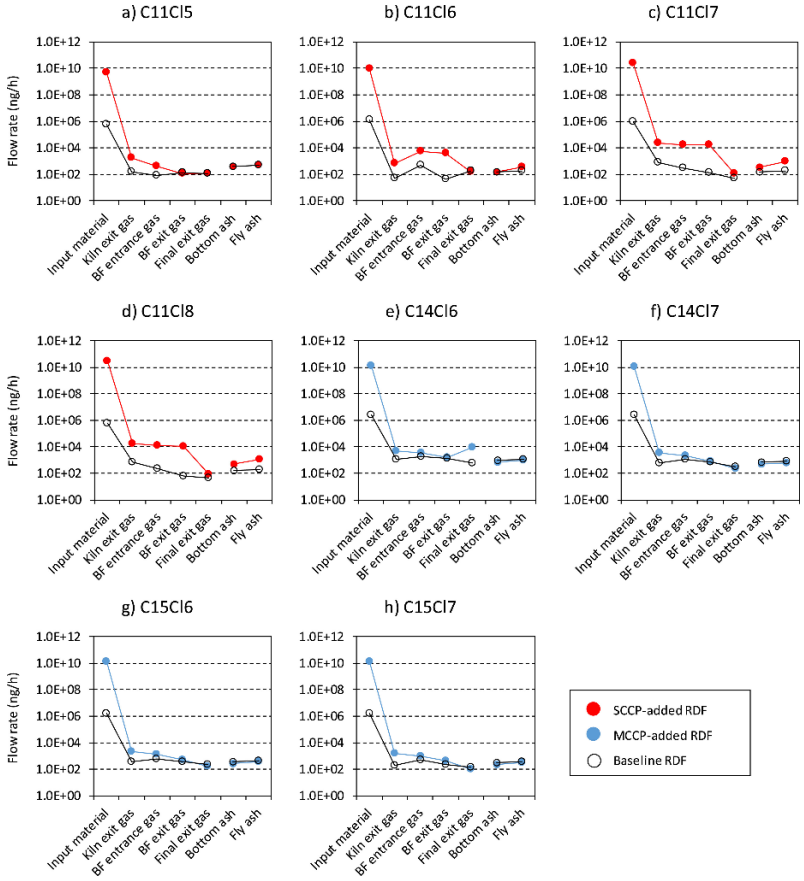

Figure.S5 Behaviors of principal homologue groups of (a–d) SCCPs and (e–h) MCCPs during the three experimental incineration runs (Matsukami and Kajiwara, 2019).

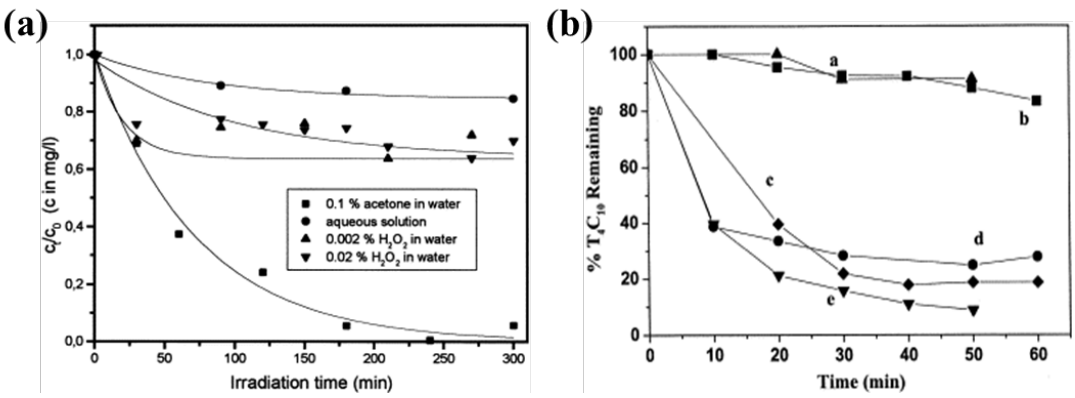

Figure.S6 (a) photodegradation of CPs by UV irradiation (c_t: residual concentration of CPs, c_0: initial concentration of CPs) (Koh & Thiemann, 2001); (b) degradation of 1,2,9,10-tetrachlorodecane (2×10^{-6} M) with 1.0×10^{-2} M H_2O_2 , a) under modified Fenton conditions (1.0×10^{-3} M $Fe(ClO_4)_3$/dark), b) under Fenton conditions (1.0×10^{-3} M $Fe(ClO_4)_2$/dark), c) using 300 nm UV light, d) under photo-Fenton conditions (1.0×10^{-3} M $Fe(ClO_4)_2$/UV), and e) under modified photo-Fenton conditions (1.0×10^{-3} M $Fe(ClO_4)_3$/UV) (Zhang et al., 2019).

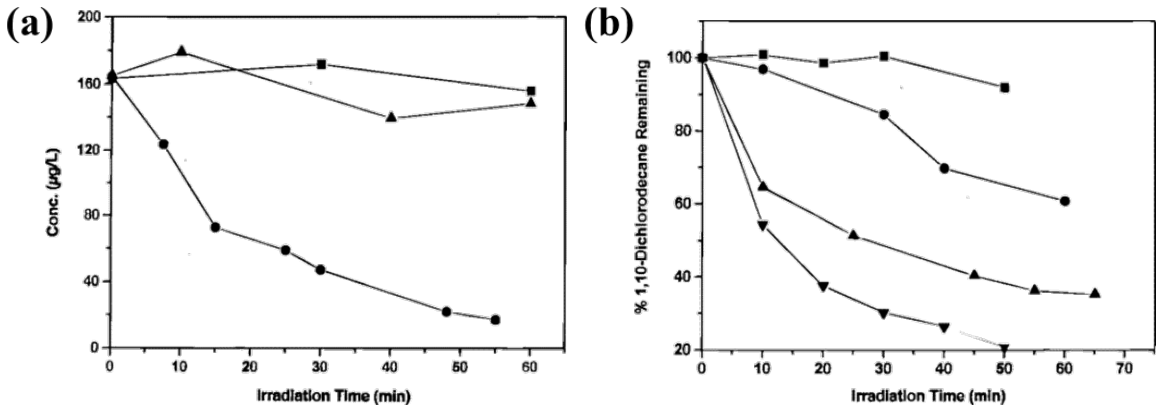

Figure.S7 (a) degradation of 1,10-dichlorodecane in a dark control (▪), in a solution without TiO_2 (▲) and in the presence of 150 mg/L of TiO_2 (●); (b) effect of the hole scavenger, methanol, on the photodegradation of 1,10-dichlorodecane in 150 mg/L of TiO_2 at a pH of 2.8. Methanol concentrations: 0 mM (▼), 1 mM (▲), 10 mM (●), and 100 mM (▪) (El-Morsi et al., 2000).

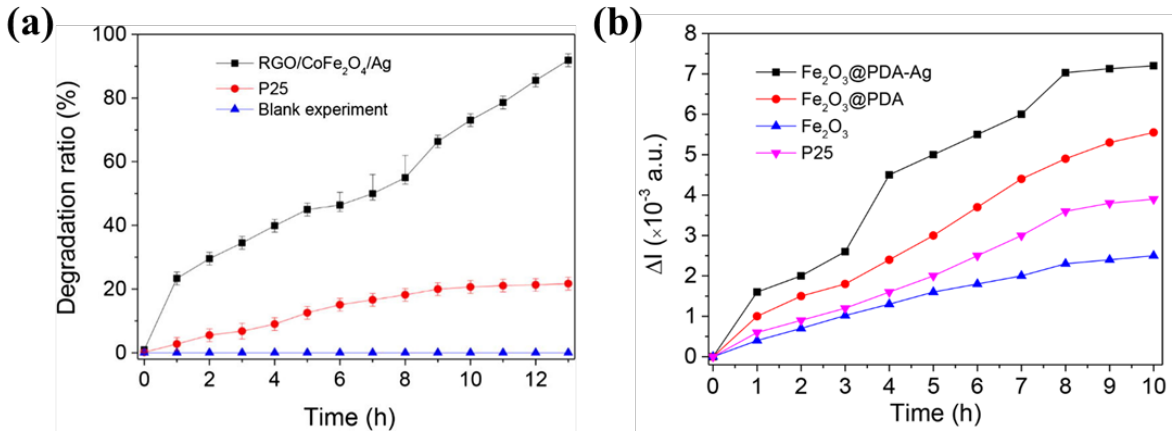

Figure.S8 (a) degradation percentage of SCCPs through blank experiment as well as over P25 and $RGO/CoFe_2O_4/Ag$ composite under the illumination of visible light (Chen et al., 2016a); (b) the change of the intensity of C-Cl band for SCCPs over different photocatalysts under the simulant solar light irradiation (Xiong et al., 2018).

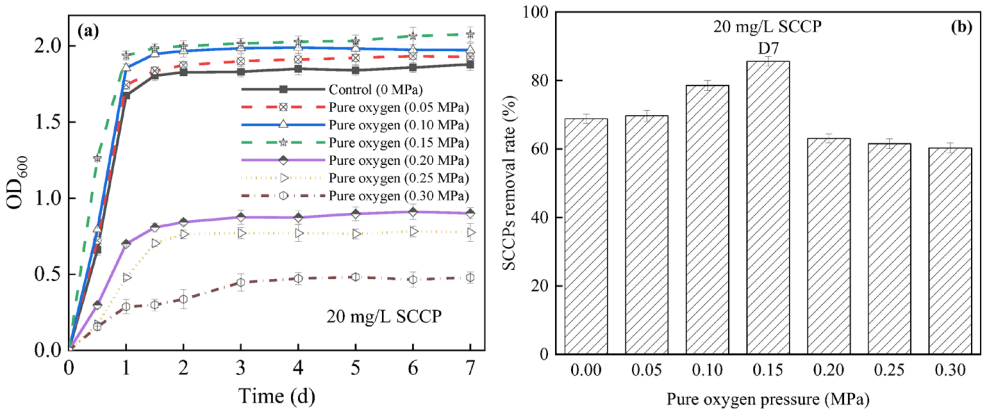

Figure.S9 Relationship between different high-purity oxygen pressures and (a) the growth of E. coli strain 2; (b) SCCP removal rate in a pressurized reactor. SCCPs, short-chain chlorinated paraffins (Qian et al., 2022).

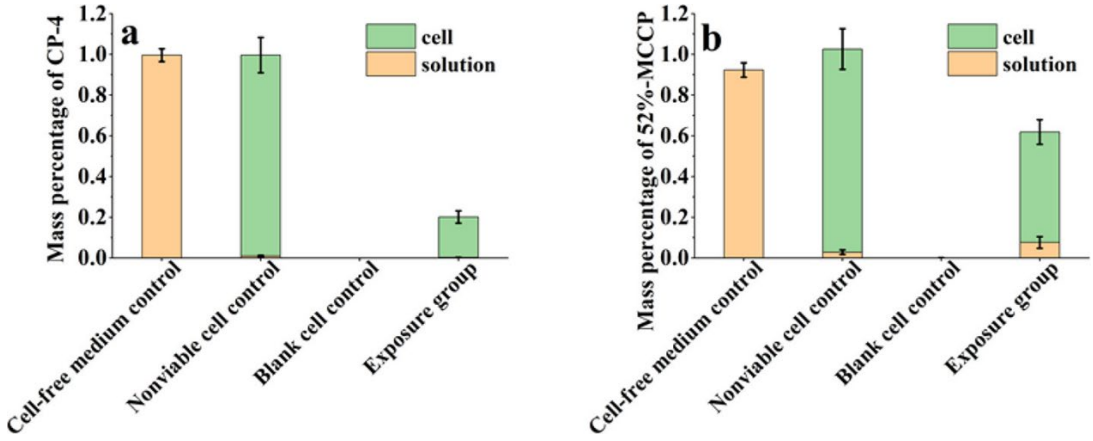

Figure.S10 Mass percentages of CP-4 (a) and 52%-MCCP (b) distributed in solutions and rice cells which account for their initial mass after 5 days exposure (Chen et al., 2020).

Reference

[1] Aamir M., Yin S., Zhou Y., Xu C., Liu K., & Liu W. (2019). Congener-specific C_{10}—C_{13} and C_{14}—C_{17} chlorinated paraffins in Chinese agricultural soils: Spatio-vertical distribution, homologue pattern and environmental behavior. *Environmental Pollution*, *245*, 789–798. https://doi.org/10.1016/j.envpol.2018.10.132

[2] Ai, Q., Zhang, P., Gao, L., Zhou, X., Liu, Y., Huang, D., Qiao, L., Weng, J., & Zheng, M. (2022). Air–soil exchange of and risks posed by short- and medium-chain chlorinated paraffins: Case study in a contaminated area in China. *Chemosphere*, *297*, 134230. https://doi.org/10.1016/j.chemosphere.2022.134230

[3] Barber J.L., Sweetman A.J., Thomas G.O., Braekevelt E., Stern G.A., & Jones K.C. (2005). Spatial and temporal variability in air concentrations of short-chain (C_{10}–C_{13}) and medium-chain (C_{14}–C_{17}) chlorinated

n-alkanes measured in the U.K. atmosphere. *Environmental Science & Technology*, *39*, 440 – 4415. https://doi.org/10.1021/es047949w

[4] Bogdal C., Alsberg T., Diefenbacher P.S., MacLeod M., & Berger U. (2015). Fast quantification of chlorinated paraffins in environmental samples by direct injection high-resolution mass spectrometry with pattern deconvolution. *Analytical Chemistry*, *87*, 2852–2860. https://doi.org/10.1021/ac504444d

[5] Bohlin-Nizzetto, P., Aas, W., & Krogseth, I. (2014) Monitoring of environmental contaminants in air and precipitation, annual report 2013. M-202-1014. Norwegian Institute for Air Research. (NILU report, 29/2014).

[6] Bohlin-Nizzetto, P., Aas, W., & Nicholas, W. (2015) Monitoring of environmental contaminants in air and precipitation, annual report 2014. M-368-2015. Norsk Institutt for Luftforskning. (NILU report, 19/2015).

[7] Bohlin-Nizzetto P., & Aas.W. (2016) Monitoring of environmental contaminants in air and precipitation, annual report 2015. M-579-2016. Norsk Institutt for Luftforskning. (NILU report, 14/2016).

[8] Bohlin-Nizzetto, P., Aas, W., & Nicholas, W. (2017) Monitoring of environmental contaminants in air and precipitation, annual report 2016. M-757-2017. Norsk Institutt for Luftforskning. (NILU report, 17/2017).

[9] Bohlin-Nizzetto, P., Aas, W., & Nicholas, W. (2018) Monitoring of environmental contaminants in air and precipitation, annual report 2017. M-1062-2018. Norsk Institutt for Luftforskning. (NILU report, 13/2018).

[10] Bohlin-Nizzetto, P., Aas, W., & Nikiforov, V. (2019) Monitoring of environmental contaminants in air and precipitation, annual report 2018. M-1419-2019. Norwegian Institute for Air Research. (NILU report, 11/2019).

[11] Bohlin-Nizzetto, P., Aas, W., & Nikiforov, V. (2020) Monitoring of environmental contaminants in air and precipitation, annual report 2019. M-1736-2020. Norwegian Institute for Air Research. (NILU report, 06/2020).

[12] Bohlin-Nizzetto, P., Aas, W., Halvorsen, H.L., Nikiforov, V., & Pfaffhuber, K.A. (2021) Monitoring of environmental contaminants in air and precipitation, annual report 2020. M-2060-2021. Norwegian Institute for Air Research. (NILU report, 12/2021).

[13] Bohlin-Nizzetto, P., Aas, W., Halvorsen, H.L., Nikiforov, V., & Pfaffhuber, K.A. (2022) Monitoring of environmental contaminants in air and precipitation, annual report 2021. M-2317-2022. (NILU report, 19/2022).

[14] Borgen A.R., Schlabach M., & Mariussen E. (2003). Screening of chlorinated paraffins in Norway. *Organohalogen Compounds*, *60*, 331-334

[15] Brandsma S.H., van Mourik L., O'Brien J.W., Eaglesham G., Leonards Pim.E.G., de Boer J., Gallen C., Mueller J., Gaus C., & Bogdal C. (2017). Medium-chain chlorinated paraffins (CPs) dominate in Australian sewage sludge. *Environmental Science & Technology*, *51*, 3364–3372. https://doi.org/10.1021/acs.est.6b05318

[16] Brits, M., de Boer, J., Rohwer, E.R., De Vos, J., Weiss, J.M., & Brandsma, S.H. (2020). Short-, medium-, and long-chain chlorinated paraffins in South African indoor dust and cat hair. *Chemosphere*, *238*, 124643. https://doi.org/10.1016/j.chemosphere.2019.124643

[17] Cao D., Gao W., Wu J., Lv K., Xin S., Wang Y., & Jiang G. (2019). Occurrence and human exposure assessment of short- and medium-chain chlorinated paraffins in dusts from plastic sports courts and synthetic turf in Beijing, China. *Environmental Science & Technology*, *53*, 443–451. https://doi.org/10.1021/acs.est.8b04323

[18] Cao X., Gao L., Jiang X., Cheng X., Zhang Y., Liu Y., Ai Q., Weng J., & Zheng M. (2024). Short- and medium-chain chlorinated paraffins in sediment from the Haihe River Basin: Sources, distributions, and ecological risk assessment. *Chemosphere*, *349*, 140856. https://doi.org/10.1016/j.chemosphere.2023.140856

[19] Castells P., Santos F.J., & Galceran M.T. (2004). Solid-phase extraction versus solid-phase microextraction for the determination of chlorinated paraffins in water using gas chromatography–negative chemical ionisation mass spectrometry. *Journal of Chromatography A*, *1025*, 157–162. https://doi.org/10.1016/j.chroma.2003.10.069

[20] Chaemfa C., Xu Y., Li J., Chakraborty P., Hussain Syed J., Naseem Malik R., Wang Y., Tian C., Zhang G., & Jones K.C. (2014). Screening of atmospheric short- and medium-chain chlorinated paraffins in India and Pakistan using polyurethane foam based passive air sampler. *Environmental Science & Technology*, *48*, 4799 – 4808. https://doi.org/10.1021/es405186m

[21] Chen, C., Ma X., Guo, W., Zhao Y., LÜ, J., Wang, Zhen., & Yao, Z. (2014). Congener specific distribution and bioaccumulation of short-chain chlorinated paraffins in Liao estuary. *Chinese Science Bulletin*, *59*, 578–585

[22] Chen H., Lam J.C.W., Zhu M., Wang F., Zhou W., Du B., Zeng L., & Zeng E.Y. (2018). Combined effects of dust and dietary exposure of occupational workers and local residents to short- and medium-chain

chlorinated paraffins in a mega e-waste recycling industrial park in South China. *Environmental Science & Technology*, *52*, 11510–11519. https://doi.org/10.1021/acs.est.8b02625

[23] Chen M., Luo X., Zhang X., He M., Chen S., & Mai B. (2011). Chlorinated paraffins in sediments from the Pearl River Delta, South China: Spatial and temporal distributions and implication for processes. *Environmental Science & Technology*, *45*, 9936–9943. https://doi.org/10.1021/es202891a

[24] Chen, W., Hou, X., Liu, Y., Hu, X., Liu, J., Schnoor, J.L., & Jiang, G. (2021). Medium- and short-chain chlorinated paraffins in mature maize plants and corresponding agricultural soils. *Environmental Science & Technology*, *55*, 4669–4678. https://doi.org/10.1021/acs.est.0c05111

[25] Chen W., Yu M., Zhang Q., Hou X., Kong W., Wei L., Mao X., Liu J., Schnoor J.L., & Jiang G. (2020). Metabolism of SCCPs and MCCPs in suspension rice cells based on paired mass distance (PMD) analysis. *Environmental Science & Technology*, *54*, 9990–9999. https://doi.org/10.1021/acs.est.0c01830

[26] Chen X., Zhao Q., Li X., & Wang D. (2016). Enhanced photocatalytic activity of degrading short chain chlorinated paraffins over reduced graphene oxide/$CoFe_2O_4$/Ag nanocomposite. *Journal of Colloid and Interface Science*, *479*, 89–97. https://doi.org/10.1016/j.jcis.2016.06.053

[27] Chen Y., Chang C., & Ding W. (2016b). Vortex-homogenized matrix solid-phase dispersion for the extraction of short chain chlorinated paraffins from indoor dust samples. *Journal of Chromatography A*, *1472*, 129–133. https://doi.org/10.1016/j.chroma.2016.10.048

[28] Choo G., Wang W., Cho H.-S., Kim K., Park K., & Oh J.-E. (2020). Legacy and emerging persistent organic pollutants in the freshwater system: Relative distribution, contamination trends, and bioaccumulation. *Environment International*, *135*, 105377. https://doi.org/10.1016/j.envint.2019.105377

[29] Cui Q., Han D., Qin H., Li H., Liu Y., Guo W., Song M., Li J., Sun Y., Luo J., Xue J., & Xu Y. (2024). Investigating the levels, spatial distribution, and trophic transfer patterns of short-chain chlorinated paraffins in the Southern Bohai Sea, China. *Water Research*, *253*, 121337. https://doi.org/10.1016/j.watres.2024.121337

[30] Diefenbacher P.S., Bogdal C., Gerecke A.C., Glüge J., Schmid P., Scheringer M., & Hungerbühler K. (2015). Short-chain chlorinated paraffins in Zurich, Switzerland—atmospheric concentrations and emissions. *Environmental Science & Technology*, *49*, 9778–9786. https://doi.org/10.1021/acs.est.5b02153

[31] El-Morsi T.M., Budakowski W.R., Abd-El-Aziz A.S., & Friesen K.J. (2000). Photocatalytic degradation of 1,10-dichlorodecane in aqueous suspensions of TiO_2: A reaction of adsorbed chlorinated alkane with

surface hydroxyl radicals. *Environmental Science & Technology*, *34*, 1018–1022. https://doi.org/10.1021/es9907360

[32] Fridén U.E., McLachlan M.S., & Berger U. (2011). Chlorinated paraffins in indoor air and dust: Concentrations, congener patterns, and human exposure. *Environment International*, *37*, 1169–1174. https://doi.org/10.1016/j.envint.2011.04.002

[33] Gao W., Cao D., Wang Y., Wu J., Wang Y., Wang Y., & Jiang G. (2018). External exposure to short- and medium-chain chlorinated paraffins for the general population in Beijing, China. *Environmental Science & Technology*, *52*, 32–39. https://doi.org/10.1021/acs.est.7b04657

[34] Gao W., Wu J., Wang Y., & Jiang G. (2016). Distribution and congener profiles of short-chain chlorinated paraffins in indoor/outdoor glass window surface films and their film-air partitioning in Beijing, China. *Chemosphere*, *144*, 1327–1333. https://doi.org/10.1016/j.chemosphere.2015.09.075

[35] Gao Y., Zhang H., Su F., Tian Y., & Chen J. (2012). Environmental occurrence and distribution of short chain chlorinated paraffins in sediments and soils from the Liaohe River Basin, P. R. China. *Environmental Science & Technology*, *46*, 3771–3778. https://doi.org/10.1021/es2041256

[36] Gillett R.W., Galbally I.E., Keywood M.D., Powell J.C., Stevenson G., Yates A., & Borgen A.R. (2017). Atmospheric short-chain-chlorinated paraffins in Melbourne, Australia – first extensive Southern Hemisphere observations. *Environmental Chemistry*, *14*, 106. https://doi.org/10.1071/EN16152

[37] Halse, A.K., Schlabach, M., Schuster, J.K., Jones, K.C., Steinnes, E., & Breivik, K. (2015). Endosulfan, pentachlorobenzene and short-chain chlorinated paraffins in background soils from Western Europe. *Environmental Pollution*, *196*, 21–28. https://doi.org/10.1016/j.envpol.2014.09.009

[38] Halvorsen, H. L., Pfaffhuber, K. A., Nipen, M., Bohlin-Nizzetto, P., Berglen, T. F., Nikiforov, V., Hartz, W. (2023). Monitoring of environmental contaminants in air and precipitation. Annual report 2022. (NILU report, 18/2023)

[39] Halvorsen, H. L., Pfaffhuber, K. A., Nipen, M., Bohlin-Nizzetto, P., Berglen, T. F., Nikiforov, V., Hartz, W. (2024). Monitoring of environmental contaminants in air and precipitation. Annual report 2023. (NILU report 18/2024)

[40] He C., Brandsma S.H., Jiang H., O'Brien J.W., van Mourik L.M., Banks A.P., Wang X., Thai P.K., & Mueller J.F. (2019). Chlorinated paraffins in indoor dust from Australia: Levels, congener patterns and preliminary assessment of human exposure. *Science of the Total Environment*, *682*, 318–323.

https://doi.org/10.1016/j.scitotenv.2019.05.170

[41] Hilger B., Fromme H., Völkel W., & Coelhan M. (2013). Occurrence of chlorinated paraffins in house dust samples from Bavaria, Germany. *Environmental Pollution*, *175*, 16–21. https://doi.org/10.1016/j.envpol.2012.12.011

[42] Hu H., Jin H., Li T., Guo Y., Wu P., Xu K., Zhu W., Zhou Y., & Zhao M. (2022). Spatial distribution, partitioning, and ecological risk of short chain chlorinated paraffins in seawater and sediment from East China Sea. *Science of The Total Environment*, *811*, 151932. https://doi.org/10.1016/j.scitotenv.2021.151932

[43] Huang D., Gao L., Qiao L., Cui L., Xu C., Wang K., & Zheng M. (2020). Concentrations of and risks posed by short-chain and medium-chain chlorinated paraffins in soil at a chemical industrial park on the southeast coast of China. *Environmental Pollution*, *258*, 113704. https://doi.org/10.1016/j.envpol.2019.113704

[44] Huang H., Gao L., Xia D., Qiao L., Wang R., Su G., Liu W., Liu G., & Zheng M. (2017). Characterization of short- and medium-chain chlorinated paraffins in outdoor/indoor PM_{10}/$PM_{2.5}$/$PM_{1.0}$ in Beijing, China. *Environmental Pollution*, *225*, 674–680. https://doi.org/10.1016/j.envpol.2017.03.054

[45] Huang Y., Chen L., Feng Y., Ye Z., He Q., Feng Q., Qing X., Liu M., & Gao B. (2016). Short-chain chlorinated paraffins in the soils of two different Chinese cities: Occurrence, homologue patterns and vertical migration. *Science of the Total Environment*, *557–558*, 644–651. https://doi.org/10.1016/j.scitotenv.2016.03.101

[46] Hüttig J., & Oehme M. (2006). Congener group patterns of chloroparaffins in marine sediments obtained by chloride attachment chemical ionization and electron capture negative ionization. *Chemosphere*, *64*, 1573–1581. https://doi.org/10.1016/j.chemosphere.2005.11.042

[47] Iino F., Takasuga T., Senthilkumar K., Nakamura N., & Nakanishi J. (2005). Risk assessment of short-chain chlorinated paraffins in Japan based on the first market basket study and species sensitivity distributions. *Environmental Science & Technology*, *39*, 859–866. https://doi.org/10.1021/es0492211

[48] J. Peters A., T. Tomy G., Jones K.C., Coleman P., & Stern G.A. (2000). Occurrence of C_{10}–C_{13} polychlorinated *n*-alkanes in the atmosphere of the United Kingdom. *Atmospheric Environment*, *34*, 3085–3090. https://doi.org/10.1016/S1352-2310(99)00479-3

[49] Ji B., Wu Y., Liang Y., Gao S., Zeng X., Yao P., & Yu Z. (2022). Occurrence, congener patterns, and potential ecological risk of chlorinated paraffins in sediments of Yangtze River Estuary and adjacent East

China Sea. *Environmental Monitoring and Assessment*, *194*, 329. https://doi.org/10.1007/s10661-022-09969-8

[50] Jiang L., Gao W., Ma X., Wang Y., Wang C., Li Y., Yang R., Fu J., Shi J., Zhang Q., Wang Y., & Jiang G. (2021). Long-term investigation of the temporal trends and gas/particle partitioning of short- and medium-chain chlorinated paraffins in ambient air of King George Island, Antarctica. *Environmental Science & Technology*, *55*, 230–239. https://doi.org/10.1021/acs.est.0c05964

[51] Koh I.-O., & Thiemann W. (2001). Study of photochemical oxidation of standard chlorinated paraffins and identification of degradation products. *Journal of Photochemistry and Photobiology, A: Chemistry*, *139*, 205–215. https://doi.org/10.1016/S1010-6030(00)00427-5

[52] Li, F., Shi, R., Wang, Y., He, A., Han, Z., Zheng, X., Li, C., Gao, W., Wang, Y., & Jiang, G. (2021a). The effect of anthropogenic activities on the environmental fate of chlorinated paraffins in surface soil in an urbanized zone of northern China. *Environmental Pollution*, *288*, 117766. https://doi.org/10.1016/j.envpol.2021.117766

[53] Li H., Fu J., Pan W., Wang P., Li Y., Zhang Q., Wang Y., Zhang A., Liang Y., & Jiang G. (2017). Environmental behaviour of short-chain chlorinated paraffins in aquatic and terrestrial ecosystems of Ny-Ålesund and London Island, Svalbard, in the Arctic. *Science of the Total Environment*, *590–591*, 163–170. https://doi.org/10.1016/j.scitotenv.2017.02.192

[54] Li H., Fu J., Zhang A., Zhang Q., & Wang Y. (2016). Occurrence, bioaccumulation and long-range transport of short-chain chlorinated paraffins on the Fildes Peninsula at King George Island, Antarctica. *Environment International*, *94*, 408–414. https://doi.org/10.1016/j.envint.2016.05.005

[55] Li H., Li J., Li H., Yu H., Yang L., Chen X., & Cai Z. (2019). Seasonal variations and inhalation risk assessment of short-chain chlorinated paraffins in $PM_{2.5}$ of Jinan, China. *Environmental Pollution*, *245*, 325–330. https://doi.org/10.1016/j.envpol.2018.10.133

[56] Li Q., Cheng X., Cui Y., Sun J., Li J., & Zhang G. (2018a). Short- and medium-chain chlorinated paraffins in the Henan section of the Yellow River: Occurrences, fates, and fluxes. *Science of the Total Environment*, *640–641*, 1312–1319. https://doi.org/10.1016/j.scitotenv.2018.05.344

[57] Li Q., Guo M., Song H., Cui J., Zhan M., Zou Y., Li J., & Zhang G. (2021b). Size distribution and inhalation exposure of airborne particle-bound polybrominated diphenyl ethers, new brominated flame retardants, organophosphate esters, and chlorinated paraffins at urban open consumption place. *Science of*

the Total Environment, *794*, 148695. https://doi.org/10.1016/j.scitotenv.2021.148695

[58] Li, Q., Jiang, S., Li, Y., Su, J., Shangguan, J., Zhan, M., Wang, Y., Su, X., Li, J., & Zhang, G. (2023a). The impact of three related emission industries on regional atmospheric chlorinated paraffins pollution. *Environmental Pollution*, *316*, 120564. https://doi.org/10.1016/j.envpol.2022.120564

[59] Li, Q., Li, J., Wang, Y., Xu, Y., Pan, X., Zhang, G., Luo, C., Kobara, Y., Nam, J.-J., & Jones, K.C. (2012). Atmospheric short-chain chlorinated paraffins in China, Japan, and South Korea. *Environmental Science & Technology*, *46*, 11948–11954. https://doi.org/10.1021/es302321n

[60] Li T., Gao S., Ben Y., Zhang H., Kang Q., & Wan Y. (2018b). Screening of chlorinated paraffins and unsaturated analogues in commercial mixtures: Confirmation of their occurrences in the atmosphere. *Environmental Science & Technology*, *52*, 1862–1870. https://doi.org/10.1021/acs.est.7b04761

[61] Li X., Guo H., Hong J., Gao Y., Ma X., & Chen J. (2023b). Short- and medium-chain chlorinated paraffins in the sediment of the East China Sea and Yellow Sea: Distribution, composition, and ecological risks. *Toxics*, *11*, 558. https://doi.org/10.3390/toxics11070558

[62] Liu D., Li Q., Cheng Z., Li K., Li J., & Zhang G. (2020). Spatiotemporal variations of chlorinated paraffins in $PM_{2.5}$ from Chinese cities: Implication of the shifting and upgrading of its industries. *Environmental Pollution*, *259*, 113853. https://doi.org/10.1016/j.envpol.2019.113853

[63] Lu, R., Xia, D., Ma, X., Zhao, S., Liu, Y., & Sun, Y. (2023). Short and medium-chain chlorinated paraffins in indoor dust from a multistory residential building in Beijing, China: Vertical distribution and potential health risks. *Science of the Total Environment*, *861*, 160642. https://doi.org/10.1016/j.scitotenv.2022.160642

[64] Ma X., Zhang H., Wang Z., Yao Z., Chen J., & Chen J. (2014a). Bioaccumulation and trophic transfer of short chain chlorinated paraffins in a marine food web from Liaodong Bay, North China. *Environmental Science & Technology*, *48*, 5964–5971. https://doi.org/10.1021/es500940p

[65] Ma X., Zhang H., Zhou H., Na G., Wang Z., Chen C., Chen J., & Chen J. (2014b). Occurrence and gas/particle partitioning of short- and medium-chain chlorinated paraffins in the atmosphere of Fildes Peninsula of Antarctica. *Atmospheric Environment*, *90*, 10–15. https://doi.org/10.1016/j.atmosenv.2014.03.021

[66] Matsukami H., & Kajiwara N. (2019). Destruction behavior of short- and medium-chain chlorinated paraffins in solid waste at a pilot-scale incinerator. *Chemosphere*, *230*, 164–172.

https://doi.org/10.1016/j.chemosphere.2019.05.048

[67] McGrath T.J., Poma G., Hutinet S., Fujii Y., Dodson R.E., Johnson-Restrepo B., Muenhor D., Dervilly G., Cariou R., & Covaci A. (2023). An international investigation of chlorinated paraffin concentrations and homologue distributions in indoor dust. *Environmental Pollution*, *333*, 121994. https://doi.org/10.1016/j.envpol.2023.121994

[68] Moeckel C., Breivik K., Nøst T.H., Sankoh A., Jones K.C., & Sweetman A. (2020). Soil pollution at a major west African E-waste recycling site: Contamination pathways and implications for potential mitigation strategies. *Environment International*, *137*, 105563. https://doi.org/10.1016/j.envint.2020.105563

[69] Nipen M., Vogt R.D., Bohlin-Nizzetto P., Borgå K., Mwakalapa E.B., Borgen A.R., Jørgensen S.J., Ntapanta S.M., Mmochi A.J., Schlabach M., & Breivik K. (2022). Spatial trends of chlorinated paraffins and dechloranes in air and soil in a tropical urban, suburban, and rural environment. *Environmental Pollution*, *292*, 118298. https://doi.org/10.1016/j.envpol.2021.118298

[70] Niu, S., Chen, R., Zou, Y., Dong, L., Hai, R., & Huang, Y. (2020). Spatial distribution and profile of atmospheric short-chain chlorinated paraffins in the Yangtze River Delta. *Environmental Pollution*, *259*, 113958. https://doi.org/10.1016/j.envpol.2020.113958

[71] Niu S., Harner T., Chen R., Parnis J.M., Saini A., & Hageman K. (2021). Guidance on the application of polyurethane foam disk passive air samplers for measuring nonane and short-chain chlorinated paraffins in air: Results from a screening study in urban air. *Environmental Science & Technology*, *55*, 11693–11702. https://doi.org/10.1021/acs.est.1c02428

[72] Pan X., Zhen X., Tian C., & Tang J. (2021). Distributions, transports and fates of short- and medium-chain chlorinated paraffins in a typical river-estuary system. *Science of the Total Environment*, *751*, 141769. https://doi.org/10.1016/j.scitotenv.2020.141769

[73] Parera J., Santos F.J., & Galceran M.T. (2004). Microwave-assisted extraction versus Soxhlet extraction for the analysis of short-chain chlorinated alkanes in sediments. *Journal of Chromatography A*, *1046*, 19–26. https://doi.org/10.1016/j.chroma.2004.06.064

[74] Qian Y., Han W., Zhou F., Ji B., Zhang H., & Zhang K. (2022). Effects of pressurized aeration on the biodegradation of short-chain chlorinated paraffins by *Escherichia coli* strain 2. *Membranes*, *12*, 634. https://doi.org/10.3390/membranes12060634

[75] Qiao L., Xia D., Gao L., Huang H., & Zheng M. (2016). Occurrences, sources and risk assessment of

short- and medium-chain chlorinated paraffins in sediments from the middle reaches of the Yellow River, China. *Environmental Pollution*, *219*, 483–489. https://doi.org/10.1016/j.envpol.2016.05.057

[76] Quinn L., Pieters R., Nieuwoudt C., Borgen A.R., Kylin H., & Bouwman H. (2009). Distribution profiles of selected organic pollutants in soils and sediments of industrial, residential and agricultural areas of South Africa. *Journal of Environmental Monitoring*, *11*, 1647–1657. https://doi.org/10.1039/B905585A

[77] Sakhi A.K., Cequier E., Becher R., Bølling A.K., Borgen A.R., Schlabach M., Schmidbauer N., Becher G., Schwarze P., & Thomsen C. (2019). Concentrations of selected chemicals in indoor air from Norwegian homes and schools. *Science of the Total Environment*, *674*, 1–8. https://doi.org/10.1016/j.scitotenv.2019.04.086

[78] Štejnarová P., Coelhan M., Kostrhounová R., Parlar H., & Holoubek I. (2005). Analysis of short chain chlorinated paraffins in sediment samples from the Czech Republic by short-column. *Chemosphere*, *58*, 253–262. https://doi.org/10.1016/j.chemosphere.2004.08.083

[79] Stevens J.L., Northcott G.L., Stern G.A., Tomy G.T., & Jones K.C. (2003). PAHs, PCBs, PCNs, organochlorine pesticides, synthetic musks, and polychlorinated n-alkanes in U.K. sewage sludge: Survey results and implications. *Environmental Science & Technology*, *37*, 462–467. https://doi.org/10.1021/es020161y

[80] Arctic Institute of North America. (2015) Synopsis of Research Conducted under the 2014–2015 Northern Contaminants Program. Northern Contaminants Program Publish.

[81] Tahir A., Abbasi N.A., He C., Ahmad S.R., Baqar M., & Qadir A. (2024). Spatial distribution and ecological risk assessment of short and medium chain chlorinated paraffins in water and sediments of river Ravi, Pakistan. *Science of the Total Environment*, *926*, 171964. https://doi.org/10.1016/j.scitotenv.2024.171964

[82] van Mourik L.M., Wang X., Paxman C., Leonards P.E.G., Wania F., de Boer J., & Mueller J.F. (2020). Spatial variation of short- and medium-chain chlorinated paraffins in ambient air across Australia. *Environmental Pollution*, *261*, 114141. https://doi.org/10.1016/j.envpol.2020.114141

[83] Wang K., Gao L., Zhu S., Cui L., Qiao L., Xu C., Huang D., & Zheng M. (2020). Spatial distributions and homolog profiles of chlorinated nonane paraffins, and short and medium chain chlorinated paraffins in soils from Yunnan, China. *Chemosphere*, *247*, 125855. https://doi.org/10.1016/j.chemosphere.2020.125855

[84] Wang, K., Gao, L., Zhu, S., Liu, X., Chen, Q., Cui, L., Qiao, L., Xu, C., Huang, D., Wang, S., & Zheng,

M. (2022). Short- and medium-chain chlorinated paraffins in soil from an urban area of northern China: Levels, distribution, and homolog patterns. *Science of the Total Environment*, *807*, 150833. https://doi.org/10.1016/j.scitotenv.2021.150833

[85] Wang P., Zhao N., Cui Y., Jiang W., Wang L., Wang Z., Chen X., Jiang L., & Ding L. (2018a). Short-chain chlorinated paraffin (SCCP) pollution from a CP production plant in China: Dispersion, congener patterns and health risk assessment. *Chemosphere*, *211*, 456–464. https://doi.org/10.1016/j.chemosphere.2018.07.136

[86] Wang X., Jia H., Hu B., Cheng H.., Zhou Y., & Fu R. (2019). Occurrence, sources, partitioning and ecological risk of short- and medium-chain chlorinated paraffins in river water and sediments in Shanghai. *Science of the Total Environment*, *653*, 475–484. https://doi.org/10.1016/j.scitotenv.2018.10.391

[87] Wang X., Wang X., Zhang Y., Chen L., Sun Y., Li M., & Wu M. (2014). Short- and medium-chain chlorinated paraffins in urban soils of Shanghai: Spatial distribution, homologue group patterns and ecological risk assessment. *Science of The Total Environment*, *490*, 144–152. https://doi.org/10.1016/j.scitotenv.2014.04.121

[88] Wang X., Zhang Y., Miao Y., Ma L., Li Y., Chang Y., & Wu M. (2013a). Short-chain chlorinated paraffins (SCCPs) in surface soil from a background area in China: occurrence, distribution, and congener profiles. *Environmental Science and Pollution Research*, *20*, 4742–4749. https://doi.org/10.1007/s11356-012-1446-3

[89] Wang Y., Li J., Cheng Z., Li Q., Pan X., Zhang R., Liu D., Luo C., Liu X., Katsoyiannis A., & Zhang G. (2013b). Short- and medium-chain chlorinated paraffins in air and soil of subtropical terrestrial environment in the Pearl River Delta, South China: Distribution, composition, atmospheric deposition fluxes, and environmental fate. *Environmental Science & Technology*, *47*, 2679–2687. https://doi.org/10.1021/es304425r

[90] Wang Y., Wang Y., & Jiang G. (2018b) Solid-phase extraction for analysis of short-chain chlorinated pa raffins in water sample. *Chinese Journal of Analytical Chemistry*, 46(07), 1102-1108. https://kns.cnki.net/kcms2/article/abstract?v=uTZa6doZ_i4MnXESF-esFPqn5F91TI5awsjaUtHFiskveAKqN-6UmBfKOz31TVkOZPqqXbv1jUvZsrc9BNdVxwhfrOZEB-DA0mdxpXUCJ2haxNZ58TgBj8f2iAdRZXbYbNU7Vl_nm9uxh-E5YjQJ-_JUQRXDVq0V0gzcV5cbZ6M=&uniplatform=NZKPT

[91] Wang Y., Zhu X., Gao Y., Bai H., Wang P., Chen J., Yuan H., Wang L., Li X., & Wang W. (2019b). Monitoring gas- and particulate-phase short-chain polychlorinated paraffins in the urban air of Dalian by a self-developed passive sampler. *Journal of Environmental Sciences*, *80*, 287–295.

https://doi.org/10.1016/j.jes.2019.01.007

[92] Weng J., Zhang P., Gao L., Zhu S., Liu Y., Qiao L., Zhao B., Liu Y., Xu M., & Zheng M. (2022). Concentrations, homolog profiles, and risk assessment of short- and medium-chain chlorinated paraffins in soil around factories in a non-ferrous metal recycling park. *Environmental Pollution*, *293*, 118456. https://doi.org/10.1016/j.envpol.2021.118456

[93] Wong F., Suzuki G., Michinaka C., Yuan B., Takigami H., & de Wit C.A. (2017). Dioxin-like activities, halogenated flame retardants, organophosphate esters and chlorinated paraffins in dust from Australia, the United Kingdom, Canada, Sweden and China. *Chemosphere*, *168*, 1248–1256. https://doi.org/10.1016/j.chemosphere.2016.10.074

[94] Wu J., Cao D., Gao W., Lv K., Liang Y., Fu J., Gao Y., Wang Y., & Jiang G. (2019). The atmospheric transport and pattern of medium chain chlorinated paraffins at Shergyla Mountain on the Tibetan Plateau of China. *Environmental Pollution*, *245*, 46–52. https://doi.org/10.1016/j.envpol.2018.10.112

[95] Wu J., Gao W., Liang Y., Fu J., Gao Y., Wang Y., & Jiang G. (2017). Spatiotemporal distribution and alpine behavior of short chain chlorinated paraffins in air at Shergyla mountain and Lhasa on the Tibetan Plateau of China. *Environmental Science & Technology*, *51*, 11136–11144. https://doi.org/10.1021/acs.est.7b03457

[96] Wu Y., Gao S., Ji B., Liu Z., Zeng X., & Yu Z. (2020a). Occurrence of short- and medium-chain chlorinated paraffins in soils and sediments from Dongguan City, South China. *Environmental Pollution*, *265*, 114181. https://doi.org/10.1016/j.envpol.2020.114181

[97] Wu Y., Gao S., Zeng X., Liang Y., Liu Z., He L., Yuan J., & Yu Z. (2023). Levels and diverse composition profiles of chlorinated paraffins in indoor dust: possible sources and potential human health related concerns. *Environmental Geochemistry and Health*, *45*, 4631–4642. https://doi.org/10.1007/s10653-023-01524-9

[98] Wu Y., Wu J., Tan H., Song Q., Zhang J., Zhong X., Zhou J., Wu W., Cai X., Zhang W., & Liu X. (2020b). Distributions of chlorinated paraffins and the effects on soil microbial community structure in a production plant brownfield site. *Environmental Pollution*, *262*, 114328. https://doi.org/10.1016/j.envpol.2020.114328

[99] Wu Y., Wu J., Wu Z., Zhou J., Zhou L., Lu Y., Liu X., & Wu W. (2021). Groundwater contaminated with short-chain chlorinated paraffins and microbial responses. *Water Research*, *204*, 117605. https://doi.org/10.1016/j.watres.2021.117605

[100] Xiong W., Li X., Zhao Q., Shi Y., & Hao C. (2018). Insight into the photocatalytic mineralization of

short chain chlorinated paraffins boosted by polydopamine and Ag nanoparticles. *Journal of Hazardous Materials*, *359*, 186–193. https://doi.org/10.1016/j.jhazmat.2018.07.066

[101] Xu C., Zhang Q., Gao L., Zheng M., Qiao L., Cui L., Wang R., & Cheng J. (2019). Spatial distributions and transport implications of short- and medium-chain chlorinated paraffins in soils and sediments from an e-waste dismantling area in China. *Science of the Total Environment*, *649*, 821–828. https://doi.org/10.1016/j.scitotenv.2018.08.355

[102] Xu C., Zhou Q., Shen C., Li F., Liu S., Yin S., & Aamir M. (2023). Short- and medium-chain chlorinated paraffins in agricultural and industrial soils from Shanghai, China: surface and vertical distribution, penetration behavior, and health risk assessment. *Environmental Geochemistry and Health*, *45*, 9087–9101. https://doi.org/10.1007/s10653-023-01632-6

[103] Xu J., Gao Y., Zhang H., Zhan F., & Chen J. (2016). Dispersion of short- and medium-chain chlorinated paraffins (CPs) from a CP production plant to the surrounding surface soils and coniferous leaves. *Environmental Science & Technology*, *50*, 12759–12766. https://doi.org/10.1021/acs.est.6b03595

[104] Yu S., Gao Y., Zhu X., Yu H., Zhang Y., & Chen J. (2023). Gas/particle partitioning of short and medium chain chlorinated paraffins from a CP production plant using passive air sampler and occupational exposure assessment. *Science of the Total Environment*, *858*, 159875. https://doi.org/10.1016/j.scitotenv.2022.159875

[105] Yuan B., Tay J.H., Padilla-Sánchez J.A., Papadopoulou E., Haug L.S., & de Wit C.A. (2021). Human exposure to chlorinated paraffins via inhalation and dust ingestion in a Norwegian cohort. *Environmental Science & Technology*, *55*, 1145–1154. https://doi.org/10.1021/acs.est.0c05891

[106] Zeng L., Chen R., Zhao Z., Wang T., Gao Y., Li A., Wang Y., Jiang G., & Sun L. (2013). Spatial distributions and deposition chronology of short chain chlorinated paraffins in marine sediments across the Chinese Bohai and Yellow Seas. *Environmental Science & Technology*, *47*, 11449–11456. https://doi.org/10.1021/es402950q

[107] Zeng L., Wang T., Han W., Yuan B., Liu Q., Wang Y., & Jiang G. (2011a). Spatial and vertical distribution of short chain chlorinated paraffins in soils from wastewater irrigated farmlands. *Environmental Science & Technology*, *45*, 2100–2106. https://doi.org/10.1021/es103740v

[108] Zeng L., Wang T., Ruan T., Liu Q., Wang Y., & Jiang G. (2012a). Levels and distribution patterns of short chain chlorinated paraffins in sewage sludge of wastewater treatment plants in China. *Environmental Pollution*, *160*, 88–94. https://doi.org/10.1016/j.envpol.2011.09.004

[109] Zeng L., Wang T., Wang P., Liu Q., Han S., Yuan B., Zhu N., Wang Y., & Jiang G. (2011b). Distribution and trophic transfer of short-chain chlorinated paraffins in an aquatic ecosystem receiving effluents from a sewage treatment plant. *Environmental Science & Technology*, *45*, 5529–5535. https://doi.org/10.1021/es200895b

[110] Zeng L., Zhao Z., Li H., Wang T., Liu Q., Xiao K., Du Y., Wang Y., & Jiang G. (2012b). Distribution of short chain chlorinated paraffins in marine sediments of the East China Sea: Influencing factors, transport and implications. *Environmental Science & Technology*, *46*, 9898–9906. https://doi.org/10.1021/es302463h

[111] Zeng Y., Tang B., Luo X., Zheng X., Peng P., & Mai B. (2016). Organohalogen pollutants in surface particulates from workshop floors of four major e-waste recycling sites in China and implications for emission lists. *Science of the Total Environment*, *569–570*, 982–989. https://doi.org/10.1016/j.scitotenv.2016.06.053

[112] Zhang W., Gao Y., Qin Y., Wang M., Wu J., Li G., & An T. (2019). Photochemical degradation kinetics and mechanism of short-chain chlorinated paraffins in aqueous solution: A case of 1-chlorodecane. *Environmental Pollution*, *247*, 362–370. https://doi.org/10.1016/j.envpol.2019.01.065

[113] Zhao N., Cui Y., Wang P., Li S., Jiang W., Luo N., Wang Z., Chen X., & Ding L. (2019). Short-chain chlorinated paraffins in soil, sediment, and seawater in the intertidal zone of Shandong Peninsula, China: Distribution and composition. *Chemosphere*, *220*, 452–458. https://doi.org/10.1016/j.chemosphere.2018.12.063

[114] Zhou Q., Xu C., Shen C., Li F., Liu S., & Aamir M. (2023). Congener profiles, air-soil exchange, and potential risks of short- and medium-chain chlorinated paraffins in demonstration zone of Yangtze River Delta. *Atmospheric Pollution Research*, *14*, 101639. https://doi.org/10.1016/j.apr.2022.101639

[115] Zhou T., Yang Q., Weng J., Gao L., Liu Y., Xu M., Zhao B., & Zheng M. (2024a). Characterization and health risks of short- and medium-chain chlorinated paraffins in the gas and size-fractionated particulate phases in ambient air. *Chemosphere*, *358*, 142225. https://doi.org/10.1016/j.chemosphere.2024.142225

[116] Zhou W., Huang K., Bu D., Zhang Q., Fu J., Hu B., Zhou Y., Chen W., Fu Y., Zhang A., Fu J., & Jiang G. (2024b). Remarkable contamination of short- and medium-chain chlorinated paraffins in free-range chicken eggs from rural Tibetan Plateau. *Environmental Science & Technology*, *58*, 5093–5102. https://doi.org/10.1021/acs.est.3c08815

[117] Zhu X., Bai H., Gao Y., Chen J., Yuan H., Wang L., Wang W., Dong X., & Li X. (2017). Concentrations

and inhalation risk assessment of short-chain polychlorinated paraffins in the urban air of Dalian, China. *Environmental Science and Pollution Research*, *24*, 21203–21212. https://doi.org/10.1007/s11356-017-9775-x

[118] Zhuo M., Ma S., Li G., Yu Y., & An T. (2019). Chlorinated paraffins in the indoor and outdoor atmospheric particles from the Pearl River Delta: Characteristics, sources, and human exposure risks. *Science of the Total Environment*, *650*, 1041–1049. https://doi.org/10.1016/j.scitotenv.2018.09.107

[119] Zitko V. (1980). Chlorinated paraffins. In Anliker R., Butler G.C., Clarke E.A., Förstner U., Funke W., Hyslop C., Kaiser G., Rappe C., Russow J., Tölg G., Zander M. & Zitko V. (Eds.), *Anthropogenic Compounds* (pp. 149–156). Springer, Berlin, Heidelberg.